THE ROLE OF DISTAL-LESS (DLX) 3 IN THE PATHOPHYSIOLOGY OF PLACENTAL DEVELOPMENT

by Patricia A. Clark

THE ROLE OF DISTAL-LESS (DLX) 3 IN THE PATHOPHYSIOLOGY OF PLACENTAL DEVELOPMENT

A Dissertation

Presented to the Faculty of the Graduate School

of Cornell University

in Partial Fulfillment of the Requirements for the Degree of

Doctor of Philosophy

by

Patricia A. Clark

August 2010

THE ROLE OF DISTAL-LESS (DLX) 3 IN THE PATHOPHYSIOLOGY OF PLACENTAL DEVELOPMENT

Patricia A. Clark, Ph.D.

Cornell University 2010

Proper placentation is critical for normal fetal growth, development, and fitness throughout gestation. This research examines the central hypothesis that Dlx3 and the gene targets of Dlx3 help to direct normal placental labyrinth morphogenesis in the mouse placenta. Further, misregulation of key features of this gene network appears to be correlated with changes in gene expression associated with the pathophysiology of preeclampsia (PE).

Yeast-two hybrid screening of a placental cDNA library identified Smad6 as a binding partner of Dlx3. Investigation using immunoprecipitation assays mapped the Smad6 interaction domain to Dlx3 residues 80-163. Further, studies indicate Smad6 has the ability to repress Dlx3 transcriptional activity on the human glycoprotein hormone α subunit promoter in JEG3 cells likely through allosteric interference.

Gene profiling using Affymetrix microarray was performed on RNA from wildtype and $Dlx3^{-/-}$ placentas and identified 401 genes that were differentially expressed following the loss of Dlx3, including expression of matrix metalloproteinase (MMP-) 9, an extracellular matrix (ECM) remodeler. Analysis of cultured media using Western blot and zymography from Dlx3 $^{+/+}$, $^{+/-}$, and $^{-/-}$ placental explants corroborated these findings. Using luciferase reporter gene analysis and DNA binding studies, Dlx3 was shown to bind and transactivate a 1.9kb portion of the mouse MMP-9 gene promoter in a dose dependent manner in JEG3 cells. Further siRNA-mediated reduction of Dlx3 resulted in decreased human MMP-9 protein levels and activity. Consistent with this result, chromatin immunoprecipitation (ChIP) assays revealed

Dlx3 is capable of binding to the human MMP-9 gene promoter. Lastly, Dlx3 and MMP-9 were both coordinately misregulated in a mouse model of preeclampsia. These studies indicate the potential role for the interaction between Dlx3 and MMP-9 during placental development and potentially the causal pathophysiology of PE.

Analysis of fetal weights during gestation revealed a potential intrauterine growth retardation (IUGR) phenotype in $Dlx3^{+/-}$ animals. Analysis of $Dlx3^{+/-}$ placentas throughout gestation found evidence for an accumulation of reactive oxygen species (ROS) likely leading to a high apoptotic index in these placentas relative to controls. Antioxidant therapy using the superoxide dismutase mimetic, Tempol, resulted in amelioration of ROS and a rescue of the IUGR phenotype. Tempol treatment also rescued a subset of $Dlx3^{-/-}$ embryos 3 days beyond their normally identified embryonic demise. Additionally, micro computer tomography (micro-CT) and histological analyses of $Dlx3^{+/+}$ and $^{+/-}$ placentas identified important changes in maternal spiral arteries associated with $Dlx3^{+/-}$ which were reversed by antioxidant supplementation. These findings support the conclusion that loss of a single Dlx3 allele is detrimental to fetal growth *in utero*. Antioxidant therapy rescued fetal growth abnormalities due to oxidative stress suggesting potential treatment for pregnancy complications associated with placental insufficiency.

Together, these studies provide evidence for the novel role of Dlx3 in the regulation of an important gene network during placental development. This includes Dlx3-dependent regulation of a key MMP linked to placental ECM remodeling. Both Dlx3 and MMP-9 are misregulated in a mouse model of PE indicating involvement in pregnancy complications. Additionally, these studies characterize a new IUGR model due to haploinsufficiency at the Dlx3 locus. Studies also provide support for the possible benefits of gestational antioxidant therapy in controlling ROS accumulation that can occur during abnormal placentation as observed in the Dlx3 mouse model.

BIOGRAPHICAL SKETCH

Patricia Clark was born and raised in Seneca Falls, New York. In 1999, she attended the University at Albany in Albany, New York majoring molecular biology. While at the University at Albany, Patty volunteered at the Albany Medical Center and the Five-Quad Ambulance Squad. In the summer of 2002, she was awarded a fellowship to study estrogen dependent progression of breast cancer under the leadership of Dr. Fengzhi Li at Roswell Park Cancer Institute in Buffalo, New York. Under the guidance of Dr. Jeffery Travis at the University at Albany, Patty completed an honors thesis in biology titled "Characterization of the pattern of motility in *Centropyxis."* Simultaneously, she conducted research in the laboratory of Dr. Michael Fucillo at Albany Medical Center and completed a second honors thesis titled "Investigating the Role of Rad51 in *Saccharomyces cerevisiae* in response to ultraviolet DNA damage." Patty graduated, with honors, in 2003 from the University at Albany.

In August of 2005, Patty joined Dr. Mark Roberson's laboratory at Cornell University as a Ph.D. student in the Field of Molecular and Integrative Physiology.

To

my parents

ACKNOWLEDGEMENTS

I would first like to express a heartfelt gratitude to my mentor and advisor, Dr. Mark S. Roberson, for his excellent guidance and unwavering support both in and out of the laboratory over the last five years. I would not have been able to produce the breadth and scope of data that is presented in this document without the patience and direction of such a fantastic, gifted, and understanding advisor.

I would also like to thank my committee members, Drs. O'Brien, Place and Schaffer. Working with you all for the last five years has been a wonderful experience. Your time, input and support have helped mold me into the scientist that I am today.

I am grateful for the numerous opportunities I have had for collaborations at Cornell University. I have been extremely fortunate to work with many brilliant thought provoking, problem-solving individuals. More specifically, I would like to thank Robin Davisson and members of her lab for their generous support, use of lab equipment, and reagents. I have worked closely with Ashley Woods from Robin Davisson's laboratory on numerous studies over the years including the micro-CT analysis of the Dlx3 mouse model that appears in Chapter 4. Thank you Ashley, for all of the your time, work, and efforts that have contributed to this body of work. I also would like to thank Chris Schaffer for the opportunity to collaborate with him and members of his laboratory on studies assessing placental vasculature of the Dlx3 mouse model with two-photon excited microscopy techniques.

My labmates in the Roberson lab were always available to discuss potential experiments, dry a tear, or share a laugh. Thank you all for your support.

Thank you to the rest of my third floor family, including Dr. Paula Cohen and the members of her laboratory, for use of equipment, reagents, and the superb working environment we have shared for the past five years.

Finally, I would like to thank my parents, my family and my friends. Their constant love, support, and general optimism gave me the courage and ambition to pursue my goals.

TABLE OF CONTENTS

LIST OF FIGURES

LIST OF ABBREVIATIONS

Ac-H3	acetylated-histone H3
Ang1	Angiotensin 1
AI	Amelogenesis imperfecta
bHLH	basic helix-loop-helix
BMI	body mass index
BMP	bone morphogenetic protein
BSA	bovine serum albumin
ChIP	chromatin immunoprecipitation assay
CG	chorionic gonadotropin
COX	cyclooxygenase
COX-1	cyclooxygenase 1
CT	tomography
Dlx3	Distal-less 3
DMEM	Dulbecco's Modified Eagle's medium
DPBS	Dulbecco's phosphate buffered saline
E	embryonic day
ECM	extracellular matrix
EDTA	ethylenediaminetetraacetic acid
EGF	epidermal growth factor
EMSA	electrophoretic mobility shift assay
ERRβ	Estrogen-related receptor β
ERK	extracellular signal-regulated kinase
Esx-1	extra-embryonic tissue-spermatogenesis-homeobox gene-1
EVT	extravillous trophoblasts

FGF	fibroblast growth factor
Flt-1	fms-like tyrosine kinase-1
GCM-1	glial cells missing-1
GFP	green fluorescence protein
HA	hemagglutinin
Hand1	heart- and neural crest derivatives-expressed
HIFβ1	hypoxia-inducible factor 1β
HO•	hydroxyl radical
H_2O_2	hydrogen peroxide
HOCl	hypochlorous acid
Id	inhibitors of DNA binding
IL-1β	interleukin-1β
Itga5	integrin 5
IUGR	intrauterine growth restriction
JRE	junctional regulatory element
KDR	kinase-insert domain region
MAPK	mitogen-activated protein kinase
micro-CT	microcomputer tomography
MMPs	matrix metalloproteinases
MMP-9	matrix metalloproteinase-9
NF-κB	nuclear factor-κB
NIH	National Institute of Health
NO•	nitric oxide
O_2•-	superoxide anion radical
Oct4	Octamer-4
ONOO-	peroxynitrite anion

ORD	Office of Rare Disease
PE	preeclampsia
PGE_2	prostaglandin E_2
PGF	placental growth factor
POU	Pit-Oct-Unc
qPCR	quantitative polymerase chain reaction
rDlx3	recombinant Dlx3
ROS	reactive oxygen species
SDS	sodium dodecyl sulfate
SDS-PAGE	SDS-polyacrylamide gel electrophoresis
siRNA	small interference ribonucleic acid
SOD	superoxide dismutase
TDO	tricho-dento-osseous
TNF-α	tumor necrosis factor-α
TGF-β	transforming growth factor-β
TIMP-1	tissue inhibitor of metalloproteinase-1
TSP-2	thrombospondin 2
Vcam	vascular cell adhesion molecule
VEGF	vascular endothelial growth factor

CHAPTER ONE

REVIEW OF THE LITERATURE

1 Introduction

The placenta is the first functional organ formed in the mammalian embryo and is essential for fetal growth and survival throughout gestation. This collection of extra-embryonic membranes serves as the main site of exchange for a variety of materials between mother and fetus including gases, nutrients, hormones, growth factors and waste products of metabolism. Both fetal circulation and maternal blood flow contribute to normal placental perfusion. Maternal contributions to proper placental development are affected by nutrition, age, and body mass index (BMI), to name a few. Improper placentation, regardless of the cause, could lead to a multitude of placental disease conditions including intrauterine growth retardation (IUGR), placental insufficiency, preeclampsia and possibly fetal death. Thus, this important interface functions to meet fetal metabolic demands to maintain fetal fitness and normal growth during gestation.

The Office of Rare Diseases (ORD) of the National Institute of Health (NIH) lists placental disease conditions as a "rare disease." By definition this identifies less than 200,000 people each year in the United States affected by placental disease. Despite this "rare disease" designation, health care costs associated with pregnancy-associated diseases including pathologies within the placenta are substantial. For example, a population survey examining 17,415 patients carrying singleton pregnancies (single placentas) found the incidence of defective placental maturation was 5.7%, and was associated with fetal mortality in 2.3% of cases. In control patients displaying normally developed placentas, fetal mortality due to placental pathologies occurred in only 0.033% of cases [1]; a ~70 fold decrease in fetal mortality. These findings indicate the importance of proper placentation to facilitate the appropriate growth trajectory and health of the fetus and mother.

2 Placental Development in the Mouse

Placental development is likely best understood in the mouse, since this species has been the focus of numerous genetic studies due to the relative ease of genetic manipulation in this model animal. Recent work from the laboratories of James Cross, Janet Rossant and colleagues have described the developing mouse placenta in great detail providing the field of placentology key insights into the genetic and molecular mechanisms of productive and successful fetal and maternal communication throughout gestation. The following sections of this dissertation provide an overview of murine placental development.

2.1 Placental Establishment Timeline

In mice, the placenta begins developing at embryonic day (E) 3.5 in the blastocyst when the trophectoderm is separated from the inner cell mass [2 3] essentially creating a two compartment embryo; the inner cell mass contributing to development of the embryo proper while the trophectoderm contributes to the placenta. Several trophoblast cell populations or lineages emerge from the trophoectoderm during establishment of the placenta. During the peri-implantation period trophoblast giant cells differentiate emerging from the outer trophectoderm layer of the blastocyst. After implantation, trophoblast giant cells, derived from the mural trophectoderm, line the embryonic cavity, where they form part of the parietal yolk sac. These giant cells are referred to as 'primary' or 'parietal' giant cells, named for their time of differentiation [4]. A second wave of trophoblast giant cells differentiates after implantation occurs. These cells are known as 'secondary' trophoblast giant cells or polar trophoblast cells, again based on the timing of differentiation and their directional invasive function during formation of the fetal-maternal interface [2,4].

Secondary giant cells also form a discontinuous border towards the maternal decidua and line the maternal vascular canals that deliver maternal blood into the fetal-maternal interface [4].

At E8.5 the extraembryonic mesoderm (allantois) fuses with the chorion derived from the trophectoderm defining the chorioallantoic attachment in the murine placenta [2 5]. At this point, the vascular portion of the placenta commences formation. The chorion begins to fold to form not only dense villus structures, but also additional space and surface area for fetal blood vessels to grow from the allantois [5]. From this point throughout the remainder of gestation, branching morphogenesis of the fetal villi continue to create a vast and intricate vascular network within the placenta. In the mouse, the fetal-maternal interface, termed the labyrinth, is structurally supported by the spongiotrophoblast cells of the junctional zone, which are derived from the ectoplacental cone and largely serves as the interface between fetal tissues and the maternal decidua. The labyrinth is formed by the proliferation and migration of polar trophoblasts to the mesometral side of the uterus [2 5 6]. The full establishment of the labyrinth reflects the key compartment where exchange of maternal and fetal components occurs during gestation.

Concurrent with the formation of vasculature within the labyrinth, chorionic trophoblast cells begin to differentiate into two labyrinth cell types, syncytiotrophoblast and cytotrophoblast cells. Both cell types play integral roles in the vascularization of the placenta. Syncytiotrophoblast cells are multinucleated, formed by the fusion of cytotrophoblast cells, and function as the cellular layer adjacent to the fetal capillary endothelium. Meanwhile, the mononuclear cytotrophoblast cells line maternal blood sinuses that form within the labyrinth. The villi, which are composed of an outer epithelial layer derived from syncytiotrophoblast cells and an inner core of stromal cells and blood vessels, are bathed in maternal blood

spaces, allowing for direct contact between maternal circulation and fetal trophoblasts [7 6]. As gestation progresses, the vasculature within the labyrinth continue to expand to meet the growing metabolic needs of the growing fetus [5]. The mechanisms associated with normal placentation are clearly regulated by numerous factors including specific gene networks, hormones, growth factors and many other key determinants. A wide variety of these factors have been shown to be of great importance for proper placentation and the establishment of the fetal-maternal interface in the mouse largely due to extensive genetic studies taking advantage of naturally occurring mutations and experimentally defined gene disruption studies. A disruption in the formation of this critical communication between fetus and mother has the possibility of creating devastating effects on fetal fitness.

3 Genetic Factors Influencing Placental Development

Numerous knockout models have led to the discovery of the involvement of specific genes in normal placental development. The following sections provide important examples of these types of genetic knockout studies; however, due to space constraints, these are not an exhaustive list of examples of gene knockouts affecting placental function. Spongiotrophoblast cells of the junctional zone border the labyrinth and the outer giant cells. Maternal blood supply passes through this layer via large arterial sinuses to bath the fetal blood vessels of the labyrinth [8]. The survival and growth of the spongiotrophoblast cells depend on the basic helix-loop-helix (bHLH) factor Mash-2 [9]. In the absence of Mash-2, the spongiotrophoblast layer within the mouse placenta is greatly reduced, leading to midgestation embryonic lethality due to placental failure associated with a lack of spongiotrophoblasts and reduced trophoblast layers within the labyrinth [10]. In addition to Mash-2, hypoxia-inducible factor 1β

(HIF1β) serves an essential function in the development and maintenance of spongiotrophoblasts. HIF1β forms a heterodimer with HIF1α and induces target genes under low oxygen tension; targeted deletion of HIF1β in mice reduces the size of the spongiotrophoblast layer. These findings indicate low oxygen levels within the developing placenta are important for maintenance and function of spongiotrophoblast [11].

Secondary trophoblast giant cells also develop from precursors of the ectoplacental cone and require the action of bHLH proteins heart- and neural crest derivatives-expressed protein (Hand1) 1 and I-mfa. Both proteins have been shown to increase in expression during giant cell differentiation *in vitro* [12,13]. Analyses of homologous genetic deletions of these genes in mice demonstrate a total reduction of giant cells due to decreased proliferation [13 14]. Additionally, both factors are able to antagonize the activity of Mash-2 through two different mechanisms. I-mfa directly binds to Mash-2, while Hand1 competes for other bHLH binding partners; both mechanisms result in a decrease in Mash-2 transcriptional activity [15 13]. Members of the inhibitors of DNA binding (Id) family may also play a role in trophoblast giant cell formation. These proteins have a HLH dimerization domain, but lack the basic domain required for DNA-binding. Both Id-1 and Id-2 proteins are present in the chorion but absent from trophoblast giant cells [16]. More specifically, overexpression of Id-1 in Rcho-1 trophoblast stem cells inhibits giant cell differentiation in this *in vitro* model [12]. In addition to its' role in differentiation of trophoblast giant cells outlined above, Hand1 is expressed in numerous developing tissues including heart, limbs, neural crest derivatives and extra-embryonic membranes and Hand1 knockout embryos die at E8.5, due to numerous developmental defects, mainly involving a failure of vascular growth and remodeling within the yolk sac. Despite the observation that placental angiogenic genes such as vascular endothelial growth factor

(VEGF) and Angiotensin1 (Ang1) were expressed normally, Hand1 mutant yolk sacs lacked proper distribution of smooth muscle cells that provide structural support to vasculature [17]. This study provides an important example of the critical function of Hand1 during yolk sac vascular development. These findings support the conclusion that genes like Hand1 serve multiple functions within the establishment of the placenta.

The Ets winged helix-turn-helix family of transcription factors have been identified in trophoblast tissues as early as day 6.5 and are also expressed in many other cell types in the developing mouse embryos, including limb buds and embryonic skin. Targeted deletion of Ets-2 resulted in embryonic lethality at E8.5 due to a defect in both the migration and differentiation of trophoblast cells and deficient expression of matrix metalloproteinase-9 (MMP-9) [18 19]. MMP-9 functions in a variety of physiological and pathophysiological processes, including placental development, wound healing, angiogenesis, inflammation and metastasis [20]. Most relevant, MMP-9 is expressed in extravillous trophoblast cells during trophoblast invasion in the beginning stages of gestation, where it helps degrade and remodel extracellular matrix (ECM) within the uterine endometrium associated with implantation [21]. Further discussion of the role MMP-9 plays in placentation is described in sections of Chapter 1 below. Similar to the Ets-2 null mouse, the Distal less (Dlx) 3 null mouse dies between E9.5 and 10 as a result of poor differentiation of the spongiotrophoblast and labyrinth layers and an overall decrease in vascularization within the placental labyrinth [22 23]. Dlx3 is the focus of this dissertation and will also be discussed in more detail in a later section; briefly, Dlx3 is a member of a larger class of homeodomain-containing transcription factors involved in many aspects of embryonic and placental development.

Together, these findings indicate the involvement of multiple genes and or gene networks in the systematic interplay responsible for normal placental cell lineage commitment and proliferation as well as important features of vascular development within the maternal-fetal interface. The key use of knockout mouse models have aided greatly in our more global understanding of how single gene deletions can contribute to placental insufficiency. There is a strong likelihood that these types of models will serve to better support our understanding of the many molecular determinants that give rise to this complex tissue. For the purposes of this dissertation placental insufficiency is defined as improper placental development resulting in a decreased fetal growth trajectory.

4 Signaling In Placental Development

The inner cell mass of the developing embryo provides important positive signaling for trophoblast cell proliferation and differentiation [8 6]. Early studies by Gardner and colleagues have shown that transplantation of an inner cell mass into a trophectodermal vesicle can result in normal development [24]. These important early studies provided the initial framework for how cell-cell interactions within the blastocyst regulate key developmental decisions. Additional evidence for the important communication between the trophectoderm and the inner cell mass comes from the failure of cultured extra-embryonic ectoderm and ectoplacental cone tissues to proliferate and form trophoblast giant cells in the absence of signaling from an inner cell mass [25 26]. These findings, led to speculation that the trophoectodermal cells, which surround the inner cell mass, and the early extraembryonic ectoderm facilitate the proliferation and differentiation of trophoblast lineages. Initial signaling arises from the inner cell mass and as cells migrate away from the signaling source, they

then differentiate to form the ectoplacental cone and trophoblast giant cells. This section of Chapter 1 seeks to provide important examples of these signaling relationships and how these signaling pathways regulate trophoblast cell function.

4.1 Fibroblast growth factor (FGF) as a signaling molecule

Recent work has focused on fibroblast growth factor (FGF) as a pathway involved in the signaling between the inner cell mass and trophoblast differentiation. More specifically, out of the 23 FGF family members found in vertebrates, the experiments highlighted below focus on Fgf4 since this family member appears to play a crucial role in trophoblast lineage determination. Fgf4 null mouse embryos die at implantation and are characterized by poor development of all trophoblast cell lineages [27]. Fgf4 is expressed within the inner cell mass at the preimplantation blastocyst and expression continues throughout the epiblast following implantation [28] [29]. Interestingly, embryonic stem cells derived from the inner cell mass of Fgf4 homozygous null embryos can be readily isolated and cultured [30]. This finding indicates the mechanisms associated with the embryonic lethality of the $Fgf4^{-/-}$ mouse model might result from a failure of trophoblast cell lineage differentiation and/or proliferation. The most persuasive evidence supporting the important role of Fgf signaling in trophoblast proliferation comes from additional mouse experiments. Octamer-4 (Oct4) is a mammalian Pit-Oct-Unc (POU) transcription factor expressed in the early stages of the developing embryo and expression is restricted to the inner cell mass. Homozygous Oct4 mutant mice develop only until the blastocyst stage due to a lack of an inner cell mass resulting in decreased trophoblast proliferation. Importantly in these studies, treatment of Oct4 null mutants with exogenous Fgf4 resulted in an increase in trophectoderm cell proliferation [31]. These studies provide

evidence of the key interactions between inner cell mass and the surrounding trophectoderm that support the early developmental decisions directing trophoblast cell fate determination and subsequent proliferation.

4.2 Other Signaling Pathways

Studies have indicated the involvement of signaling pathways other than Fgf4 in early trophoblast cell proliferation and differentiation. Estrogen-related receptor (ERRβ) is one such pathway. Mutating the gene encoding for ERRβ, results in a complete absence of the diploid trophoblast layers of the placenta, an abnormally thick layer of giant trophoblast cells, and embryonic lethality around embryonic day (E) 9 [32]. Investigating ERRβ mutant embryos earlier in gestation (~E6), the extra embryonic ectoderm forms normally. However, the demise of these embryos appears to be a failure of chorion formation resulting from the inability of trophoblast cell differentiation [32]. These findings indicate the potential role of ERRβ in early trophoblast differentiation and proliferation. Whether the ERRβ pathway is independent of the Fgf4 signaling pathway requires further analysis.

Additional studies have highlighted the involvement of the mitogen-activated protein kinase (MAPK) pathways in mouse embryonic development and placentation. These pathways are evolutionarily conserved and involved in transducing extracellular signals from growth factors such as Fgfs into intracellular responses [33]. The prototypical MAPK pathway is the extracellular signal-regulated kinase (ERK)1/2 pathway. The two related MAPK isoforms are known as ERK1 and ERK2. Several studies have implicated these enzymes in the control of cell proliferation and differentiation [34]. Both Erk1 and Erk2 are widely expressed throughout the early-stage embryos. Disruption of the Erk2 locus leads to embryonic lethality after implantation

in mouse development. Erk2 mutants fail to form the ectoplacental cone and extra-embryonic ecotderm. Additionally, Erk1 fails to compensate for Erk2 function suggesting a novel function of Erk2 in normal trophoblast development in the mouse, likely via regulating the proliferation potential of trophectoderm cells during placentation [35].

Although this list is not exhaustive, together, these findings indicate the dynamic relationship of multiple pathways governing normal placental development. Like a number of transcription factors, disruption of discrete signaling pathways or downstream signaling intermediates regulated by these pathways can lead to detrimental effects during placental development.

5 Comparative Placental Development: humans and mice

The discussion thus far has focused on the use of mouse models to describe basic genetic mechanisms associated with placental development and function. This is entirely consistent with the use of important mouse models (such as the Dlx3 null mouse) in the research described in this dissertation. However, my fundamental goal is to use these crucial animal models to help inform our understanding of basic mechanisms at play that lead to human pathophysiology during pregnancy. Thus, a brief discussion of the comparison of form and function between the mouse and human placentas is warranted.

The basic architecture of both mouse and human placentas is remarkably similar with only a few differences observed at the microscopic level of these two species. The placentas of both species are characterized as chorioallantoic, hemochorial placentas; perhaps the most intimate placental vascular relationship in mammals. The fetal and maternal circulatory interface of both species contains three

trophoblast cell layers (trichorial); two syncytiotrophoblast layers surrounding fetal endothelial cells of the fetal vasculature and a single cytotrophoblast cell layer adjacent to the maternal blood spaces [5 8 36]. Further, comparison of placental anatomy and gene expression of the murine and human placentas suggest analogous cell types exist between the two species [36].

Consistent with mice, the structure of the human placenta is established during the first half of gestation [37]. Additionally, both mouse and human placentas are classified as discoid, meaning the functional exchange portion of the placenta reflects one discrete unit with a single place of attachment within the uterus. In both species, maternal blood enters the placenta through a remodeled blood vessel network of large diameter, low-resistance vessels, known as maternal spiral arteries. The remodeling that occurs to create these low-resistant vessels involves migration of fetal trophoblasts into these vessels. The remodeling carried out by these trophoblasts is largely characterized by a loss of smooth muscle surrounding these vessels. The site of fetal-maternal exchange in humans is referred to as the villus tree, while in the mouse, the labyrinth, and reflects the interface between fetal and maternal blood supplies. Within the fetal-maternal interface, the fetal chorionic branches and maternal blood sinusoids of both species are similar in tortuosity and dimension [36 8]. Additionally, the umbilical vessels of both species connect the fetal capillaries of the placental exchange region with the fetal circulation [36].

The similarities between mouse and human placentas are more pronounced when investigating the actual cell types. Human extravillous trophoblasts (EVT) develop from anchoring villi and attach to the uterine basement membrane. EVT's are analogous to the trophobast giant cells of the murine placenta. Both have the ability to be polyploid due to multiple rounds of DNA replication in the absence of intervening cytokinesis. Human EVT's and mouse trophoblast giant cells are similar in function

as well; both mediate the maternal invasion of the uterus. Trophoblast invasion in both species is a precursor to the remodeling of maternal endothelium resulting in large diameter, low resistance spiral artery vessels. Maternal spiral arteries present in both species facilitate proper placental profusion [38] [39]. The cytotrophoblast cells of the anchoring villi are similar in function to the murine spongiotrophoblasts cells, due to the ability of the spongiotrophoblast cells to differentiate into giant cells. Thus, murine giant trophoblast cells and the cytotrophoblast cells of the human anchoring villi serve in the formation of the interface of fetal-maternal exchange.

A comparative proteomic and transcriptome investigation of microdissected placental tissue from the mouse labyrinth and the human villous tree near the end of gestation reveals 70% co-expression of orthologous genes in both species; over 80% of genes known that regulate placental differentiation in the mouse are co-expressed in both species. More importantly, 34 novel candidate proteins identified in both mouse and humans are likely important in placental structure and/or function [40]. For example, integrin (Itga) 5 was identified in this screen. Integrins mediate cell adhesion to basement membranes and extracellular matrix in addition to cell signaling in both humans and mice. Homozygous loss of Itga5 in mouse models results in defects in yolk sac mesodermal structures leading to midgestation embryonic lethality at E10 [41]. Altogether, these findings highlight key similarities between mouse and human placental structures and indicate an important role of mouse models for studying placental pathophysiology characteristic of human disease.

6 Abnormal Placentation

Disruption in fetal-maternal communication(s) within the labyrinth layer (mouse) or the villous tree (human) could lead to a multitude of disease states

including intrauterine growth restriction (IUGR), placental insufficiency, preeclampsia, and possibly fetal death. As suggested earlier, numerous mouse knockout models have aided in the study of abnormal placentation. In general, three critical areas can be defined as necessary for placental development: chorioallantoic attachment, branching morphogenesis at the chorioallantoic interface, and morphogenesis of the labyrinth layer. The following discussion will outline the role each plays in establishment of the normal placenta and how disruption of these processes can result in compromised pregnancies.

6.1 Chorioallantoic Attachment

As discussed above, the initial stage of the formation of the labyrinth layer in the mouse is chorioallantoic attachment and defects at this stage of placentation have been characterized by midgestation embryonic lethality. One notable pathway believed to be associated with this phenotype is the bone morphogenetic protein (Bmp) signaling pathway. Knockouts of Bmp 2, -4, -5, and -7 have led to mesodermal differentiation defects culminating in aberrant development of the allantois [42,43]. For example, Bmp5/Bmp7 double mouse mutants die at E10.5 due to abnormal placental development. More specifically, these mutants have defects in promoting the necessary proliferation and maintenance of trophoblast cells governing chorioallintoic fusion [43].

In addition to Bmp signaling, cell adhesion molecules such as vascular cell adhesion molecule (Vcam) 1 and the gene encoding for integrin α (Itga) 4, are also believed to be involved in the process associated with chorioallantoic fusion. Vcam1 is expressed on the tip of the expanding allantois and binds to alpha 4 integrin, which is expressed on the basal surface of the chorion. This key interaction results in the fusion of the chorioallantoic membranes. Loss of function mutations in mice in both

Vcam1 [44] and Itga4 [45] genes result in abnormal chorioallantoic fusion and in some cases, defects in the establishment of the placental labyrinth. The similar placental phenotype observed in these separate mouse mutants argues for a mechanism whereby the interaction between these two cell adhesion molecules is necessary for chorioallantoic attachment. However, these two molecules alone may not be mediating the entire fusion between the allantois and the chorion. Mammalian relative of DnaJ (MrJ) null mice exhibit defective chorioallantoic fusion and die at midgestation, around E8.5 despite having normal expression of both Vcam1 and alpha 4 integrin. However, MrJ null mice do express reduced levels of specific transcription factors such as glial cells missing-1 (Gcm-1), which is necessary for fetal branching morphogenesis in the labyrinth layer [46]. MrJ appears to play a role, in conjunction with other genes, in facilitating branching morphogenesis responsible for proper placental vascularization. Thus, chorioallantoic fusion is mediated by multiple genes likely via discrete mechanisms. Lesions at any step results in failure in the fusion of the chorion and allantois and disruption of a viable pregnancy.

6.2 Branching Morphogenesis

In addition to chorioallantoic attachment, branching morphogenesis is critical for placental vascularization and fetal growth. A large surface area is created by extensive branching morphogenesis of trophoblast-derived epithelium to create a villous network. These fetal villi are subsequently vascularized with an elaborate capillary network. This branching allows for the complex vascular interface necessary for fetal and maternal exchange in the placenta.

Branching morphogenesis in the placenta is facilitated by the transcription factor glial cells missing-1 (Gcm-1). Areas in the chorionic plate where folding

occurs and enagination of the allantoic mesoderm is initiated are preceded by the expression of Gcm-1. Gcm-1 is expressed at focal sites in the chorionic plate as early as E8.0. Trophoblast cells expressing the Gcm-1 gene initiate branching and coordinate the differentiation of trophoblast cells to fuse and form syncytiotrophoblast layers. Gcm-1 is expressed at the distal tip of the branching villi [47]. Gcm-1 is expressed as long as the labyrinth continues to enlarge by villus branching processes [8]. Mice with a mutation in Gcm-1 lack chorioallantoic branching, the chorion layer remains flat, trophoblast cells fail to differentiate and the fetal vasculature does not interact with the maternal blood sinuses [47]. The hallmark of the Gcm-1 gene deletion is the absence of the labyrinth compartment of the mouse placenta. Additionally, Fgf signaling is required for chorioallantoic branching as indicated by the labyrinth defects found in Fgf receptor 2 mutant mice [48]. Thus, similar to chorioallantoic fusion, placental branching morphogenesis is due to the interplay between numbers of genes.

6.3 Morphogenesis of the Labyrinth

Trophoblast stem cells reside in the chorion and remain as a self-renewing population of stem cells or differentiate into spongiotrophoblasts, trophoblast giant cells or syncytiotrophoblast cells found within the labyrinth. Several key transcription factors appear to regulate this important balance of stem cell self-renewal or differentiation of stem cells into cell lineages in the developing placenta. For example, the mammalian *Achaete-Scute* homologues (Mash-2) is involved in trophoblast cell proliferation. Targeted deletion of this basic helix-loop-helix (bHLH) transcription factor results in a decreased spongiotrophoblast layer due to a restriction of trophoblast proliferation with a concurrent sustained rate of trophoblast cell differentiation into giant cells [18]. The labyrinth of Mash-2 mutants is reduced and

presumable not functional [9]. Another bHLH protein, Hand1, involved in yolk sac formation, as described above, also indirectly plays a role in morphogenesis of the labyrinth layer. Hand1 has been implicated in trophoblast stem cell differentiation. Overexpression of Hand1 in trophoblast stem cells promoted trophoblast giant cell differentiation indicating its function to restrict cells toward trophoblast giant cell fate in the formation of the labyrinth [49]. Recent mouse studies have identified the transcription factor extra-embryonic tissue-spermatogenesis-homeobox gene (Esx)1 as a regulator of trophoblast function and vascularization of the labyrinth layer. Esx1 is exclusively expressed in the chorion and is later expressed in the trophoblast compartment of the labyrinth [50]. Homozygous null Esx1 mutant mice exhibit a larger labyrinth, but the overall vascularization of the labyrinth is reduced [51]. These findings help to define the ability of Esx1to regulate the vascularization of the placental labyrinth.

Another mouse model associated with placental insufficiency and abnormal labyrinth morphology is the BPH/5 mouse model of preeclampsia. The BPH/5 mouse has been developed by Robin Davisson's lab here at Cornell University. The phenotype for this mouse was originally discovered while searching for a suitable model of hypertension. At E12.5 the BPH/5 mouse exhibits reduced and irregular fetal blood vessel branching within the labyrinth layer and an overall reduction in expansion of the labyrinth compared to C57 control mice [52]. It is unknown whether failure in the expansion of the labyrinth layer dictates the other classic preeclamptic phenotypes, including spontaneous late gestational hypertension and intrauterine growth restriction found in this mouse model. To date, not a single gene or subset of genes has been deemed responsible for any phenotype including abnormal labyrinth morphogenesis observed in the BPH/5 mouse. A more in depth discussion of the BPH/5 mouse will follow below.

These studies from mice indicate a complex organization of genes involved in the development of the fetal-derived labyrinth vasculature. The dependence of this organization on genetic contributions, numerous signaling pathways and potentially, other external signals, is clearly closely regulated. Aberrant expression of any one labyrinthine vascularization contributor may result in placental insufficiency and compromised fetal health.

7 External Factors Affecting Placental Function

Disease states such as intrauterine fetal growth retardation (IUGR) and preeclampsia can arise due to a number of factors including abnormal placentation caused at least in part by aberrant gene expression, as described above, an imbalance of angiogenic potential and oxidative stress caused by an inappropriate accumulation of reactive oxygen species. The following sections of Chapter 1 provide some important examples of mechanisms associated with placental dysfunction leading to fetal distress and failed pregnancies.

Barker and colleagues carried out a key study, which provided the field of placental dysfunction novel insights into the potential link between maternal metabolic well-being, placental growth abnormalities and risk associated with adult onset of disease. This longitudinal study examined weight and placental size at birth of 449 fetuses and those measurements were correlated with adult blood pressure at ~50 years of age. Examination of the data revealed adult mean systolic pressure rose by 15 mm Hg as placental weight increased from less than or equal to 1 lb to greater than 1.5 lb. Further, blood pressure fell by 11mm Hg as birth weight increased from less than or equal to 5.5 lb to greater than 7.5 lb. In general, these correlations suggest that the highest blood pressure found in these adults was associated with a low birth weight

and relatively large placentas [53]. The findings from this study suggest altered placentation may lead to an abnormal fetal circulatory adaptation, and ultimately present as hypertension in the adult. Further studies have analyzed this same theory of fetal programming within the uterus due to maternal well-being in the context of type 2 diabetes [54]. These findings indicate the same trend of adult onset of disease that was found in the hypertension study. This theory of intrauterine fetal programming based on maternal well-being became known as the "Barker hypothesis", and provides the basis for our understanding of the critical role maternal health may have, not only on the fetus during development, but also the major repercussions that may occur well into adult life. As such, any placental dysfunction has the unique ability to not only affect fetal well-being during gestation but increase the "risk" of that fetus to some adult diseases.

8 Placental Dysfunction in Preeclampsia

Preeclampsia affects 5-10% of all pregnancies worldwide and is responsible for both maternal and neonatal morbidity and mortality. This disease is characterized by a late gestational onset of maternal hypertension and proteinuria [55 56]. Preeclampsia is also frequently related to maternal edema and hyperuricemia, which is a high level of uric acid in the blood. Hemolytic anemia Elevated Liver enzymes and Low Platelet count or HELLP syndrome is also frequently associated with preeclampsia. Although the symptoms of preeclampsia have been well characterized, the causes of this disease are unknown. Several studies indicate that generalized endothelial dysfunction, along with placental and maternal accumulation of free radicals, may promote a cycle of events that account for a majority of the clinical aspects of preeclampsia. The relevance of preeclampsia to this dissertation comes

from recent observations that in the Dlx3 null mouse model, misregulation of placental morphogenesis occurs concurrent with reduced expression of placental growth factor, a key marker of preeclampsia [57]. Moreover, studies reported in this dissertation reveal that in a mouse model of preeclampsia, Dlx3 and several key Dlx3 target genes are mis-expressed early in gestation in the BPH/5 mouse supporting the possibility that the Dlx3 gene network may be playing an important role in early genetic determination of this disease. The following sections provide an overview of key features of placental dysfunction during preeclampsia.

8.1 Endothelial Cell Dysfunction in Preeclampsia

Data reported from several laboratories indicates that preeclampsia is a maternal response to a generalized endothelial cell dysfunction. Increased circulating fibronectin, factor VIII antigen, and thrombomodulin, which are all markers of endothelial cell injury, have been found in preeclamptic patients [55,58]. A decreased production of endothelial-derived vasodilators such as prostacyclins, increased production of endothelins and enhanced vascular reactivity to angiotensin II also suggests abnormal endothelial function during preeclampsia [56]. Additionally, misregulation of vascular endothelial growth factor (VEGF) in maternal circulation has also been linked to the pathogenesis of preeclampsia. VEGF is an endothelial-specific mitogen that promotes angiogenesis and its activities are mediated primarily by interaction with two high-affinity cell surface receptor tyrosine kinases: kinase-insert domain region (KDR) and fms-like tyrosine kinase-1 (Flt-1) [55,59]. Alternative splicing of Flt-1 leads to an endogenously secreted soluble protein, sFlt-1, which lacks the cytoplasmic and transmembrane domain of the full length receptor, but maintains the ligand-binding domain [60]. sFlt-1 can antagonize not only circulating VEGF, but

also placental growth factor (PGF) by binding to these molecules in circulation and preventing their interactions with endogenous receptors located in the placental vasculature. PGF is another member of the VEGF family that is placentally derived and predominately acts to promote angiogenesis in the placenta. Karumanchi and colleagues have recently reported that in a nested case-control study of preeclamptic and control patients, serum concentrations of sFlt-1 are increased, while levels of PGF are markedly reduced providing important biomarkers with predictive value in the subsequent development of preeclampsia [59,61]. Consistent with these observations, the BPH/5 mouse displays abnormal endothelial cell function and secretion of pro-angiogenic factors such as VEGF and PGF. Close examination of E10.5 decidual vessels in the BPH/5 placentas reveal narrowed lumens and indicate a thickened arterial wall, in contrast to the open lumens and thin arterial walls of C57 control mouse placentas [52]. These data suggest that maternal spiral artery remodeling may be disrupted in the BPH/5 model.

Although preeclampsia is clearly a multi system disease, endothelial cell dysfunction appears to play a major role in the phenotype. The differential patterns of angiogenic factor(s) expression found in human PE, in conjunction with the abnormal placental morphology in the BPH/5 mouse, strongly indicate the role of endothelial cell dysfunction in the pathophysiology responsible for preeclampsia.

8.2 Contribution of Fetal and Maternal Free Radicals in Preeclampsia

In some reports, the pathology associated with preeclampsia may be accounted for by an increase in placental and maternal free radicals during gestation. A free radical is any molecule containing one or more unpaired electron [62]. Free radicals are part of a broader category of reactive oxygen species (ROS), which include oxygen-

containing free radicals, like hydroxyl radical (HO•), superoxide anion radical (O_2•-), and nitric oxide (NO•). ROS also consist of reactive molecules that do not contain unpaired electrons, such as hydrogen peroxide (H_2O_2), hypochlorous acid (HOCl), and peroxynitrite anion (ONOO-). ROS can function as signal transducers in normal physiological states [62], but overproduction of ROS can result in numerous health problems including atherosclerosis, ischemic heart disease, cancer, diabetes, preeclampsia, and neurodegenerative diseases such as Alzheimer's disease, Parkinson's disease, and Huntington's disease [63].

Preeclampsia has been characterized by distinct pathological lesions of the decidual arterioles, known as acute atherosis [64]. More specifically, the ROS associated with nitrotyrosine was detected by immunostaining around foam cells in human placenta atherosclerotic lesions [65]. This condition may be due to an increase in ROS caused by lipid peroxidation or nitrotyrosine formation, or a decrease in superoxide dismutase (SOD) expression and activity. SOD's are responsible for converting ROS into hydrogen peroxide, where cellular components such as catalase can convert it into oxygen and water. Two different SOD isoforms have been identified in the placenta in response to antioxidant therapy, mitochondrial (Mn)SOD isoform and cytosolic Cu,Zn-SOD isoform. The Mn SOD isoform is expressed in the syncytiotrophoblast cells and in villous vascular endothelium. While the cytosolic Cu,Zn-SOD isoform is expressed primarily in the villous stroma [66]. The two different SOD isoforms found in different cell types in the placenta, as a result of antioxidant therapy, may indicate different SOD requirements of specific cell types or the SOD expression is a direct correlation to the degree of placental oxygenation [67].

Several studies have investigated the contribution of natural antioxidants, such as vitamins C and E, in the maternal diet, on the occurrence of preeclampsia. While potentially exciting, the overall effect(s) of antioxidant therapy on the incidence of

preeclampsia has been controversial and inconsistent [68]. This inconsistency in response to antioxidant therapy may be attributed to a particular critical time frame of antioxidant administration. Antioxidants administered during preconception and early gestation may be key for counterbalancing abnormal oxidative stress associated with the onset of preeclampsia [69]. Any placental "insult" including abnormally high levels of ROS within the developing placenta during this timeframe may lead to abnormal placentation and potentially direct effects on fetal growth.

Antioxidant therapy using the SOD mimetic, Tempol, in the BPH/5 mouse model of preeclampsia has demonstrated positive effects. Chronic administration of Tempol to BPH/5 mice throughout gestation significantly improved fetal growth and survival. Further, Tempol administration ameliorated pregnancy-induced maternal hypertension and proteniuria in this model. Tempol therapy normalized levels of ROS in all placental zones in the BPH/5 mouse placenta [70]. Using the BPH/5 mouse as a model for preeclampsia indicates the potential benefits of antioxidant therapy on maternal and fetal health during preeclampsia. A more in depth analysis of the possible benefits of antioxidant therapy on the Dlx3 mouse model will be discussed in Chapter 4.

9 Distal-less (Dlx) 3 Mouse Model of Placental Insufficiency

The Roberson lab became interested in the transcription factor Distal-less (Dlx) 3 when examining transcriptional mechanisms associated with the control of the glycoprotein hormone α subunit gene in placental trophoblasts [71]. The α subunit is a key subunit for chorionic gonadotropin (CG) expressed in the primate placenta. Dlx3 was identified as a key transcriptional regulator of the α subunit by virtue of its binding to the junctional regulatory elements within the promoter region of this gene.

Loss of Dlx3 function in choriocarcinoma cells results in diminished expression of the α subunit [71]. Studies of human placental section obtained from pregnancies terminated at 8 weeks gestation suggest that in humans, Dlx3 is expressed in cyto- and syncytiotrophoblasts at the time of peak CG production [72]. These studies support speculation that Dlx3 may be playing a key role in the regulation of expression of CG subunits, thus aiding in maintenance in maternal recognition of pregnancy in women. Dlx3 null mouse dies mid-gestation ~ E 9.5 due to placental insufficiency [22]. More specifically, Dlx3 is expressed largely within trophoblasts of the labyrinth and Dlx3 null placentas lack expansion in the labyrinth layer of the placenta [23]. The gene profile associated with the Dlx3 mouse model may give insight into the placental insufficiency exhibited in preeclampsia and other placental diseases. The features of the Dlx3 gene network will be described in more detail below.

9.1 Dlx Family Members

Dlx3 is one of a six-member (Dlx1-6) Distal-less family of homeodomain-containing transcription factors [73]. Dlx proteins are homologs of *Drosophila* Distal-less (Dll) genes; in flies, Dll appears to contribute to limb specification and development [74]. Loss of Dll function results in a homeotic change in the identity of ventral appendages (for example, legs and antennae) resulting in the loss of the appendage [74]. Both mouse and human Dlx genes are found in three convergently transcribed pairs linked to Hox clusters. Hox genes are critical in embryonic development for the proper number and placement of embryonic segment structures (such as legs, antennae, and eyes) [75]. In both humans and mice, Dlx1 and Dlx2 are linked to the Hoxd cluster, Dlx3 and Dlx4 are linked to the Hoxb cluster and Dlx5 and Dlx6 are linked to Hoxa cluster [22,73]. The distinct clustering pattern of Dlx and Hox

genes suggest important relationships between the two classes of homeobox genes in the developmental processes they control.

9.2 Dlx3 Expression Pattern

Dlx genes are expressed primarily in the forebrain, branchial arches, and tissues derived from the epithelial/mesenchymal interactions during development [22,73]. More specifically, Dlx3 is expressed in hair follicles, tooth germ, branchial arch mesenchyme, and in the interfollicular epidermis [76]. Dlx3 also functions in the normal differentiation of mammalian epidermis. Ectopic expression of Dlx3 in the basal layer of mouse epidermis resulted in cessation of proliferation and the activation of profilaggin, a late differentiation marker of keratinocytes, resulting in the transformation of basal cells into more differentiated keratinocytes [77]. The profilaggin gene has a Dlx3 binding site located in the 5' regulatory region and Dlx3 has been shown to be a positive transcriptional regulator of this structural protein [77]. Interestingly, Dlx3 and Dlx4 expression is both spatially and temporally separate from other Dlx genes. As outlined above, mammalian Dlx genes are arranged in distinct bigene clusters (Dlx1/Dlx2, Dlx5/Dlx6, Dlx3/Dlx4, formally known as Dlx7) and exhibit nested patterns of expression in developing visceral branchial arches. Each bigene cluster is under different regulatory mechanisms. Ruddle and colleagues have demonstrated that the 245 bp enhancer element located in the intercistronic region of the Dlx3-4 cluster, whose DNA sequence is highly conserved between mice and humans, and can regulate a visceral branchial arch specific expression pattern of the Dlx3 gene [78]. Despite the observation that both Dlx3 and 4 are expressed within the placental in mice and humans, the precise role of this intercistronic regulatory region within the Dlx3/4 cluster in the placenta is currently not known.

In humans, the aberrant expression of Dlx3 is of clinical significance leading to two known disease states: tricho-dento-osseous (TDO) syndrome [76,79] and Amelogenesis imperfecta (AI) [80]. TDO is inherited as an autosomal dominant trait leading to tooth defects, kinky hair at birth and craniofacial bone abnormalities; it is characterized by a four-nucleotide deletion downstream of the DNA-binding homeodomain, resulting in a premature truncation of the protein. Similarly, AI shares characteristics associated with TDO and is the result of a two nucleotide deletion that causes a frameshift, altering the last two amino acids of the DNA-binding homeodomain, resulting in a premature truncation of the protein [80]. Interestingly, there have been no reports regarding the incidence of failed pregnancy outcomes in TDO or AI patients. This may not be unexpected since these Dlx3 mutations are thought to result in a partial loss of function rather than complete cessation of Dlx3 activity. Moreover, TDO and AI are exceedingly rare disorders leaving open the question of the role of these Dlx3 mutations on placental function and pregnancy outcomes.

9.3 Dlx3 Transcriptional Activity

The DNA-binding homeodomain of Dlx3 is similar to many other transcription factors in that it displays high affinity for a core TAATT DNA-binding motif indicating that it can recognize specific sequences and function as a transcriptional activator or a repressor depending on cell type and physiological state. The full consensus DNA-binding sequence of Dlx3, (A/C/G)TAATT(G/A)(C/G), has been shown by our lab as a cis-acting element necessary for the transactivation of the promoter for the human α subunit gene of chorionic gonadotropin hormone [71]. In most cases, Dlx3 functions as a cell-type-specific transcriptional activator in placental

trophoblast cells. However, Dlx3 has also been shown to repress pan neural markers in the anterior neural plate in the developing *Xenopus* embryo [81]. Therefore, the functional outcome of the transcriptional activity of Dlx3 may depend on not only cell context and physiological state, but also the availability of heterodimeric binding partners, which may have positive or negative transcriptional activities. One of the key questions examined in the research outlined in the dissertation focuses on Dlx3 binding partners and how these putative interacting partners influence transaction potential in placental trophoblasts.

9.4 Identification of the Dlx3 gene network

In placental cells, the research from the Roberson lab suggests that Dlx3 is largely playing a transcription stimulating role in trophoblasts. To more fully investigate the Dlx3 gene network, our lab set out to use microarray analyses to examine changes in transcript abundance within the placental disk, specifically comparing $Dlx3^{+/+}$ and $Dlx3^{-/-}$ placentas at E9.5. These genes were identified by gene profiling analysis using an Affymetrix microarray. Results revealed 401 genes that were differentially expressed and the signal-log-ratio absolute value of 33 genes was higher or lower than 0.5 when compared to the wildtype mouse placenta [57]. The genes were subjected to gene network analysis revealing two interrelated gene networks that were strongly impacted by the loss of Dlx3; a cell-to-cell signaling and interaction gene network and a network composed of genes related to hematological disease. Several important molecules emerged from this analysis. As indicated earlier, PGF transcript levels were markedly reduced with the loss of Dlx3 suggesting a potential transcriptional role in the regulation of the PGF gene. A second important molecule discovered in the cell-to-cell signaling interaction network was matrix

metalloproteinase-9 (MMP-9), a proteinase involved in extracellular matrix (ECM) remodeling. Both microarray analysis and subsequent validation by qRT-PCR demonstrated that the expression of MMP-9 mRNA was reduced in the $Dlx3^{-/-}$ mouse placenta [57]. Studies described in this dissertation take advantage of the data obtained from the array analyses and use MMP-9 gene expression as a model system for how Dlx3 can serve as a transcriptional activator in placental cells. Moreover, our studies suggest that both Dlx3 and MMP-9 are misregulated in a mouse model of preeclampsia, leaving open the question of the role of Dlx3 and the Dlx3 gene network in regulation of disease progression during preeclampsia. The following sections help to frame the background of how MMP-9 (as well as other MMPs) aid in regulating placental morphogenesis.

10 The Role of MMPs in Placental Development

As indicated above, maternal vascular remodeling is essential for proper perfusion of the developing placental vascular bed. This process is dependent on the invasion of cytrotrophoblasts through the ECM of the maternal decidua. Ultimately this process results in the remodeling of the maternal spiral arteries and sustained blood flow into the intervillious space [82]. MMPs appear to play a key role in this process. The placental abnormalities exhibited in the Dlx3 mouse model and a link between aberrant Dlx3 expression and MMP-9 transcript levels indicate the potential role of MMP-9 in the gene profile associated with the pathophysiology of placental insufficiency in the Dlx3 null mouse model.

10.1 Matrix Metalloproteinase-9 (MMP-9) Function

MMP-9 is a member of the zinc-dependent proteinase family known for their ability to degrade ECM [83]. Early studies provide evidence that MMP-9 degrades denatured collagens and basement membrane components [84]. More recently, MMP-9 is has been shown to cleave fibrin [85], serpin α_1-proteinase inhibitor [86], interleukin-1β (IL-1β) [87], and transforming growth factor-β (TGF-β) [88] revealing the involvement of MMP-9 in many processes including tissue remodeling, inflammatory responses, and metastasis in the progression of cancer. Pro-inflammatory cytokines such as tumor necrosis factor-α (TNF-α) and IL-1β selectively up-regulate the expression of MMP-9 in macrophages [89]. However, TGF-β has been shown to have an inhibitory effect on several members of the MMP family, including MMP-1, MMP-3 and MMP-9 in fibroblasts [90]. Studies from Chen and colleagues indicate that a nuclear factor-κB (NF-κB) site is responsible for the suppressive activity of TGF-β in the regulation of MMP-9 gene transcription [91]. As indicated above, the Ets family of transcription factors also governs MMP-9 transcriptional activity. For example, reporter transfection assays revealed epidermal growth factor (EGF) activation of MMP-9 gene promoter required Ets-1 and Ets-2 [92]. Together these findings indicating there are numerous pathways responsible for the expression and activity of MMP-9.

10.2 Matrix Metalloproteinase-9 (MMP-9) Contribution(s) to Preeclampsia

The exact role MMP-9 plays in the pathophysiology of preeclampsia remains unclear and somewhat controversial. In normal placental development, MMP-9 functions to degrade various components of the extracellular matrix (ECM) including type IV, V, VII and X collagens, fibronectin, and gelatin [93]. Degradation of these ECM components is necessary for proper remodeling of the maternal spiral arties from

high-resistance, low capacity arteries to low-resistance, high capacity venous-like structures [82,94] to facilitate proper placental profusion [95].

Extravillous trophoblast invasion of maternal spiral arteries is a multistep process. This process first requires proteolytic degradation of decidual/endothelial ECM followed by active cell migration through the degraded matrix [96]. Briefly, MMP-2 and MMP-9 are secreted as latent enzymes and are activated outside invading fetal trophoblast cells where their activity is further regulated by tissue inhibitors of metallopeptidases (TIMP) 1, 2, and 3 [97]. Cell adhesion molecules, particularly integrins, play an important role in the transformation of extravillous trophoblasts from stationary to mobile [98]. During the invasion process, key receptors are upregulated or down regulated by the invading extravillous trophoblasts. For example, invasion into the maternal decidua requires downregulation of ITGA6B4 (a laminin receptor), but upregulation of ITGA5B1 (a fibronectin receptor) and ITGA1B1 (a laminin/collagen receptor) [99].

As integral components to the extravillous trophoblast invasion process, MMP-9 and family member MMP-2 are expressed in invasive extravillous trophoblasts. Increased secretion of MMP-9 and MMP-2 have also been detected in intrauterine tissue at parturition in several species including humans and rats [100]. Interestingly, several studies indicate decreased MMP-9 mRNA expression [101] and immuno-staining [102] in human preeclamptic placentas.

Despite these findings, other studies indicate no difference in MMP-2 and MMP-9 expression levels in normal pregnancies compared to pregnancies complicated by preeclampsia. For example, specific immuno-capture assays examining placental bed biopsies revealed no change in MMP-2 and MMP-9 transcript levels across normal and complicated pregnancies [93]. Additionally, human plasma examined from normal and pregnancies complicated by preeclampsia again found no difference in

MMP-9 levels [103]. A more in depth discussion of MMP-9, its relationship to Dlx3 and its potential role in the pathophysiology of abnormal placentation related to the Dlx3 mouse model and preeclampsia will follow in Chapter 3.

11 Imaging of Placental Vasculature

Central to the studies described in Chapter 4 in this dissertation is the ability to visualize placental vasculature in the healthy and diseased state. As such, some preliminary discussion regarding vascular imaging is warranted here to set the framework for my later discussion of imaging in Chapter 4 and reflect efforts to develop novel and innovative methodologies for vascular imaging within the mouse placenta.

11.1 Historical Imaging Tools

Traditionally, placental vasculature has been imaged in a fixed state with the aid of latex/plastic casts and analyses of structure using an electron microscopy. In what is now considered one of the most important papers on placental vasculature in mice, Adamson and colleagues [5] prepared vascular casts of mouse placenta from E10.5 to term and found remarkable changes in placental vascular morphology throughout gestation. For example, maternal arteries carrying maternal blood into the uterus branched into 5-10 dilated maternal spiral arteries. The endothelial-lined spiral arteries converge into a small set of vascular channels at the trophoblast giant cell layer and carry maternal blood directly to the base of the placenta. Maternal blood was then found to flow through the intervillous spaces of the labyrinth layer towards the maternal side of the placenta, countercurrent to the direction of the fetal capillary blood flow.

Trophoblast cells from the early embryo were found to invade the uterus in two distinct patterns. Trophoblast giant cells expressing the proliferin gene invaded following implantation in a pattern associated with remodeling the maternal spiral arteries. Dilation of the spiral arteries was obvious between E10.5 and E14.5. Meanwhile, the second pathway detected trophoblast cell invasion after E12.5, invading the interstitial spaces within the labyrinth layer [5]. Most importantly, Adamson and colleagues found that the transition from endothelial-lined maternal artery to trophoblast-lined blood spaces is associated with the invasion of trophoblast giant cells [5]. Although this imaging technique has led to a novel view of the placental vascular beds, the static nature of these images does not allow for complete spatial and temporal resolution of placental vasculature.

11.2 Advancements in Imaging Techniques

11.2.1 2-Photon Excited Fluorescence Microscopy

Advancements in imaging capabilities have allowed for greater resolution of vasculature. One such innovative technique is 2-photon excited fluorescence microscopy (2PE). Briefly, a femtosecond laser is tightly focused inside a specimen that has been labeled with a fluorescent molecule (ie GFP); at the focus of the laser beam, the intensity can become high enough to induce two-photon excitation of the fluorescent molecule. Due to the non-linear excitation, the resulting fluorescence is only produced in the focal volume where the laser intensity is the highest. 2PE excitation is spatially localized due to the dependence of two photons arriving at the same time for excitation to occur. Moreover, the fluorescence depends on the square of the intensity, rather than it being linearly proportional, as in the case of one-photon excitation. After exciting fluorescent molecules at one location, the laser beam raster

scans the entire surface of the specimen resulting in a three-dimensional map representing the distribution of the fluorescently labeled tissue. Additionally, because 2PE occurs only at the focus of the laser, sample artifacts due to photobleaching and photo-damage of the tissues are negligible compared to linear imaging tools [104].

2PE also allows for imaging depths up to 500μm as shown in brain, skin, and kidney without the loss of image resolution [105]. More recent studies have shown the capability of reaching an imaging depth of 1mm in *in vivo* imaging of adult mouse brains at 1280 nm with approximately 1-nJ pulse energy at the sample surface [106]. Further, 2PE allows for quantification of the velocity of red blood cells (RBC) *in vivo* [107]. This method has recently been used to quantify blood flow changes in rat cortex following optically induced microstrokes [108]. 2PE also has the capability to capture live cells as demonstrated in the imaging of *Drosophila* embryonic neural stem cells by Rebollo and colleagues [109]. Additionally, 2PE live cell imaging has advanced the understanding of sensory axon regeneration in live transgenic zebrafish embryos expressing green fluorescence protein (GFP) driven by a sensory neuron specific promoter [110]. 2PE has the potential to surpass previous vascular casting techniques, allowing for microscopic definition of placental vasculature and the ability to image in real time.

11.2.2 Micro-computed Tomography (micro-CT)

Another breakthrough in vascular imaging capabilities has come by way of utilizing micro-computed tomography (micro-CT). Higher spatial and temporal resolutions are key technical advancements to obtain quantitative three-dimension (3D) vascular reconstructions such as with mouse placental vasculature. This technique is used and discussed in studies outlined in Chapter 4 of this dissertation.

Essentially micro-CT, much like tomography (CT), utilizes X-rays to create cross-sections of a 3D object that will later be analyzed by computer software to render a virtual image in the x, y and z planes. The term "micro" indicates the micrometer range of the pixels representing the cross-sections. Generally, there are two different principle constructions of micro-CT scanners. The first is consistent with clinical CT scanners. For this construction, the X-ray detector is rotated around the stationary specimen [111]. The second construction principle is utilized mainly in *ex vivo* experiments. The object in this design is rotated around a stationary X-ray source. This set up allows the object to be rotated vertically [112] or horizontally [113] orthogonal to the X-ray source allowing for optimization of geometric magnification.

The first advances in micro-CT were mainly driven by a need for evaluating bone anatomy and density [114]. This technology has allowed for complex quantization of bone density [115], osteogenesis [116], osteoporosis [117], bone resorption [118], bone remodeling [119], bone regeneration [120] and many more. With the use of contrast agents, evaluation of vascular structures in small animals was made possible with micro-CT. To date numerous studies have investigated the vasculature of organ systems in healthy and diseased conditions, namely renal vasculature [107,121], hepatic vasculature [122], cerebral vasculature [123], and coronary arteries [124].

Recent work from Rennie and colleagues, has taken advantage of the ability to evaluate vascular structures using micro-CT imaging technology. By injecting a micro-CT specific compound into the placental vasculature of mice preceding micro-CT imaging, Rennie et. al. obtained surface renderings of arterial and venous placental mouse vasculature at embryonic days (E) 13.5, 15.5 and 18.5. Surface area and volume measurements were determined for vessels greater than the micro-CT machine's minimum resolvable diameter of 0.03 mm. More importantly, this imaging analysis allowed for a greater understanding of placental vasculature through

gestation. Specifically, these findings determined arterial surface area and volume were unchanged from E13.5-15.5, but increased significantly at E18.5 (to 170 ± 13mm^2 and 7.2 ± 0.8mm^2, respectively). The trend of increased diameter of venous surface areas and volumes were similar to arterial measurements, but smaller in scale [125].

Together these findings demonstrate the superb imaging potential of mouse vasculature using micro-CT analysis. Employing micro-CT imaging tools, we sought to explore the placental insufficiency associated with the Dlx3 mouse model. Chapter 4 will reveal an in depth analysis of the Dlx3 mouse placental vasculature.

12 Study Aims

Recent findings indicate that the homeodomain transcription factor, Dlx3, exhibits placental insufficiency resulting in early embryonic death [22,23]. The research presented in this dissertation examines the central hypothesis that Dlx3 and the gene targets of Dlx3 help to direct normal placental labyrinth morphogenesis in the mouse placenta. Further, misregulation of key features of this gene network appears to be correlated with changes in gene expression associated with the pathophysiology of preeclampsia in women. To further understand fundamental aspects of the molecular genetic control of placental morphogenesis by the Dlx3 gene network, a number of *in vitro* and *in vivo* studies were carried out to examine my central hypothesis. In Chapter 2, studies focus on the function of Dlx3, its interacting partners, and the effect this physical interaction has on Dlx3 function. Chapter 3 explores the link between Dlx3 and its' target gene, MMP-9. Finally, Chapter 4 reveals the effects of incremental loss of Dlx3 on fetal fitness by investigations into fetal growth patterns during gestation. This collection of studies provide a number of new insights into the

role of Dlx3 as a placental-specific transcriptional regulator and how the Dlx3 gene network may underlie important gene expression decisions that lead to preeclampsia.

REFERENCES

[1] Stallmach, T. et al., Rescue by birth: defective placental maturation and late fetal mortality. *Obstet Gynecol* **97** (4), 505 (2001).

[2] Cross, J. C., Simmons, D. G., and Watson, E. D., Chorioallantoic morphogenesis and formation of the placental villous tree. *Ann N Y Acad Sci* **995**, 84 (2003).

[3] Cross, J. C., Werb, Z., and Fisher, S. J., Implantation and the placenta: key pieces of the development puzzle. *Science* **266** (5190), 1508 (1994).

[4] Hemberger, M., IFPA award in placentology lecture - characteristics and significance of trophoblast giant cells. *Placenta* **29 Suppl A**, S4 (2008).

[5] Adamson, S. L. et al., Interactions between trophoblast cells and the maternal and fetal circulation in the mouse placenta. *Dev Biol* **250** (2), 358 (2002).

[6] Watson, E. D. and Cross, J. C., Development of structures and transport functions in the mouse placenta. *Physiology (Bethesda)* **20**, 180 (2005).

[7] Cross, J. C. et al., Genes, development and evolution of the placenta. *Placenta* **24** (2-3), 123 (2003).

[8] Rossant, J. and Cross, J. C., Placental development: lessons from mouse mutants. *Nat Rev Genet* **2** (7), 538 (2001).

[9] Guillemot, F. et al., Essential role of Mash-2 in extraembryonic development. *Nature* **371** (6495), 333 (1994).

[10] Tanaka, M., Gertsenstein, M., Rossant, J., and Nagy, A., Mash2 acts cell autonomously in mouse spongiotrophoblast development. *Dev Biol* **190** (1), 55 (1997).

[11] Adelman, D. M. et al., Placental cell fates are regulated in vivo by HIF-mediated hypoxia responses. *Genes Dev* **14** (24), 3191 (2000).

[12] Cross, J. C. et al., Hxt encodes a basic helix-loop-helix transcription factor that regulates trophoblast cell development. *Development* **121** (8), 2513 (1995).

[13] Kraut, N. et al., Requirement of the mouse I-mfa gene for placental development and skeletal patterning. *EMBO J* **17** (21), 6276 (1998).

[14] Riley, P., Anson-Cartwright, L., and Cross, J. C., The Hand1 bHLH transcription factor is essential for placentation and cardiac morphogenesis. *Nat Genet* **18** (3), 271 (1998).

[15] Scott, I. C. et al., The HAND1 basic helix-loop-helix transcription factor regulates trophoblast differentiation via multiple mechanisms. *Mol Cell Biol* **20** (2), 530 (2000).

[16] Jen, Y., Manova, K., and Benezra, R., Each member of the Id gene family exhibits a unique expression pattern in mouse gastrulation and neurogenesis. *Dev Dyn* **208** (1), 92 (1997).

[17] Morikawa, Y. and Cserjesi, P., Extra-embryonic vasculature development is regulated by the transcription factor HAND1. *Development* **131** (9), 2195 (2004).

[18] Stepan, H. et al., Structure and regulation of the murine Mash2 gene. *Biol Reprod* **68** (1), 40 (2003).

[19] Yamamoto, H. et al., Defective trophoblast function in mice with a targeted mutation of Ets2. *Genes Dev* **12** (9), 1315 (1998).

[20] Van den Steen, P. E. et al., Biochemistry and molecular biology of gelatinase B or matrix metalloproteinase-9 (MMP-9). *Crit Rev Biochem Mol Biol* **37** (6), 375 (2002).

[21] Roth, I. and Fisher, S. J., IL-10 is an autocrine inhibitor of human placental cytotrophoblast MMP-9 production and invasion. *Dev Biol* **205** (1), 194 (1999).

[22] Morasso, M. I. et al., Placental failure in mice lacking the homeobox gene Dlx3. *Proc Natl Acad Sci U S A* **96** (1), 162 (1999).

[23] Berghorn, K. A. et al., Smad6 represses Dlx3 transcriptional activity through inhibition of DNA binding. *J Biol Chem* **281** (29), 20357 (2006).

[24] Gardner, R. L., Papaioannou, V. E., and Barton, S. C., Origin of the ectoplacental cone and secondary giant cells in mouse blastocysts reconstituted from isolated trophoblast and inner cell mass. *J Embryol Exp Morphol* **30** (3), 561 (1973).

[25] Jenkinson, E. J. and Billington, W. D., Differential susceptibility of mouse trophoblast and embryonic tissue to immune cell lysis. *Transplantation* **18** (3), 286 (1974).

[26] Rossant, J. and Ofer, L., Properties of extra-embryonic ectoderm isolated from postimplantation mouse embryos. *J Embryol Exp Morphol* **39**, 183 (1977).

[27] Feldman, B. et al., Requirement of FGF-4 for postimplantation mouse development. *Science* **267** (5195), 246 (1995).

[28] Rappolee, D. A., Basilico, C., Patel, Y., and Werb, Z., Expression and function of FGF-4 in peri-implantation development in mouse embryos. *Development* **120** (8), 2259 (1994).

[29] Niswander, L. and Martin, G. R., Fgf-4 expression during gastrulation, myogenesis, limb and tooth development in the mouse. *Development* **114** (3), 755 (1992).

[30] Wilder, P. J. et al., Inactivation of the FGF-4 gene in embryonic stem cells alters the growth and/or the survival of their early differentiated progeny. *Dev Biol* **192** (2), 614 (1997).

[31] Nichols, J. et al., Formation of pluripotent stem cells in the mammalian embryo depends on the POU transcription factor Oct4. *Cell* **95** (3), 379 (1998).

[32] Luo, J. et al., Placental abnormalities in mouse embryos lacking the orphan nuclear receptor ERR-beta. *Nature* **388** (6644), 778 (1997).

[33] Widmann, C., Gibson, S., Jarpe, M. B., and Johnson, G. L., Mitogen-activated protein kinase: conservation of a three-kinase module from yeast to human. *Physiol Rev* **79** (1), 143 (1999); Pearson, G., English, J. M., White, M. A., and Cobb, M. H., ERK5 and ERK2 cooperate to regulate NF-kappaB and cell transformation. *J Biol Chem* **276** (11), 7927 (2001).

[34] Whitmarsh, A. J. and Davis, R. J., Analyzing JNK and p38 mitogen-activated protein kinase activity. *Methods Enzymol* **332**, 319 (2001); Bliss, S. P. et al., ERK signaling in the pituitary is required for female but not male fertility. *Mol Endocrinol* **23** (7), 1092 (2009).

[35] Saba-El-Leil, M. K. et al., An essential function of the mitogen-activated protein kinase Erk2 in mouse trophoblast development. *EMBO Rep* **4** (10), 964 (2003).

[36] Georgiades, P., Ferguson-Smith, A. C., and Burton, G. J., Comparative developmental anatomy of the murine and human definitive placentae. *Placenta* **23** (1), 3 (2002).

[37] Reynolds, L. P. et al., Animal models of placental angiogenesis. *Placenta* **26** (10), 689 (2005).

[38] Pijnenborg, R. et al., Placental bed spiral arteries in the hypertensive disorders of pregnancy. *Br J Obstet Gynaecol* **98** (7), 648 (1991).

[39] McFadyen, I. R., Price, A. B., and Geirsson, R. T., The relation of birthweight to histological appearances in vessels of the placental bed. *Br J Obstet Gynaecol* **93** (5), 476 (1986).

[40] Cox, B. et al., Comparative systems biology of human and mouse as a tool to guide the modeling of human placental pathology. *Mol Syst Biol* **5**, 279 (2009).

[41] Yang, J. T., Rayburn, H., and Hynes, R. O., Embryonic mesodermal defects in alpha 5 integrin-deficient mice. *Development* **119** (4), 1093 (1993).

[42] Fujiwara, T., Dehart, D. B., Sulik, K. K., and Hogan, B. L., Distinct requirements for extra-embryonic and embryonic bone morphogenetic protein 4 in the formation of the node and primitive streak and coordination of left-right asymmetry in the mouse. *Development* **129** (20), 4685 (2002); Ying, Y. and Zhao, G. Q., Cooperation of endoderm-derived BMP2 and extraembryonic ectoderm-derived BMP4 in primordial germ cell generation in the mouse. *Dev Biol* **232** (2), 484 (2001).

[43] Solloway, M. J. and Robertson, E. J., Early embryonic lethality in Bmp5;Bmp7 double mutant mice suggests functional redundancy within the 60A subgroup. *Development* **126** (8), 1753 (1999).

[44] Gurtner, G. C. et al., Targeted disruption of the murine VCAM1 gene: essential role of VCAM-1 in chorioallantoic fusion and placentation. *Genes Dev* **9** (1), 1 (1995).

[45] Yang, J. T., Rayburn, H., and Hynes, R. O., Cell adhesion events mediated by alpha 4 integrins are essential in placental and cardiac development. *Development* **121** (2), 549 (1995).

[46] Hunter, P. J. et al., Mrj encodes a DnaJ-related co-chaperone that is essential for murine placental development. *Development* **126** (6), 1247 (1999).

[47] Anson-Cartwright, L. et al., The glial cells missing-1 protein is essential for branching morphogenesis in the chorioallantoic placenta. *Nat Genet* **25** (3), 311 (2000).

[48] Xu, X. et al., Fibroblast growth factor receptor 2 (FGFR2)-mediated reciprocal regulation loop between FGF8 and FGF10 is essential for limb induction. *Development* **125** (4), 753 (1998).

[49] Hughes, M. et al., The Hand1, Stra13 and Gcm1 transcription factors override FGF signaling to promote terminal differentiation of trophoblast stem cells. *Dev Biol* **271** (1), 26 (2004).

[50] Li, Y., Lemaire, P., and Behringer, R. R., Esx1, a novel X chromosome-linked homeobox gene expressed in mouse extraembryonic tissues and male germ cells. *Dev Biol* **188** (1), 85 (1997).

[51] Li, Y. and Behringer, R. R., Esx1 is an X-chromosome-imprinted regulator of placental development and fetal growth. *Nat Genet* **20** (3), 309 (1998).

[52] Dokras, A. et al., Severe feto-placental abnormalities precede the onset of hypertension and proteinuria in a mouse model of preeclampsia. *Biol Reprod* **75** (6), 899 (2006).

[53] Barker, D. J., Bull, A. R., Osmond, C., and Simmonds, S. J., Fetal and placental size and risk of hypertension in adult life. *BMJ* **301** (6746), 259 (1990).

[54] Barker, D. J. et al., Type 2 (non-insulin-dependent) diabetes mellitus, hypertension and hyperlipidaemia (syndrome X): relation to reduced fetal growth. *Diabetologia* **36** (1), 62 (1993).

[55] Hsu, C. D. et al., Elevated circulating thrombomodulin in severe preeclampsia. *Am J Obstet Gynecol* **169** (1), 148 (1993).

[56] Taylor, R. N. et al., High plasma cellular fibronectin levels correlate with biochemical and clinical features of preeclampsia but cannot be attributed to hypertension alone. *Am J Obstet Gynecol* **165** (4 Pt 1), 895 (1991); Mills, J. L. et al., Prostacyclin and thromboxane changes predating clinical onset of preeclampsia: a multicenter prospective study. *JAMA* **282** (4), 356 (1999).

[57] Han, L. et al., Analysis of the gene regulatory program induced by the homeobox transcription factor distal-less 3 in mouse placenta. *Endocrinology* **148** (3), 1246 (2007).

[58] Friedman, S. A. et al., Biochemical corroboration of endothelial involvement in severe preeclampsia. *Am J Obstet Gynecol* **172** (1 Pt 1), 202 (1995).

[59] Levine, R. J. et al., Circulating angiogenic factors and the risk of preeclampsia. *N Engl J Med* **350** (7), 672 (2004).

[60] Dvorak, H. F., Vascular permeability factor/vascular endothelial growth factor: a critical cytokine in tumor angiogenesis and a potential target for diagnosis and therapy. *J Clin Oncol* **20** (21), 4368 (2002); He, H. et al., Vascular endothelial growth factor signals endothelial cell production of nitric oxide and prostacyclin through flk-1/KDR activation of c-Src. *J Biol Chem* **274** (35), 25130 (1999).

[61] Thadhani, R. et al., First trimester placental growth factor and soluble fms-like tyrosine kinase 1 and risk for preeclampsia. *J Clin Endocrinol Metab* **89** (2), 770 (2004).

[62] Halliwell, B., Gutteridge, J. M., and Cross, C. E., Free radicals, antioxidants, and human disease: where are we now? *J Lab Clin Med* **119** (6), 598 (1992).

[63] Sen, C. K. and Packer, L., Antioxidant and redox regulation of gene transcription. *FASEB J* **10** (7), 709 (1996); Schon, E. A., Mitochondrial genetics and disease. *Trends Biochem Sci* **25** (11), 555 (2000).

[64] Hubel, C. A., Oxidative stress in the pathogenesis of preeclampsia. *Proc Soc Exp Biol Med* **222** (3), 222 (1999).

[65] Roberts, L. J., 2nd and Morrow, J. D., The isoprostanes: novel markers of lipid peroxidation and potential mediators of oxidant injury. *Adv Prostaglandin Thromboxane Leukot Res* **23**, 219 (1995).

[66] Myatt, L. et al., Differential localization of superoxide dismutase isoforms in placental villous tissue of normotensive, pre-eclamptic, and intrauterine growth-restricted pregnancies. *J Histochem Cytochem* **45** (10), 1433 (1997).

[67] Hempstock, J. et al., Intralobular differences in antioxidant enzyme expression and activity reflect the pattern of maternal arterial bloodflow within the human placenta. *Placenta* **24** (5), 517 (2003).

[68] Poston, L. et al., Vitamin C and vitamin E in pregnant women at risk for pre-eclampsia (VIP trial): randomised placebo-controlled trial. *Lancet* **367** (9517), 1145 (2006); Rumbold, A. R. et al., Vitamins C and E and the risks of preeclampsia and perinatal complications. *N Engl J Med* **354** (17), 1796 (2006).

[69] Catov, J. M. et al., Association of periconceptional multivitamin use and risk of preterm or small-for-gestational-age births. *Am J Epidemiol* **166** (3), 296 (2007); Myatt, L., Review: Reactive oxygen and nitrogen species and functional adaptation of the placenta. *Placenta* **31 Suppl**, S66.

[70] Hoffmann, D. S. et al., Chronic tempol prevents hypertension, proteinuria, and poor feto-placental outcomes in BPH/5 mouse model of preeclampsia. *Hypertension* **51** (4), 1058 (2008).

[71] Roberson, M. S. et al., A role for the homeobox protein Distal-less 3 in the activation of the glycoprotein hormone alpha subunit gene in choriocarcinoma cells. *J Biol Chem* **276** (13), 10016 (2001).

[72] Berghorn, K. A. et al., Developmental expression of the homeobox protein Distal-less 3 and its relationship to progesterone production in mouse placenta. *J Endocrinol* **186** (2), 315 (2005).

[73] Feledy, J. A., Morasso, M. I., Jang, S. I., and Sargent, T. D., Transcriptional activation by the homeodomain protein distal-less 3. *Nucleic Acids Res* **27** (3), 764 (1999).

[74] Cohen, S. M. and Jurgens, G., Proximal-distal pattern formation in Drosophila: cell autonomous requirement for Distal-less gene activity in limb development. *EMBO J* **8** (7), 2045 (1989).

[75] Mallo, M., Wellik, D. M., and Deschamps, J., Hox genes and regional patterning of the vertebrate body plan. *Dev Biol*.

[76] Robinson, G. W. and Mahon, K. A., Differential and overlapping expression domains of Dlx-2 and Dlx-3 suggest distinct roles for Distal-less homeobox genes in craniofacial development. *Mech Dev* **48** (3), 199 (1994).

[77] Morasso, M. I., Markova, N. G., and Sargent, T. D., Regulation of epidermal differentiation by a Distal-less homeodomain gene. *J Cell Biol* **135** (6 Pt 2), 1879 (1996).

[78] Sumiyama, K. and Ruddle, F. H., Regulation of Dlx3 gene expression in visceral arches by evolutionarily conserved enhancer elements. *Proc Natl Acad Sci U S A* **100** (7), 4030 (2003); Ghanem, N. et al., Regulatory roles of conserved intergenic domains in vertebrate Dlx bigene clusters. *Genome Res* **13** (4), 533 (2003).

[79] Price, J. A. et al., Identification of a mutation in DLX3 associated with tricho-dento-osseous (TDO) syndrome. *Hum Mol Genet* **7** (3), 563 (1998); Price, J. A. et al., A common DLX3 gene mutation is responsible for tricho-dento-osseous syndrome in Virginia and North Carolina families. *J Med Genet* **35** (10), 825 (1998); Haldeman, R. J. et al., Increased bone density associated with DLX3 mutation in the tricho-dento-osseous syndrome. *Bone* **35** (4), 988 (2004).

[80] Dong, J. et al., DLX3 mutation associated with autosomal dominant amelogenesis imperfecta with taurodontism. *Am J Med Genet A* **133A** (2), 138 (2005).

[81] Feledy, J. A. et al., Inhibitory patterning of the anterior neural plate in Xenopus by homeodomain factors Dlx3 and Msx1. *Dev Biol* **212** (2), 455 (1999).

[82] Pijnenborg, R., Vercruysse, L., and Hanssens, M., The uterine spiral arteries in human pregnancy: facts and controversies. *Placenta* **27** (9-10), 939 (2006).

[83] Raza, S. L. and Cornelius, L. A., Matrix metalloproteinases: pro- and anti-angiogenic activities. *J Investig Dermatol Symp Proc* **5** (1), 47 (2000).

[84] Hibbs, M. S., Hoidal, J. R., and Kang, A. H., Expression of a metalloproteinase that degrades native type V collagen and denatured collagens by cultured human alveolar macrophages. *J Clin Invest* **80** (6), 1644 (1987).

[85] Lelongt, B. et al., Matrix metalloproteinase 9 protects mice from anti-glomerular basement membrane nephritis through its fibrinolytic activity. *J Exp Med* **193** (7), 793 (2001).

[86] Liu, Z. et al., The serpin alpha1-proteinase inhibitor is a critical substrate for gelatinase B/MMP-9 in vivo. *Cell* **102** (5), 647 (2000).

[87] Ito, A. et al., Degradation of interleukin 1beta by matrix metalloproteinases. *J Biol Chem* **271** (25), 14657 (1996).

[88] Yu, Q. and Stamenkovic, I., Cell surface-localized matrix metalloproteinase-9 proteolytically activates TGF-beta and promotes tumor invasion and angiogenesis. *Genes Dev* **14** (2), 163 (2000).

[89] Zhang, Y., McCluskey, K., Fujii, K., and Wahl, L. M., Differential regulation of monocyte matrix metalloproteinase and TIMP-1 production by TNF-alpha, granulocyte-macrophage CSF, and IL-1 beta through prostaglandin-dependent and -independent mechanisms. *J Immunol* **161** (6), 3071 (1998).

[90] Edwards, D. R. et al., Transforming growth factor beta modulates the expression of collagenase and metalloproteinase inhibitor. *EMBO J* **6** (7), 1899 (1987).

[91] Ogawa, K., Chen, F., Kuang, C., and Chen, Y., Suppression of matrix metalloproteinase-9 transcription by transforming growth factor-beta is mediated by a nuclear factor-kappaB site. *Biochem J* **381** (Pt 2), 413 (2004).

[92] Watabe, T. et al., The Ets-1 and Ets-2 transcription factors activate the promoters for invasion-associated urokinase and collagenase genes in response to epidermal growth factor. *Int J Cancer* **77** (1), 128 (1998).

[93] Huisman, M. A. et al., Matrix-metalloproteinase activity in first trimester placental bed biopsies in further complicated and uncomplicated pregnancies. *Placenta* **25** (4), 253 (2004).

[94] Zhang, J. et al., Dynamic changes occur in patterns of endometrial EFNB2/EPHB4 expression during the period of spiral arterial modification in mice. *Biol Reprod* **79** (3), 450 (2008).

[95] Gallery, E. D. et al., Preeclamptic decidual microvascular endothelial cells express lower levels of matrix metalloproteinase-1 than normals. *Microvasc Res* **57** (3), 340 (1999); Campbell, S., Rowe, J., Jackson, C. J., and Gallery, E. D., In vitro migration of cytotrophoblasts through a decidual endothelial cell monolayer: the role of matrix metalloproteinases. *Placenta* **24** (4), 306 (2003).

[96] Staun-Ram, E. and Shalev, E., Human trophoblast function during the implantation process. *Reprod Biol Endocrinol* **3**, 56 (2005).

[97] Cohen, M., Meisser, A., and Bischof, P., Metalloproteinases and human placental invasiveness. *Placenta* **27** (8), 783 (2006).

[98] Damsky, C. H. et al., Integrin switching regulates normal trophoblast invasion. *Development* **120** (12), 3657 (1994).

[99] Zhou, Y. et al., Human cytotrophoblasts adopt a vascular phenotype as they differentiate. A strategy for successful endovascular invasion? *J Clin Invest* **99** (9), 2139 (1997).

[100] Myers, J. E. et al., MMP-2 levels are elevated in the plasma of women who subsequently develop preeclampsia. *Hypertens Pregnancy* **24** (2), 103 (2005); Vadillo-Ortega, F. et al., 92-kd type IV collagenase (matrix metalloproteinase-9) activity in human amniochorion increases with labor. *Am J Pathol* **146** (1), 148 (1995); Lei, H., Vadillo-Ortega, F., Paavola, L. G., and Strauss, J. F., 3rd, 92-kDa gelatinase (matrix metalloproteinase-9) is induced in rat amnion immediately prior to parturition. *Biol Reprod* **53** (2), 339 (1995).

[101] Li, J. K., Xiong, Q., Zhou, S., and Yang, P. F., [Differences between the expression of matrix metalloproteinase-2, 9 in preeclampsia and normal placental tissues]. *Zhonghua Fu Chan Ke Za Zhi* **42** (2), 73 (2007); Qiao, C., Wang, C. H., Shang, T., and Lin, Q. D., [Clinical significance of KiSS-1 and matrix metalloproteinase-9 expression in trophoblasts of women with preeclampsia and their relation to perinatal outcome of neonates]. *Zhonghua Fu Chan Ke Za Zhi* **40** (9), 585 (2005).

[102] Shokry, M. et al., Expression of matrix metalloproteinases 2 and 9 in human trophoblasts of normal and preeclamptic placentas: preliminary findings. *Exp Mol Pathol* **87** (3), 219 (2009); Zhang, H., Lin, Q. D., and Qiao, C., [Expression of trophoblast invasion related genes mRNA and protein in human placenta in preeclampsia]. *Zhonghua Fu Chan Ke Za Zhi* **41** (8), 509 (2006).

[103] Palei, A. C., Sandrim, V. C., Cavalli, R. C., and Tanus-Santos, J. E., Comparative assessment of matrix metalloproteinase (MMP)-2 and MMP-9, and their inhibitors, tissue inhibitors of metalloproteinase (TIMP)-1 and TIMP-

2 in preeclampsia and gestational hypertension. *Clin Biochem* **41** (10-11), 875 (2008).

[104] Tsai, P. S. et al., All-optical histology using ultrashort laser pulses. *Neuron* **39** (1), 27 (2003).

[105] Schaffer, C. B. et al., Two-photon imaging of cortical surface microvessels reveals a robust redistribution in blood flow after vascular occlusion. *PLoS Biol* **4** (2), e22 (2006); Schelhas, L. T., Shane, J. C., and Dantus, M., Advantages of ultrashort phase-shaped pulses for selective two-photon activation and biomedical imaging. *Nanomedicine* **2** (3), 177 (2006); Tirlapur, U. K. et al., Femtosecond two-photon high-resolution 3D imaging, spatial-volume rendering and microspectral characterization of immunolocalized MHC-II and mLangerin/CD207 antigens in the mouse epidermis. *Microsc Res Tech* **69** (10), 767 (2006).

[106] Kobat, D. et al., Deep tissue multiphoton microscopy using longer wavelength excitation. *Opt Express* **17** (16), 13354 (2009).

[107] Kleinfeld, D., Mitra, P. P., Helmchen, F., and Denk, W., Fluctuations and stimulus-induced changes in blood flow observed in individual capillaries in layers 2 through 4 of rat neocortex. *Proc Natl Acad Sci U S A* **95** (26), 15741 (1998).

[108] Nishimura, N. et al., Targeted insult to subsurface cortical blood vessels using ultrashort laser pulses: three models of stroke. *Nat Methods* **3** (2), 99 (2006).

[109] Rebollo, E. and Gonzalez, C., Time-lapse imaging of embryonic neural stem cell division in Drosophila by two-photon microscopy. *Curr Protoc Stem Cell Biol* **Chapter 1**, Unit1H 2.

[110] O'Brien, G. S. et al., Two-photon axotomy and time-lapse confocal imaging in live zebrafish embryos. *J Vis Exp* (24) (2009).

[111] Schambach, S. J. et al., Application of micro-CT in small animal imaging. *Methods* **50** (1), 2.

[112] Schambach, S. J. et al., Vascular imaging in small rodents using micro-CT. *Methods* **50** (1), 26.

[113] Badea, C., Hedlund, L. W., and Johnson, G. A., Micro-CT with respiratory and cardiac gating. *Med Phys* **31** (12), 3324 (2004).

[114] Feldkamp, L. A. et al., The direct examination of three-dimensional bone architecture in vitro by computed tomography. *J Bone Miner Res* **4** (1), 3 (1989).

[115] Engelke, K. et al., [Micro-CT. Technology and application for assessing bone structure]. *Radiologe* **39** (3), 203 (1999).

[116] Liu, H. W. et al., Heterobifunctional poly(ethylene glycol)-tethered bone morphogenetic protein-2-stimulated bone marrow mesenchymal stromal cell differentiation and osteogenesis. *Tissue Eng* **13** (5), 1113 (2007).

[117] Borah, B. et al., Three-dimensional microimaging (MRmicroI and microCT), finite element modeling, and rapid prototyping provide unique insights into bone architecture in osteoporosis. *Anat Rec* **265** (2), 101 (2001).

[118] Freeman, T. A. et al., Micro-CT analysis with multiple thresholds allows detection of bone formation and resorption during ultrasound-treated fracture healing. *J Orthop Res* **27** (5), 673 (2009).

[119] Umoh, J. U. et al., In vivo micro-CT analysis of bone remodeling in a rat calvarial defect model. *Phys Med Biol* **54** (7), 2147 (2009).

[120] Kempen, D. H. et al., Effect of local sequential VEGF and BMP-2 delivery on ectopic and orthotopic bone regeneration. *Biomaterials* **30** (14), 2816 (2009).

[121] Garcia-Sanz, A. et al., Three-dimensional microcomputed tomography of renal vasculature in rats. *Hypertension* **31** (1 Pt 2), 440 (1998); Fortepiani, L. A. et

al., Effect of losartan on renal microvasculature during chronic inhibition of nitric oxide visualized by micro-CT. *Am J Physiol Renal Physiol* **285** (5), F852 (2003).

[122] Ananda, S. et al., The visualization of hepatic vasculature by X-ray micro-computed tomography. *J Electron Microsc (Tokyo)* **55** (3), 151 (2006).

[123] Abruzzo, T. et al., Microscopic computed tomography imaging of the cerebral circulation in mice: feasibility and pitfalls. *Synapse* **62** (8), 557 (2008).

[124] Clauss, S. B. et al., Patterning of coronary arteries in wildtype and connexin43 knockout mice. *Dev Dyn* **235** (10), 2786 (2006).

[125] Rennie, M. Y. et al., 3D visualisation and quantification by microcomputed tomography of late gestational changes in the arterial and venous feto-placental vasculature of the mouse. *Placenta* **28** (8-9), 833 (2007).

CHAPTER TWO

SMAD6 REPRESSES DLX3 TRANSCRIPTIONAL ACTIVITY THROUGH INHIBITION OF DNA BINDING

This research was originally published in Journal of Biological Chemistry. Kathie A. Berghorn*, Patricia A. Clark*, Li Han*, Michael McGrattan, Robert S. Weiss and Mark S. Roberson. Smad6 represses Dlx3 transcriptional activity through inhibition of DNA binding. *Journal of Biological Chemistry*. 2006; 281:20357-20367. * These authors contributed equally to this work.
Figure 2.1 was kindly provided by Dr. Kathie A. Berghorn. Figures 2.5-2.9 were kindly provided by Ms. Li Han.

Abstract

Dlx3 is a homeobox-containing transcription factor required for normal placental development in mice. Here we demonstrate that DLX3 interacts with SMAD6, a member of a larger family of transcriptional regulators generally thought to regulate transforming growth factor β/bone morphogenetic protein signaling. Immunocytochemical and immunoprecipitation studies demonstrate overlapping nuclear localization and physical interaction between DLX3 and SMAD6 in human choriocarcinoma cells and in differentiated trophoblasts from human placenta. *In vitro* protein interaction studies mapped the SMAD6 interaction domain within DLX3 to residues 80-163, a region of DLX3 that includes a portion of the homeodomain. DLX3 and DLX4 share homology within this region, and DLX4 was also found to bind SMAD6. Using the *Esx1* gene promoter as a model for a Dlx3-responsive gene, studies demonstrate two near consensus Dlx3 binding sites within the proximal 2.3 kb of the transcription start site. Interestingly, binding of DLX3 to one of these two sites was inhibited by interaction with SMAD6. Consistent with this result, expression of an *Esx1* promoter luciferase reporter was increased by overexpression of DLX3; this effect was reversed with co-expression of SMAD6. Further, small interfering RNA mediated knockdown of endogenous SMAD6 increased DLX3-dependent expression of the *Esx1* gene promoter. Thus, SMAD6 appears to functionally interact with DLX3, altering the ability of DLX3 to bind target gene promoters. SMAD6 appears to play a modulatory role in the regulation of DLX3-dependent gene transcription within placental trophoblasts.

Introduction

The Dlx family of transcriptional regulators includes six members in mammals, arrayed in pairs and aligned with the *Hox* gene clusters along different chromosomes [1,2]. *DLX3* is tandemly arrayed with *DLX4* on human chromosome 17 and is involved in developmental determination of multiple tissues, including the first and second branchial arches, teeth, bone, and multiple epithelia, including the skin, mammary gland primordia, and the placenta [3]. The relationship between convergently transcribed pairs of Dlx family members and specific *Hox* gene clusters has suggested that, although independent of *Hox* gene expression patterns, these homeodomain-containing transcription factors are clearly involved in important aspects of developmental morphogenesis (reviewed in Ref. [2]). The importance of Dlx3 during development and in the adult arises from several different observations of disease states. Mutations in *DLX3* are believed to be causally related to TDO, a genetic disorder manifested by taurodontism, hair abnormalities, and increased bone density in the cranium [4-6]. The defect in *DLX3* leading to TDO appears to be associated with a four-nucleotide deletion just downstream of the homeodomain, resulting in a premature truncation of the protein. AI with taurodontism has similar characteristics as TDO and has also been associated with mutations with *DLX3* in some families investigated, albeit distinct from the four nucleotide deletion/mutation described above [7]. AI is an autosomal dominant trait leading to dental enamel defects and enlarged pulp chambers and has been associated with a two-nucleotide deletion within the homeodomain of *DLX3*. This deletion again results in a frameshift and premature truncation of DLX3 in the carboxyl terminus, primarily downstream of the homeobox. In addition to TDO and AI, *Dlx3/Dlx4* have been identified in the gene interval thought to be involved in some forms of craniofacial abnormalities, including cleft

palate [8]. The putative involvement of Dlx3 in the occurrence of cleft palate is also supported by the murine model deficient in endothelin-A receptor, which results in cleft palate and hypoplasia of the mandible [9-11]. In this model, *Dlx3* expression is thought to be dependent upon endothelin-1 through a Gαq/Gα11-dependent mechanism. In the Gαq/Gα11-deficient mouse, *Dlx3*, among other factors, is specifically down-regulated, supporting the speculation of the importance of Dlx3 in cranio-facial morphogenesis [12]. Thus, the role and importance of Dlx3 in morphogenic aspects of development and in epithelial differentiated function is rather far reaching.

The *Dlx3* null mouse dies *in utero* by E10 due to putative placental failure [13]. This was associated with a failure in the development/morphogenesis of the placental labyrinth compartment of the murine placenta. Further, genetic loss of *Dlx3* was correlated with reduced expression of an additional homeobox factor, Esx1, suggesting that Dlx3 may be an important transcriptional regulator of *Esx1* promoter activity. Studies from our laboratory identified DLX3 as a cell type-specific transcriptional activator in placental trophoblasts. DLX3 binds to and transactivates the promoter for the glycoprotein hormone α subunit gene via a cis-acting element required for full basal activity of this gene [14]. The glycoprotein hormone α subunit is a subunit of the heterodimeric glycoprotein hormone, CG. Trophoblast-derived CG has been identified in primates and equine and appears to play a critical role in the maintenance of early pregnancy in women, providing early gonadotropic support to the CL and maintenance of progesterone production [15-17]. Both for the case of the α subunit promoter and regulation of *Esx1* in the *Dlx3* null mouse, Dlx3 appears to function as a putative transcriptional activator. However, it has also been proposed that Dlx3 can serve as a negative regulator of gene transcription in amphibian models [2]. This apparent activation/repression capability may be due to variable heterodimeric partners of Dlx3 (as proposed in Ref. [2]), dependent upon cell context and

physiological state. This observation was the impetus for us to examine potential binding partners of DLX3 in the context of the human placenta. The present studies identify SMAD6 as a binding partner for DLX3 using a yeast two-hybrid screen of a human term placental cDNA library. DLX3 and SMAD6 are co-localized in the nucleus of cells of trophoblast origin including cytotrophoblasts and syncytial trophoblasts from fully differentiated human term placenta. Interaction between DLX3 and SMAD6 alters the DNA binding properties of DLX3 such that SMAD6 serves as a negative regulator of DLX3-dependent gene transcription of the *Esx1* promoter.

Materials and Methods

Plasmids and cDNAs

All plasmids used in these studies were prepared by two cycles through cesium chloride using standard protocols. Expression vector for human DLX3 was generously provided by Dr. Maria Morasso (National Institutes of Health, Bethesda MD). A series of deletion mutants of the *DLX3* cDNA were constructed by PCR. To facilitate cloning into the pKH3 vector (generously provided by Dr. Jun-Lin Guan, Cornell University, Ithaca, NY), EcoR I and Cla I restriction sites were added to the forward and reverse primers, respectively. The forward primers used in these reactions were as follows: forward 1, 5'-TCAGGAAT TCAAATGAGCGGCTCCTTCGATCGC-3', forward 40, 5'-TCAGGAATTCAACTGGGC TATTACAGCGCTCCTCAG-3', forward 80, 5'-TCAGGAATTCAATACTCGCCCAAGT CGGAATATACC-3', forward 121, 5'-TCAGGAATTCAAATGGTGAACGGCAAGCCCAAAAAG-3', and forward 195, 5'-TCA GGAATTCAACTGGAACACAGCCCCAACAACAGT-3'. The reverse primers used in these reactions were as follows: reverse 128, 5'-GTACATCGATCACGGCTTTCGGACC TTCTTGGGCTTCCC-3', reverse 163, 5'-GTACATCGATCAAGCTAGCTCGGCGCGCTCAGGCAA-3', reverse 202, 5'-

GTACATCGATCAACTGTATTGGGACTGTGCTCCAG-3', and reverse 287, 5'-GTACATCGATTCAGTACACAGCCCCAGGGTT-3'. PCR products were cloned initially into the pGEM T-Easy vector (Promega Corp., Madison, WI). Once verified by nucleotide sequence analysis, fragments were subcloned into the pKH3 vector for use in studies. SMAD6 expression plasmid was a gift from Dr. Ali Hemmati-Brivanlou (The Rockefeller University, New York, NY). SMAD4 expression vector was a gift from Dr. Colin Clay (Colorado State University, Fort Collins, CO). The human *DLX4* cDNA was obtained by PCR from RNA isolated from JEG3 cells using the following primers: 5'-TCAGGAATTCAAATGACCTC TTTACCCTGTCCC-3' and 5-GTACATCGA TCACATCATCTGAGGCAG TGC-3'. The resulting *DLX4* cDNA was cloned into pKH3 and verified by nucleotide sequence analysis. *Esx1*-2.3kb promoter was obtained by PCR using mouse genomic DNA and the following primers: 5' primer (5'-GGTACCAGCACCGAGCTATCACAACCATCA-3') and 3' primer (5'-GCTAGCTACCAGCTGCTTCTCCCGTA-3'). To facilitate cloning, Kpn I and Nhe I restriction enzyme sites were engineered at the end of the 5' primer and 3' primer respectively. The PCR products were cloned into pGEM T-Easy vector. After Kpn I and Nhe I digestion, the promoter fragment was subcloned into a luciferase reporter vector. The fidelity of the construct was confirmed by nucleotide sequence analysis. PCR-based site-directed mutagenesis was used to disrupt the distal DLX3 binding site within the *Esx1* luciferase reporter. This mutation substituted a Not I restriction site for the near consensus DLX3 binding site. The mutation was confirmed using nucleotide sequence analysis. The human α subunit gene promoter luciferase reporter has been reported previously [14].

Yeast two-hybrid screen

To investigate novel protein-protein interactions, full-length DLX3 served as the bait protein with a human term placental cDNA library serving as the target. The bait, human *DLX3* cDNA was cloned into the vector pGBKT7 and transformed in the yeast strain AH109. A pretransformed human term placental Matchmaker cDNA library was in yeast strain Y187 (BD Biosciences/Clontech, Palo Alto, CA). The bait and library plasmids were expressed as GAL4 fusion proteins. 3-amino-1,2,4-triazole was titrated (5-35 mM) using the bait strain to control background yeast growth. A concentration of 12 mM 3- amino-1,2,4-triazole was used in the library screen. The bait and library strains were mated with an efficiency of approximately 4%. The bait strain required Leu^- Synthetic Dropout (SD) minimal medium, and the library strain required Trp^- SD minimal medium. Mating was carried out in YPDA media containing 0.003% adenine hemisulfate. Following mating of the bait strain with the human placental library, yeast was initially plated on medium stringency SD media ($His^-/Leu^-/Trp^-$) plates. When colonies were of sufficient size, colonies were replicate plated on high stringency SD medium ($Ade^-/His^-/Leu^-/Trp^-$/X-α-Gal) plates to verify that they maintained the correct phenotype. A colony filter lift assay was performed to access β-galactosidase activity to identify and rank the strength of potential interactions. Once identified, yeast plasmids were isolated using disruption with glass beads and plasmids rescued/purified using the Qiagen Miniprep reagents and spin column (Qiagen Inc., Valencia, CA). Identity of the rescued plasmids was verified by nucleotide sequence analysis. The interaction between DLX3 and target genes was examined using a reconstitution assay where both plasmids were co-transformed into the AH109 yeast strain and plated on high stringency SD medium.

Preparation of JEG3 cell nuclear extracts

Subconfluent JEG3 cells were used for the preparation of nuclear extracts. Cells were washed twice with ice-cold Dulbecco's Phosphate Buffered Saline (PBS; Invitrogen Corp., Carlsbad, CA). Cells were collected by scraping in ice-cold PBS supplemented with 1:1000 dilution of protease inhibitor cocktail (referred to as protease inhibitor cocktail; Sigma-Aldrich Corp., St. Louis, MO), 5 mM benzamidine, and 0.2 mM phenylmethylsulfonyl fluoride (PMSF). Cells were pelleted by centrifugation and resuspended in a hypotonic buffer consisting of 120 mM potassium chloride, 30 mM sodium chloride, 30 mM Hepes (pH 8.0), 0.3 M sucrose, protease inhibitor cocktail, 5 mM benzamidine, and 0.2 mM PMSF and allowed to swell for 15 min on ice. Cells were lysed by douncing and nuclei were isolated by layering the broken cell lysate over a sucrose cushion (0.9 M sucrose) followed by centrifugation at 2000×g for 30 min at 4˚C. The nuclear pellet was resuspended in a buffer containing 10 mM Tris (pH 7.5), 50 mM NaCl, 5% glycerol, 1 mM ethylenediamine tetraacetic acid (EDTA), protease inhibitor cocktail, 5 mM benzamidine, and 0.2 mM PMSF. Additional sodium chloride was added to a final concentration of 450 mM and nuclear proteins were extracted with constant rocking at 4˚C for 30 min. Nuclear extracts were clarified by centrifugation (85,000×g for 60 min) and the nuclear extract was stored in aliquots at –80˚C until later use. Protein concentrations of the nuclear extracts were determined by Bradford assay.

Immunoprecipitation (IP) from JEG3 nuclear extracts and Western blotting analysis

JEG3 cell nuclear extracts (200µg) were suspended in 1ml of 0.1% Triton X buffer (50 mM Tris (pH 7.6), 50 mM sodium chloride, 0.1% Triton X, protease inhibitor cocktail, 5 mM benzamidine, and 0.2 mM PMSF). To pre-clear the nuclear extracts,

protein A/G-agarose (Santa Cruz Biotechnology Inc., Santa Cruz, CA) was added to each suspension and allowed to mix for 1 h at 4˚C with gentle rocking. Following centrifugation (1200×g for 1 min) to remove protein A/G-agarose, antibodies were added at the following dilutions: normal rabbit serum at 1:1000; Dlx3 antibody at 1:1000; SMAD6 antibody (Santa Cruz Biotechnology Inc., Santa Cruz, CA) at 1:100. Following 2 h at 4˚C of gentle rocking, protein A/G-agarose (Santa Cruz Biotechnology Inc., Santa Cruz, CA) was added and allowed to mix for an additional 2 h. Complexes were then washed four times with 0.1% Triton X buffer. Samples were then suspended in an equal volume of 2×SDS loading buffer (100mM Tris (pH 6.8), 4% SDS, 20% glycerol and 200 mM dithiothreitol). Protein samples were boiled for 3 min and chilled for 5 min on ice. Proteins were resolved by SDS-polyacrylamide gel electrophoresis and transferred to polyvinylidine difluoride membranes by electroblotting. Membranes were blocked with nonfat dried milk (5%) in Tris-buffered saline [10 mM Tris (pH 7.6), 150mM sodium chloride] containing 0.1% Tween 20 (TBST). For western blots, the DLX3 antibody was used at 1:5000 in TBST, 5% nonfat dried milk. The reciprocal western blot from IPs using the SMAD6 antibody was not possible since the IP heavy chain IgG blocked visualization of SMAD6 on western blot due to similar molecular size. In other western blot studies, the SMAD6 antibody was used at 1:500 and the actin antibody (Santa Cruz Biotechnology Inc., Santa Cruz CA) was used at 1:1000 dilution. Proteins bands were visualized by chemiluminescence reagents (PerkinElmer Life Sciences, Wellesley, MA).

Immunocytochemistry

JEG3 cells were cultured on glass slides or coverslips for 24 h, rinsed one time with potassium phosphate buffered saline (KPBS), then fixed for 20 min with 4% paraformaldehyde. Slides or coverslips were then stored in 70% ethanol until used.

Prior to use, slides were rinsed in KPBS seven times over 1 hour. JEG3 cells were incubated with primary antibody (SMAD6 at 1:100; DLX3 at 1:500) overnight at 4˚C. Slides were again rinsed with KPBS followed by incubation with a fluorescent-conjugated secondary antibody (Alexa 594, Molecular Probes, Eugene OR; and Cy2, Jackson Immunoresearch Labs, Westgrove, PA) in KPBS-Triton X at 37˚C for 2 h. Cells were rinsed in KPBS, dehydrated through a graded series of ethanol, cleared with xylene and coverslips attached with Krystalon (EM Science, Gibbstown NJ).

Samples of human term placenta (derived from elective caesarian section) were obtained from Cayuga Medical Center, Ithaca, NY under the guidelines and approval of the Cornell University and the Cayuga Medical Center Committees on the Use of Human Subjects in Research. Samples were collected, fixed with 4% paraformaldehyde for 48 h and transferred to 70% ethanol until processing. Tissues were paraffin embedded and 5 μm sections were obtained. Immunocytochemistry was performed as previously described [14], except that fluorescent-conjugated secondary antibodies were used as described above.

Recombinant proteins and immuno-precipitation analysis

Recombinant SMAD6, SMAD4, DLX4, DLX3 and deletions of DLX3 were prepared using a coupled transcription and translation Wheat Germ Extract System (Promega Corp., Madison, WI) following the prescribed protocol. Proteins were radioactively labeled using ^{35}S methionine (1,000Ci/mmol at 10mCi/ml; Amersham, Piscataway, NJ). A portion (10%) of each recombinant protein was saved for input analysis. Protein combinations were added at a 1:1 (by volume) mixture to a 0.1% Triton X buffer along with appropriate antibody at specified concentrations (DLX3 at 1:1000; SMAD6, Santa Cruz Biotechnology Inc., Santa Cruz, CA at 1:100; and SMAD4, Santa Cruz Biotechnology Inc., Santa Cruz, CA at 1:500). Following 2 h of

gentle rocking at 4˚C, protein A/G-agarose (Santa Cruz Biotechnology Inc., Santa Cruz, CA) was added and allowed to mix for an additional 2 h. Complexes were then washed four times with 0.1%Triton X buffer. Proteins were resolved by SDS-polyacrylamide gel electrophoresis, the gel was fixed in 25% methanol, and 15 % glacial acetic acid for 1 h with gentle rocking at room temperature. The gel was then washed three times in 40% isopropanol solution, dried and bands visualized by autoradiography.

Electrophoretic mobility shift assay

Electrophoretic mobility shift assays (EMSA) were carried out as described previously [14,18] using the indicated antibodies. Reactions (without probe) were maintained at room temperature for 30 min followed by addition of ^{32}P-labeled oligonucleotide DLX3 binding site probes (the junctional regulatory element or JRE from the glycoprotein hormone α subunit promoter [14] and two putative DLX3 binding sites identified within the *Esx1* promoter). The binding reactions were maintained an additional 30 min then resolved on native polyacrylamide gels. To determine if SMAD6 could displace prebound DLX3 in EMSA, binding reactions containing DLX3 alone were allowed to incubate with probe for 30 min to reach equilibrium. SMAD6 protein was then added and the reactions were incubated for an additional 30 min. These reactions were compared to binding reactions where both DLX3 and SMAD6 were added together and incubated for the full 60 min. Following electrophoresis, the gels were dried and DNA-protein complexes were visualized by autoradiography. All DNA binding studies were conducted at least three times with similar results. The nucleotide sequences for probes were as follows (only one strand indicated): JRE: 5'-ACGTCATGGTAATTACACCAAG-3' Distal binding site: 5'-

ACA AGGAGCTAATTTACTTCCT-3' Proximal binding site: 5'-TTAGGGCTCTAATTCAGACTCT-3'.

Cell culture and transient transfection studies

JEG3 cells were cultured in monolayer using Dulbeco's Modified Eagle's Medium (DMEM) supplemented with 10% fetal bovine serum (FBS). Before transfection studies, cells were split to 35 mm dishes and sub-confluent cultures were used. JEG3 cells were transiently co-transfected with an *Esx1* promoter luciferase reporter construct, DLX3 expression vector at a constant dose (2.0 µg) and increasing doses of SMAD6 expression vector using lipofection (FuGENE 6 transfection reagent; Roche Diagnostics Inc., Indianapolis, IN). All transfections were carried out with a constant amount of DNA by supplementing reactions with the parent vector pKH3. Luciferase activity was determined after 24 h of transfection using reagents from the Luciferase Reporter Assay System (Promega Corp., Madison, WI), and luciferase activity was standardized by total cell protein amount (luciferase/1.0 µg) as determined by Bradford assay. All transfection studies were conducted in triplicate on at least three separate occasions with similar results. Data are shown as means (n=3) ± standard errors of the mean of a representative experiment.

Preparation of stable cell lines expressing small interference RNA (siRNA)

The mammalian expression vector, pSUPER-retro-neo (pSR; OligoEngine, Seattle, WA) was used for preparation of retrovirus containing specific siRNAs and expression of siRNAs in JEG3 cells following viral infection. Each gene-specific insert targeted a 19-nucleotide sequence within the human *SMAD6* mRNA. The siRNA sequences were as follows: *SMAD6*-#1: 5'CACATTGTCTTACACTGAA *SMAD6*-#2: 5'TCAAGGTGTTCGACTTCGA *SMAD6*-#3: 5'GCCACTGGATCTGTCCGAT The

plasmids were referred to as *SMAD6* siRNA #1, #2 and #3. A control siRNA vector (also prepared in pSR) was constructed using a 19-nucleotide sequence (5'TTCTCCGAAC GTGTCACGT) putatively without significant similarity to any mammalian gene sequence and therefore served as an appropriate negative control (OligoEngine, Seattle, WA). The forward and reverse strands of oligonucleotides containing the siRNAs and nonsense sequence also contained Bgl II and Hind III sites at the 5'end of the forward and reverse oligonucleotides, respectively. The oligonucleotides were annealed and inserted into the pSR vector after digestion of the vector with Bgl II and Hind III. These siRNAs were a self-contained hairpin loop for the double stranded siRNA. All siRNA sequences were confirmed by nucleotide sequencing.

Cell culture, transfection and retroviral infection of siRNAs

HEK293 Phoenix Ampho packaging cells (American Type Culture Collection; Manassa, VA) were cultured in DMEM containing 10% FBS and were transfected with the pSUPER-retro-neo siRNA plasmids using FuGENE 6 transfection reagent (Roche Diagnostics Inc., Indianapolis IN). Forty-eight hours following transfection, the culture media containing the retrovirus for individual siRNAs and control siRNA were filtered through a 0.45-μm filter, and the viral supernatant was used for infection of JEG3 cells in the presence of 8 μg/ml polybrene. JEG3 cells were exposed to the retrovirus overnight, cell were then washed with fresh medium and allowed to recover for 24 h. Following infection, stable cell lines were selected using neomycin at 500 μg/ml for 7 days (time until untransfected cells all died) then cultures were maintained in medium containing 500 μg/ml neomycin. Transient transfections of the siRNA cell lines were carried out as described above.

Statistical analysis

Luciferase data were subjected to analysis of variance and differences between treatments were determined using Tukey's Studentized Range Test. Probability of less than 0.05 ($p<0.05$) was considered statistically significant.

Results

DLX3 and SMAD6 functionally interact in a yeast two-hybrid screen

Full-length human DLX3 was used as a bait protein in a yeast two-hybrid screen of a human term placental library. The screen included coverage of approximately 3.4×10^6 independent clones. Once colonies were identified from the original screen and library plasmids were rescued, plasmids were retransformed in a reconstitution assay with the bait vector into the AH109 yeast strain. The library plasmid resulting in the most robust interaction (as measured by β-galactosidase activity) with *DLX3* was a cDNA containing the entire coding region of *SMAD6*. Transformation of the *SMAD6* library vector alone did not support yeast growth on high stringency SD medium (Ade^-/His^-/Leu^-/Trp^-/X-α-Gal) plates in the presence of 12 mM 3-amino-1,2,4-triazole. Transformation of Dlx3 bait vector minimally supported yeast growth under the same conditions. Co-transformation of *DLX3* bait and *SMAD6* library plasmid resulted in rescue of yeast growth (Figure 2.1A).

DLX3 and SMAD6 are co-localized in the nucleus in choriocarcinoma cells and in human placental trophoblasts

Initially, studies focused on examining localization of DLX3 and SMAD6 proteins in cells of trophoblast origin. DLX3 and SMAD6 were expressed and localized primarily in the nuclear compartment in JEG3 cells (Figure 2.1B), a choriocarcinoma cell line of trophoblast origin. Consistent with this observation, DLX3 and SMAD6

were nuclear localized to both cytotrophoblast and syncytial trophoblast within microvilli of fully differentiated term human placenta. Localization of DLX3 in term placenta provided additional insight into the expression pattern of DLX3 during gestation in primates. We have previously shown DLX3 in placental trophoblasts in human placenta obtained at 8 weeks gestation during peak production

Figure 2.1. DLX3 and SMAD6 interact in yeast two hybrid and co-localize in placental trophoblasts. A. Yeast two-hybrid screen of a human term placental library was carried out using full length DLX3 as bait. Following plasmid rescue, Gal4 DNA binding domain-*DLX3* bait was co-transformed along with Gal4 activation domain-*SMAD6* into the AH109 yeast strain and plated on ($^{-}$His, $^{-}$Leu, $^{-}$Trp) media as described in Methods. **B.** JEG3 cells were plated on glass slides and fixed as described in Materials and Methods. Double labeled immunocytochemistry was used to determine localization of DLX3 (green) or SMAD6 (red). The merged images demonstrate overlapping expression patterns. Human term placenta was obtained, fixed and sectioned as described in Materials and Methods. Similar double labeled immunocytochemistry was used to localize DLX3 and SMAD6. The white arrow head identifies nuclei in syncytial trophoblasts while the black arrow head identifies nuclei in cytotrophoblasts. Bar = 20 μm.
This figure is kindly provided by Dr. Kathie A. Berghorn.

A.

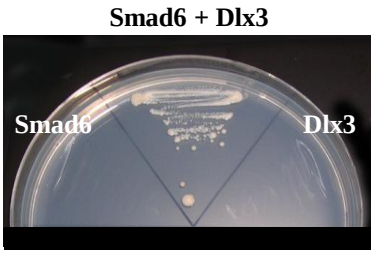
Smad6 + Dlx3
Smad6
Dlx3

B.

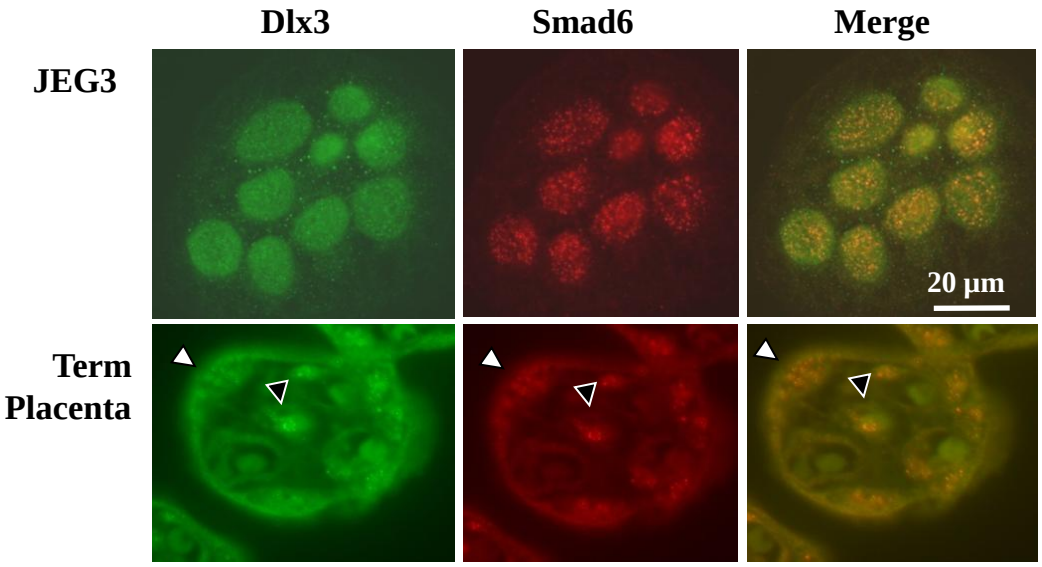
Dlx3
Smad6
Merge
JEG3
Term Placenta
20 µm

of hCG [14]. The current studies support the conclusion that DLX3 expression may be maintained within trophoblast cell populations until term in the human placenta. Since both DLX3 and SMAD6 were expressed endogenously in the JEG3 horiocarcinoma cell model, we sought to use this model for subsequent analyses. We have used JEG3 cells previously for molecular analysis of gene regulatory processes related to glycoprotein hormone and *DLX3* gene promoter expression [14,18,19]. IP studies using nuclear extracts from JEG3 cells and SMAD6 antibody revealed that DLX3 and SMAD6 interact in mammalian cells (Figure 2.2A). The reciprocal study using DLX3 antibody to IP SMAD6 was not possible due to the molecular size of SMAD6 and interference with the IgG heavy chain used in the IP studies. However, this constraint was overcome with preparation of DLX3 and SMAD6 as recombinant proteins labeled with [^{35}S] methionine. IP of recombinant DLX3 and SMAD6 with the DLX3 antibody revealed specific association with SMAD6 but not Smad4 (Figure 2.2B). Thus, the original interaction defined in the yeast system was supported by IP studies in choriocarcinoma cells that endogenously express these two proteins and *in vitro* using recombinant DLX3 and SMAD6 proteins.

Structure/function analysis of the DLX3/SMAD6 interaction interface

To further understand the mechanism of the DLX3/SMAD6 interaction, we constructed a series of deletion mutants of DLX3 (Figure 2.3A). The rationale for these mutations was predicated on existing understanding of important domains within DLX3 defined by others [20,21], centering upon the homeodomain (residues 130-189; Figure 2.3A), the centrally located DNA binding domain. DLX3 deletion mutants were prepared *in vitro* along with full-length DLX3 and SMAD6. SMAD6 IP was then used to determine the domains sufficient to support interaction with DLX3. Initially, we identified the importance of DLX3-(1-202), which bound SMAD6 at levels similar

Figure 2.2. DLX3 and SMAD6 interact in the JEG3 choriocarcinoma cell model. **A.** JEG3 cell nuclear extracts were used in immunoprecipitation (IP) studies. IPs included the use of normal rabbit serum (NRS) or antisera (ab) directed against DLX3 or SMAD6. Recombinant DLX3 (rDLX3; without HA epitope tag) and IPs were resolved by SDS-PAGE and Western blots for DLX3 were carried out (IB DLX3). Molecular size standards (MW) are depicted to the left of the panel. **B.** Recombinant DLX3, SMAD6 and SMAD4 were produced using wheat-germ lysates in a coupled transcription/translation reaction containing ^{35}S methionine (Input). DLX3 and either SMAD6 or SMAD4 were combined followed by IP with the DLX3 antibody (DLX3 IP). The input and IPs were resolved by SDS-PAGE, the gels fixed and dried and autoradiography was used to visualize bands.

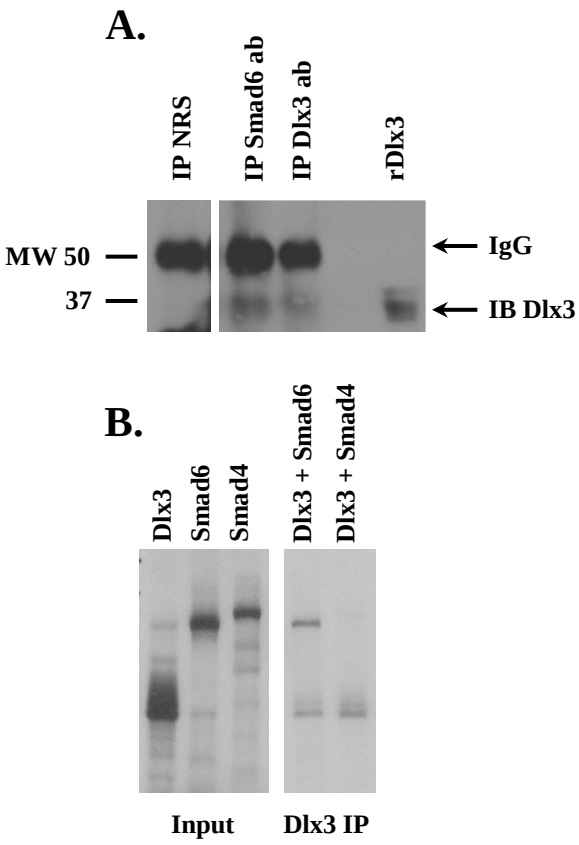
A.
IP NRS
IP Smad6 ab
IP Dlx3 ab
rDlx3
MW 50
37
IgG
IB Dlx3
B.
Dlx3
Smad6
Smad4
Dlx3 + Smad6
Dlx3 + Smad4
Input
Dlx3 IP

Figure 2.3. Deletion mutants of DLX3 reveal interaction interface with SMAD6. **A.** A series of DLX3 deletions (characterized in schematic form) were prepared using PCR. The numbers represent amino acid designations for the termini of wild type DLX3 and each mutant. **B.** Wild type DLX3, SMAD6 and the DLX3 deletion series were prepared as recombinant proteins as described in Figure 2B (Input) and subjected to IP studies using the SMAD6 antibody (SMAD6 IP) and recombinant SMAD6 and the combination of deletions mutants indicated. The input and IPs were resolved by SDS-PAGE, gels were fixed and bands visualized by autoradiography. Asterisks (*) designate bands consistent with protein-protein interactions.

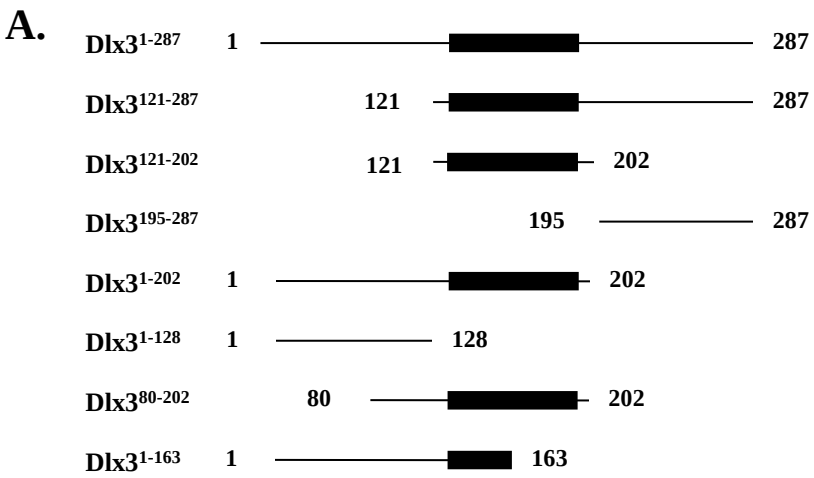
A.
Dlx3 1-287 1 287
Dlx3 121-287 121 287
Dlx3 121-202 121 202
Dlx3 195-287 195 287
Dlx3 1-202 1 202
Dlx3 1-128 1 128
Dlx3 80-202 80 202
Dlx3 1-163 1 163

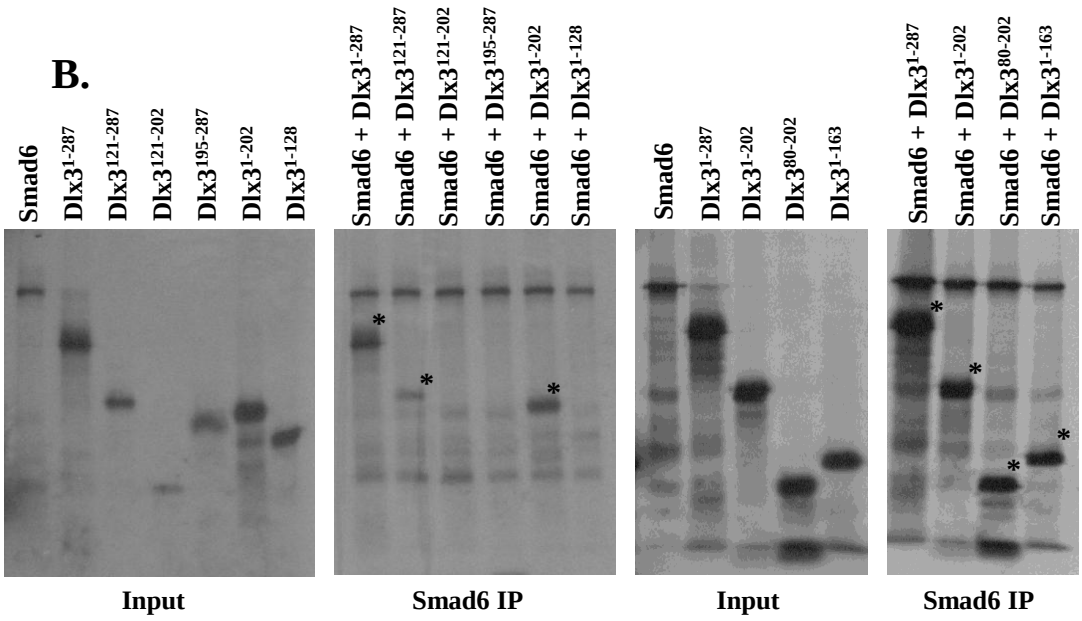
B.
Smad6
Dlx3 1-287
Dlx3 121-287
Dlx3 121-202
Dlx3 195-287
Dlx3 1-202
Dlx3 1-128
Smad6 + Dlx3 1-287
Smad6 + Dlx3 121-287
Smad6 + Dlx3 121-202
Smad6 + Dlx3 195-287
Smad6 + Dlx3 1-202
Smad6 + Dlx3 1-128
Smad6
Dlx3 1-287
Dlx3 1-202
Dlx3 80-202
Dlx3 1-163
Smad6 + Dlx3 1-287
Smad6 + Dlx3 1-202
Smad6 + Dlx3 80-202
Smad6 + Dlx3 1-163
Input
Smad6 IP
Input
Smad6 IP

to DLX3-(1-287) (Figure 2.3B). DLX3-(121-287) bound SMAD6 as well, suggesting that SMAD6 interaction domain required at least a portion of the homeodomain (Figure 2.3B). Based upon these results, we predicted that DLX3-(121-202) mutant would also bind SMAD6. This was not readily interpretable in our studies since putative degradation fragments/products of these recombinant deletion mutants were of similar molecular size as the DLX3-(121-287) mutant. Subsequent DLX3 deletion mutants defined a region of DLX3-(80-163) that was sufficient to bind SMAD6 *in vitro* (Figure 2.3B). These studies again supported the conclusion that at least the amino-terminal portion of the homeodomain was sufficient for interaction with SMAD6 *in vitro*. Alignment of DLX3 with DLX4 (another member of the DLX family expressed in placenta [22]) revealed approximately 37% amino acid conservation within this region (residues 80-163; Figure 2.4A), with higher levels of homology particularly clustered within the homeodomain, supporting the prediction that DLX4 may also bind SMAD6. Based upon *in vitro* studies, recombinant full-length DLX4 bound SMAD6 similar to DLX3-(1-287) (Figure 2.4B). DLX3-(195-287), previously shown not to bind SMAD6 (Figure 2.3B), was used in these studies as a negative control.

DLX3 binds to the 5'-flanking sequence of the Esx1 promoter

To begin to examine the functional significance of the DLX3/SMAD6 interaction on gene transcription, we cloned 2.3 kilobases of the 5'-flanking sequence of the Esx1 promoter. The report of the *Dlx3* null mouse provided evidence that the loss of *Dlx3 in vivo* was correlated with a loss of *Esx1* mRNA in mouse placenta [13]. Taking advantage of this observation, we identified two near consensus Dlx3 binding sites within the 2.3-kb promoter fragment. The distal site was located at -2135 and the more proximal site at -585 relative to the transcription start site of the *Esx1* promoter, as previously

Figure 2.4. DLX4 binds SMAD6. A. Alignment of DLX3 and DLX4 between residue 80 and 198 reveals regions of conserved sequence within the SMAD6 interaction domain (residue 80-163). The consensus amino acid sequence is listed in bold below the alignment. **B.** Wild type $DLX3^{1-287}$, $DLX3^{195-287}$, SMAD6 and DLX4 were prepared as recombinant proteins as described in Figure 2 (Input) and subjected to IP studies using the SMAD6 antibody (Smad6 IP) and recombinant SMAD6 and combinations of DLX3 or DLX4 as indicated. The input and IPs were resolved by SDS-PAGE, gels were fixed and bands visualized by autoradiography. Asterisks (*) designate bands consistent with protein-protein interactions.

A.

```
Dlx3       YSPKSEYTYGGSYRQYGAYREQPLPAQDPVSVKEEPEAEVRMVNGKPKKVRKPRTIYSSY
Dlx4       SYLPRQQQLVAPSQPFHRPAEHPQ-ELEAESEKLALSLVPSQQQSLTRKLRKPRTIYSSL
consensus                        e p       s k                k rkprtiyss
Dlx3       QLAALQRRFQKAQYLALPERAELAAQLGLTQTQVKIWFQNRRSKFKKLYKNGE-VPLEHS
Dlx4       QLQHLDQRFQHTQYLALPERAQLAAQLGLTQTQVKIWFQNKRSKYKKLLKQSSGEPEEDF
consensus  ql  l  rfq  qylalpera laaqlgltqtqvkiwfqn rsk kkl k     p e
```

B.

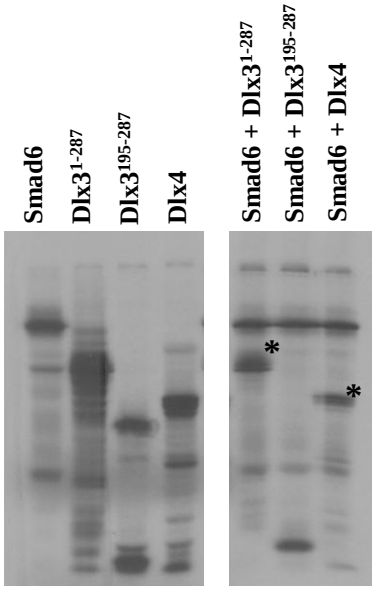

Figure 2.5. Two putative Dlx3 binding sites are present within the *Esx1* promoter. **A.** The junctional regulatory element (JRE), a consensus Dlx3 binding site from the glycoprotein hormone α subunit promoter was compared to the distal (position -2135) and proximal (position -585) binding sites from the *Esx1* promoter. The central core of the binding site is underlined. **B.** Electrophoretic mobility shift assays (EMSA) were used to compare binding complexes formed on the JRE, the distal and proximal Dlx3 binding sites within the *Esx1* promoter using JEG3 cell nuclear extract and recombinant DLX3. Equal amounts of nuclear extracts or recombinant DLX3 were added to each binding reaction. Recombinant DLX3 in these studies was epitope tagged with three copies of the HA epitope (3xHA-DLX3). Binding reactions were resolved on native polyacrylamide gels. The gels were dried and bands visualized by autoradiography. Free probe is designated by an arrow at the bottom of the gel. This figure is kindly provided by Ms. Li Han.

A.

JRE ACGTCATGGTAATTACACCAAG
Distal ACAAGGAGCTAATTTACTTCCT
Proximal TTAGGGCTCTAATTCAGACTCT
Consensus (A/C/G)TAATT(G/A)(C/G)

B.

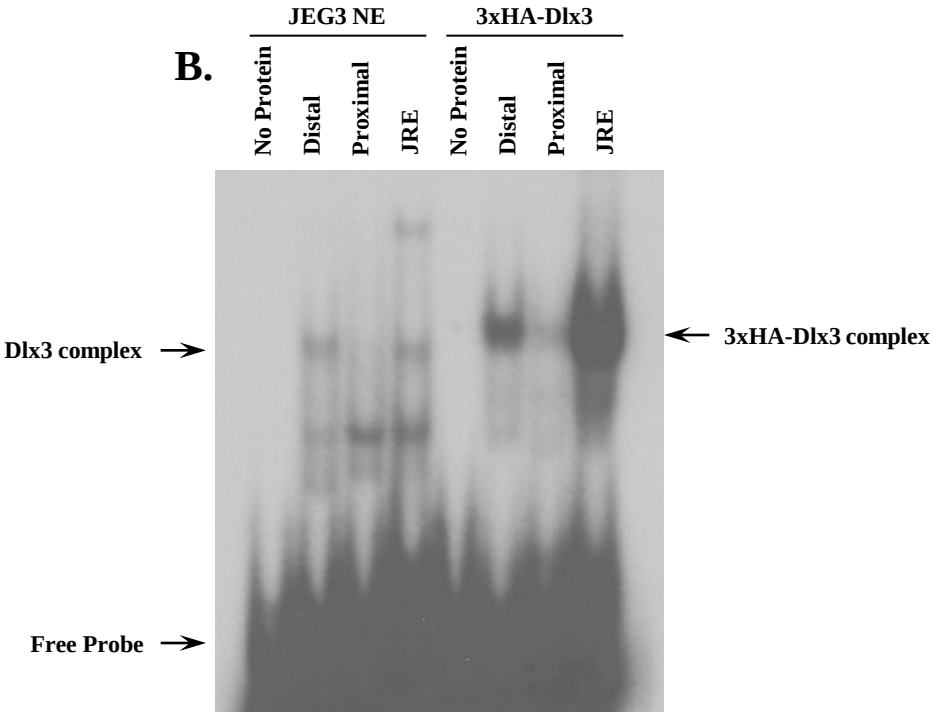

defined [23]. At both of these two sites, the central core of the binding site (TAATT) was conserved; however, the two nucleotides present on the 3' termini of this central core were not conserved (Figure 2.5A). These nucleotides varied from the consensus Dlx3 binding site [24] we defined in the human glycoprotein hormone α subunit promoter [14]. Using EMSAs, we compared the DNA binding complexes formed when using the distal (-2135) and proximal (-585) putative Dlx3 binding sites from the *Esx1* promoter and nuclear extracts from JEG3 cells (Figure 2.5B). As a positive control, the JRE from the α subunit promoter was used. Figure 2.5B depicts direct comparison of complexes formed with all three of these binding sites. The distal site was more similar to the JRE binding complex electrophoretic mobility when compared to the proximal site. When using recombinant DLX3 in EMSA (Figure 2.5B), all three sites were sufficient to bind DLX3; however, clear differences in the relative binding of DLX3 for these binding sites were revealed. The recombinant DLX3 was slightly larger in molecular size due to the presence of the three hemagglutinin (HA) epitopes engineered into the recombinant protein. The rank order of relative binding for recombinant DLX3 was the JRE (highest) > the distal site > the proximal site (lowest). We focused our attention on the distal DLX3 binding site within the *Esx1* gene promoter. EMSA studies using nuclear extracts and antiserum against DLX3 provided direct evidence that endogenous DLX3 can bind to this site (Figure 2.6A). The addition of the DLX3 antibody to EMSA binding reaction resulted in supershifted complexes that were not evident using preimmune normal rabbit serum (NRS). The addition of the SMAD6 or the C/EBP antiserum to these binding reactions did not appreciably alter complex formation in EMSA, suggesting that SMAD6 may not directly participate in DNA binding with DLX3 and that DLX3 antibody interactions were specific. To determine the importance of this site to DLX3-induced *Esx1* gene transcription, the distal site was mutagenized to a Not I restriction site and examined

Figure 2.6. The distal binding site of the *Esx1* promoter binds DLX3 and is necessary for full DLX3-induced gene transcription. A. Using only the distal binding site for DLX3 and JEG3 cell nuclear extract (JEG3 NE), studies examined if a DLX3 antibody would disrupt binding of endogenous proteins including DLX3 to this site. Binding reactions were resolved on native polyacrylamide gels, the gels were dried and bands visualized by autoradiography. Addition of a DLX3 antibody (DLX3 ab) to binding reactions resulted in the formation of a super shifted complex as indicated (supershift). Normal rabbit serum was used as a control for the DLX3 antibody. In some binding reactions, the JEG3 NE was boiled and then added to reactions containing the DLX3 ab as a negative control. Free probe is designated by an arrow at the bottom of the gel. **B.** Transient transfection studies were used to determine the relative importance of the distal DLX3 binding site on expression of the *Esx1* promoter luciferase reporter gene. JEG3 cells were transiently transfected with either wild type *Esx1* luciferase reporter or an *Esx1* luciferase reporter containing a mutation within the distal DLX3 binding site. Cells were cotransfected with control plasmid or a DLX3 expression vector (2 μg; designated – or +). Data are reported as relative luciferase activity standardized for protein for a representative study (n=3/treatment). The designations a, b and c indicate significant differences ($p<0.05$). This figure is kindly provided by Ms. Li Han.

A.

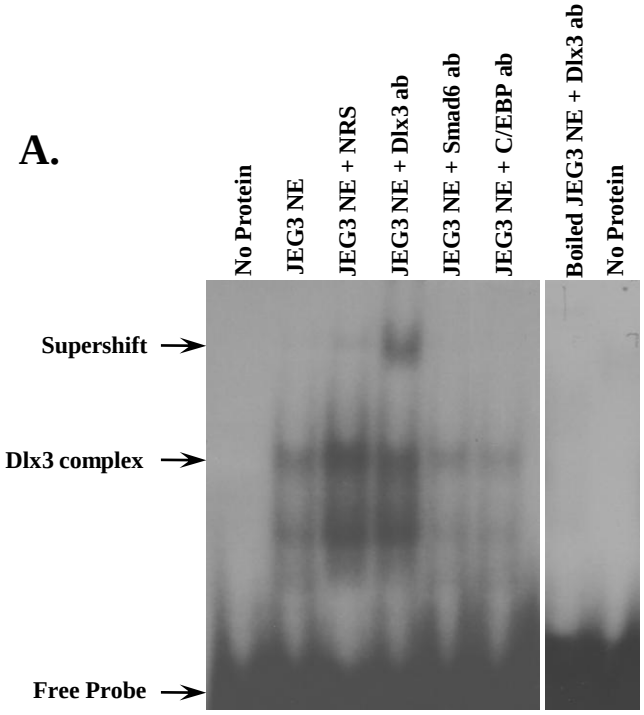
No Protein
JEG3 NE
JEG3 NE + NRS
JEG3 NE + Dlx3 ab
JEG3 NE + Smad6 ab
JEG3 NE + C/EBP ab
Boiled JEG3 NE + Dlx3 ab
No Protein
Supershift
Dlx3 complex
Free Probe

B.

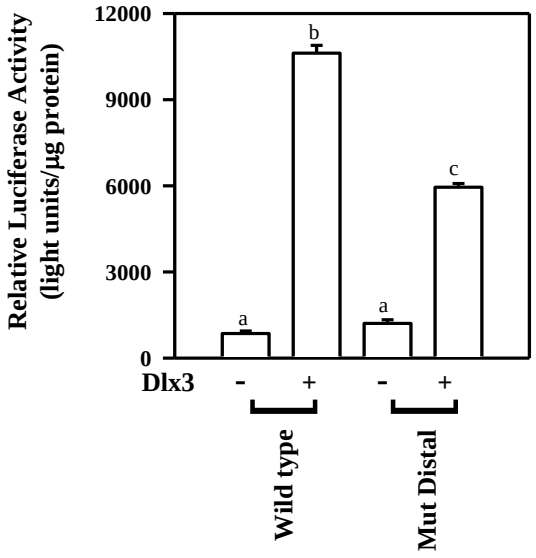
Relative Luciferase Activity
(light units/µg protein)
12000
9000
6000
3000
0
a
b
a
c
Dlx3
-
+
-
+
Wild type
Mut Distal

using a luciferase reporter gene approach in transient transfection studies (Figure 2.6B). The wild type *Esx1* promoter was strongly induced by DLX3. The mutation in the distal putative DLX3 binding site reduced DLX3-induced *Esx1* expression by >50% ($p<0.05$), suggesting that this site was important for promoter activity induced by DLX3.

We then sought to determine the impact of SMAD6 on DLX3 DNA binding. Reconstitution EMSAs using recombinant DLX3 and SMAD6 demonstrated that the DLX3/SMAD6 interaction effectively reduced/ blocked association of DLX3 with the distal DLX3 binding site within the *Esx1* promoter (Figure 2.7A). In this experiment, SMAD6 alone did not form a complex with the distal DLX3 binding site. When SMAD6 was titrated into the binding reactions containing DLX3, the DLX3 binding complex was diminished in a dose-dependent manner. Using the JRE as probe, a similar titration of SMAD6 protein reduced DLX3 binding, albeit to a lesser extent compared to the distal site of the *Esx1* promoter. Studies then focused on determining if prebound DLX3 could be displaced by SMAD6 in EMSA binding reactions (Figure 2.7B). Binding reactions compared addition of DLX3 concurrent with SMAD6 and reactions where DLX3 binding was allowed to reach equilibrium then SMAD6 was added. These studies revealed that for the distal probe, SMAD6 competed for DLX3 binding regardless of order of protein addition. Similar levels of competition were not observed using the JRE (stronger relative binding), suggesting that SMAD6 can compete for DLX3 binding particularly on gene targets that have relatively weaker DLX3 binding sites, like those characterized within the *Esx1* gene promoter.

To assess the functional consequences of the DLX3/SMAD6 interaction on the *Esx1* promoter, we again used the *Esx1* promoter-luciferase reporter construct (Figure 2.8). Based upon the binding studies described above, our prediction was that SMAD6 overexpression would probably repress expression of the *Esx1* promoter induced by

Figure 2.7. SMAD6 attenuates DLX3 DNA binding. A. To examine the effects of SMAD6 on DLX3 binding, recombinant DLX3 and SMAD6 were prepared *in vitro* and used in electrophoretic mobility shift assays (EMSA) with the distal DLX3 binding site within the *Esx1* promoter and the JRE. As observed earlier, DLX3 bound this site while increasing doses of SMAD6 (as represented by the grey triangle) did not bind. Binding reactions containing a constant dose of DLX3 and increasing doses of SMAD6 resulted in a dose dependent reduction in DLX3 binding for the distal site and to a lesser extent for the JRE. **B.** EMSA studies were carried out to determine if order of protein addition had an impact on the ability of SMAD6 to interfere with DLX3 binding. Using the distal and JRE probes, binding reactions were assembled where DLX3 was added and allowed to reach equilibrium (DLX3) then SMAD6 was added (DLX3 > SMAD6). This was compared to binding reactions where DLX3 and SMAD6 were added concurrently (DLX3 + SMAD6). For both A. and B., free probe and DLX3 complexes are designated by arrows.

This figure is kindly provided by Ms. Li Han.

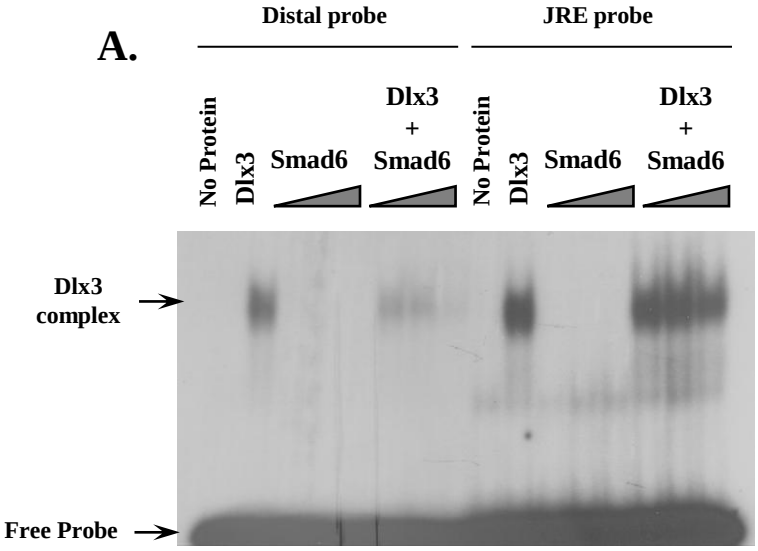
A.
Distal probe
JRE probe
No Protein
Dlx3
Smad6
Dlx3 + Smad6
No Protein
Dlx3
Smad6
Dlx3 + Smad6
Dlx3 complex
Free Probe

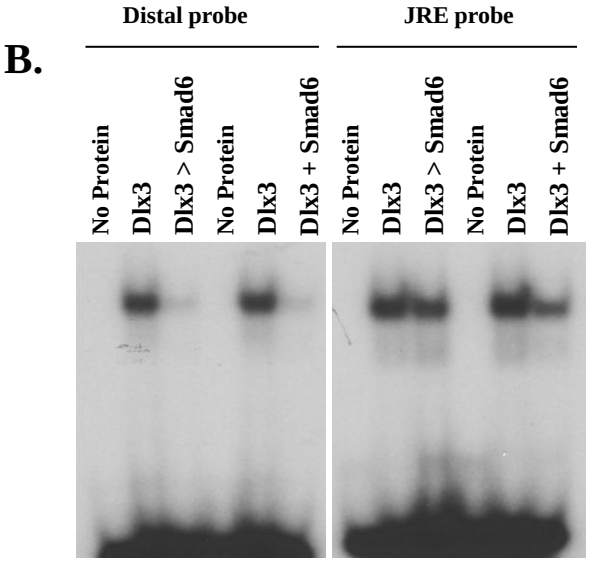
B.
Distal probe
JRE probe
No Protein
Dlx3
Dlx3 > Smad6
No Protein
Dlx3
Dlx3 + Smad6
No Protein
Dlx3
Dlx3 > Smad6
No Protein
Dlx3
Dlx3 + Smad6

DLX3. Using transient transfection in JEG3 cells, overexpression of DLX3 and SMAD6 resulted in increased levels of ectopically expressed DLX3 and SMAD6 (Figure 2.8A). Further, DLX3 overexpression increased *Esx1* luciferase activity ($p<0.05$; Figure 2.8B). Titration of SMAD6 into this system resulted in reduced basal activity of the Esx1 reporter gene ($p<0.05$). Consistent with our prediction, o-transfection with increasing doses of SMAD6 expression vector along with DLX3 resulted in a marked inhibition ($p<0.05$) of DLX3-induced *Esx1* promoter activity. DLX3-induced activation of the α subunit gene promoter was also reduced by overexpression of SMAD6 (data not shown). In an effort to determine the specificity of SMAD6 action on gene transcription in general, we examined the effects of SMAD6 on the trophoblast Kunitz domain protein (TKDP) 1 (Figure 2.8C) and Rous sarcoma virus promoters (data not shown). *TKDP1* promoter expression [25,26] is trophoblast-specific but not dependent upon DLX3 expression (Figure 2.8C). The Rous sarcoma virus promoter is constitutively active in trophoblast cells. In contrast to the effects of SMAD6 on DLX3-induced expression of the *Esx1* and α subunit promoter, SMAD6 had no appreciable effect on the *TKDP* promoter and actually increased expression of the Rous sarcoma virus promoter in a dose-dependent manner. These studies support the conclusion that SMAD6 does not confer global non-specific transcriptional repression and probably the effects of SMAD6 on *Esx1* and α subunit promoter activity are specific.

siRNA-mediated knockdown of SMAD6 resulted in increased expression of the Esx1 gene promoter.

Whereas overexpression studies can be informative, interpretation of such studies must be cautious. To examine the effects of SMAD6 on DLX3-dependent gene expression, we developed stable cell lines expressing specific *SMAD6* siRNA hairpin

Figure 2.8. SMAD6 attenuates DLX3-dependent promoter activation in JEG3 cells. A. To determine the levels of ectopic expression of DLX3 and SMAD6 in overexpression studies, JEG3 cells were transiently transfected with expression vectors for DLX3 (+DLX3; 2 μg) or SMAD6 (+SMAD6; 2 μg). Whole cell lysates were prepared and western blot analyses were carried out using the DLX3 and SMAD6 antibodies. **B.** Transient transfection studies in JEG3 cells were used to investigate the functional relevance of SMAD6 on DLX3-dependent gene expression. Co-transfection of the *Esx1* gene promoter-luciferase reporter with DLX3 (constant dose, 2 μg) and increasing doses of SMAD6 expression vector (0, 0.5, 1.0 and 2.0 μg; represented by the grey triangle) resulted in a dose dependent decrease in expression of the *Esx1* luciferase reporter. **C.** Similar studies were carried out using the *TKDP-1* gene promoter luciferase reporter. As a control for DLX3 action, the *Esx1* promoter was also used. *TKDP-1*-Luc activity was unaffected by DLX3 or increasing doses of SMAD6 expression vector. Data for all panels are reported as relative luciferase activity standardized for protein from representative studies (n=3/treatment). For B. and C. The designations a, b and c indicate significant differences ($p<0.05$) within experiment; ns = not significantly different. This figure is kindly provided by Ms. Li Han.

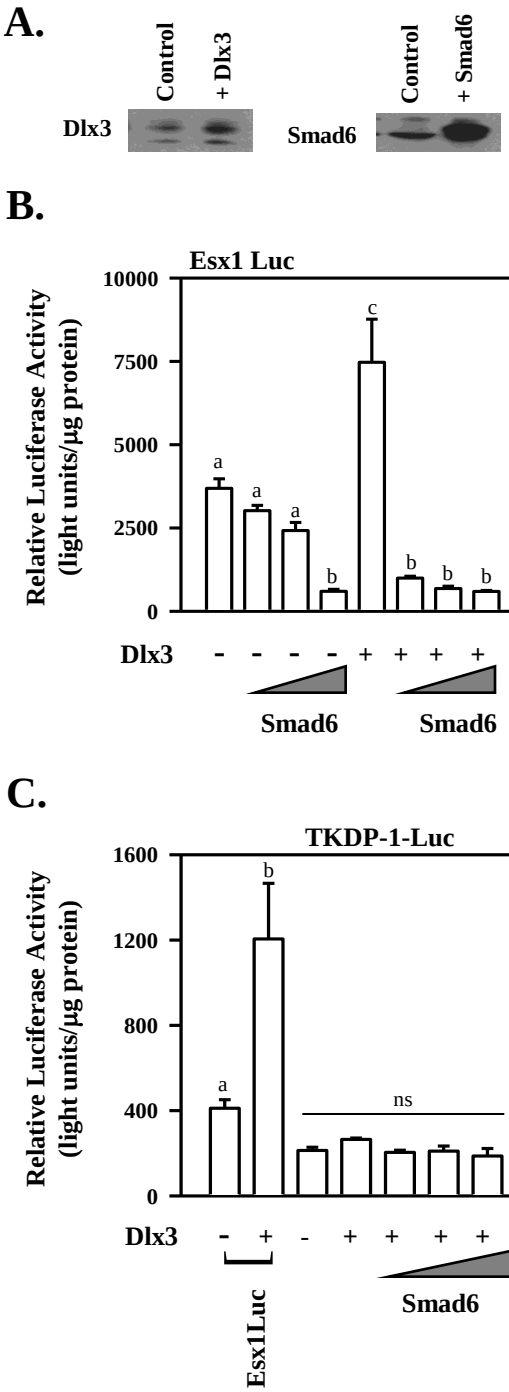
A.
Control
+ Dlx3
Dlx3
Control
+ Smad6
Smad6
B.
Esx1 Luc
Relative Luciferase Activity
(light units/µg protein)
10000
7500
5000
2500
0
a
a
a
b
c
b
b
b
Dlx3
- - - - + + + +
Smad6
Smad6
C.
TKDP-1-Luc
Relative Luciferase Activity
(light units/µg protein)
1600
1200
800
400
0
a
b
ns
Dlx3
- + - + + + +
Esx1Luc
Smad6

Figure 2.9. siRNA-mediated knockdown of SMAD6 results in enhanced DLX3-dependent expression of the *Esx1* Luc reporter. A. Stable cell lines were selected using neomycin resistance following infection with retrovirus expression empty vector (Vector Control), three separate, independent siRNAs specific for *SMAD6* (*SMAD6* siRNA #1-3) or a control siRNA (Control siRNA). Following selection, cell lysates were prepared and western blot analysis was used to determine SMAD6 protein levels. The cell lines were also assayed for DLX3 and ACTIN using specific antibodies. SMAD6 protein levels were reduced approximately 57% with siRNAs #1 and 3. **B.** The Control siRNA and *SMAD6* siRNA#1-3 cell lines were used in transient transfection studies using the Esx1 Luc reporter in the absence or presence of DLX3 expression vector (2 μg). Data are reported as relative luciferase activity standardized for protein from representative studies (n=3/treatment). The designations a, b, c and d indicate significant differences ($p<0.05$). This figure is kindly provided by Ms. Li Han.

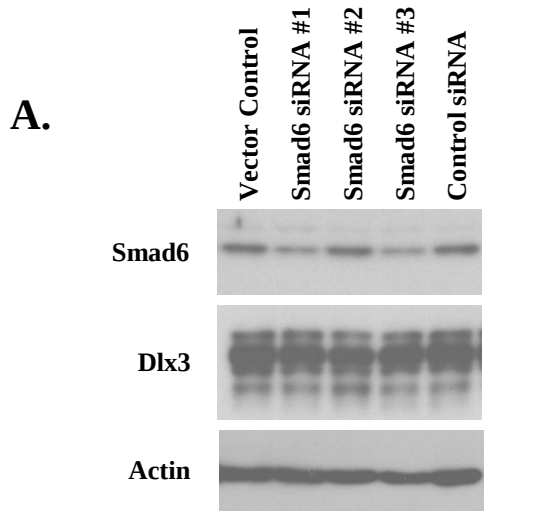
A.
Vector Control
Smad6 siRNA #1
Smad6 siRNA #2
Smad6 siRNA #3
Control siRNA
Smad6
Dlx3
Actin

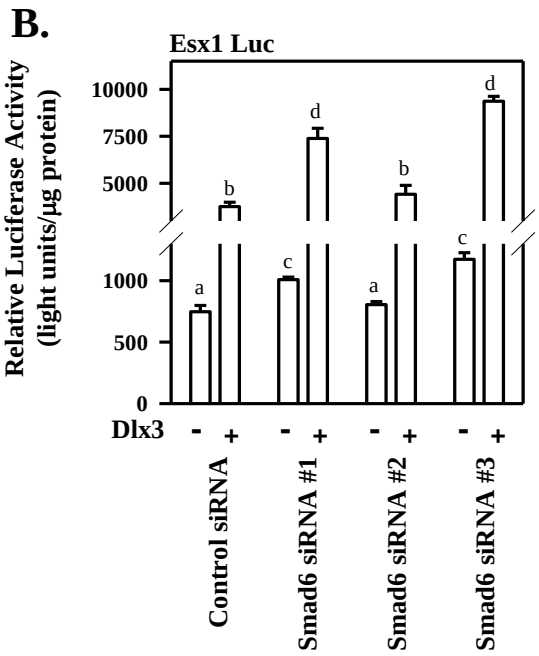
B.
Esx1 Luc
Relative Luciferase Activity
(light units/µg protein)
10000
7500
5000
1000
500
0
a
b
c
d
Dlx3
-
+
Control siRNA
Smad6 siRNA #1
Smad6 siRNA #2
Smad6 siRNA #3

loops (Figure 2.9A). Two of the three siRNA cell lines examined were found to have specific reductions in SMAD6 protein expression (*SMAD6* siRNAs #1 and #3; 57% reduction compared to control siRNA) but not expression of DLX3 nor ACTIN (internal controls; Figure 2.9A). Transfection studies in the control siRNA and the *SMAD6* siRNA cell lines using the *Esx1* luciferase reporter demonstrated that basal activity of this promoter was elevated ($p<0.05$) in the siRNA#1 and siRNA#3 cell lines but not in the control and siRNA#2 cell lines. In response to DLX3, *Esx1* luciferase promoter activity was enhanced ($p<0.05$) in *SMAD6* siRNA#1 and siRNA#3 cell lines but not in control or siRNA#2 cell lines [control siRNA (5.0-fold) *versus* siRNA#1 (7.3-fold) and siRNA#3 (8-fold)] in a manner highly correlated with the percentage loss of SMAD6 in these cell lines (Figure 2.9B). Thus, consistent with the overexpression studies, loss of endogenous SMAD6 was highly correlated with enhanced DLX3-dependent transcription of the *Esx1* gene promoter.

Discussion

The present studies provide novel evidence for the functional association between DLX3, a distal-less class homeobox factor required for normal placental development in the mouse, and an inhibitory Smad, SMAD6. The role of DLX3 as a transcriptional activator is clear based upon studies in mammalian systems, such as the glycoprotein hormone α subunit gene promoter [14], the expression of the homeobox factor *Esx1* in the *Dlx3* null mouse [13], and the role of Dlx3 in the regulation of the osteocalcin gene [27]. Moreover, Dlx3 has been linked to transcriptional activation as well as transcriptional repression in Xenopus (reviewed in Ref.[2]). The ability of Dlx3 to serve in several different ways as a transcriptional modulator may be best explained by the presence of variable tissue- and cell type-specific binding partners. The present study provides important evidence that DLX3 and SMAD6 form a complex in a yeast

system, in mammalian cells in culture and *in vitro* using recombinant proteins. DLX3 and SMAD6 also display overlapping expression in the nucleus of differentiated human term placental trophoblasts, suggesting that a functional interaction between these two proteins may be important *in vivo*. The finding that one DLX3 interacting partner is an inhibitory Smad may also reflect important cross-talk between the transforming growth factor (TGF) β/bone morphogenetic factor (BMP) signaling system and important developmental determinants that require DLX3.

Smad proteins are transcriptional regulators that can be subdivided into essentially three classes (reviewed in Refs. [28-30]). Regulated or R-Smads (Smad 1, 2, 3, 5 and 8) are substrates of the serine/threonine kinase catalytic activity of TGFβ/BMP type I receptors. Phosphorylation of R-Smads promotes the association with a common or C-Smad (Smad4) and subsequent nuclear translocation of the R- and C-Smad complex to affect TGFβ/BMP/Smad-specific target genes. Others have demonstrated an interaction between Smad4 and Dlx1 in the context of cytokine regulation of hematopoietic cells [31]. A third unique subclass of this family is the inhibitory or I-Smads (Smad 6 and 7). In the context of TGFβ/BMP signaling, I-Smads essentially oppose the activity of the stimulatory R- and C-Smads at several levels. I-Smads have been shown to compete for R-Smad binding to the type I TGFβ/BMP receptor, providing an inhibitory mechanism for R-Smad activity [32]. In addition, Smad6 has been shown to interfere with the ability of Smad1 to form a complex with Smad4, independent of Smad1 phosphorylation state [33]. I-Smads also form complexes with Smurfs, E3 ubiquitin ligases that appear to be involved in I-Smad nuclear export and marking target proteins (for example the TGFβ/BMP receptors and I-Smads themselves) for degradation by the proteosome, again contributing to an inhibitory action [28-30].

In the nuclear compartment, Smad6 appears to recruit the transcriptional co-repressor C-terminal binding protein to target genes related to BMP action [34]. Based upon the present studies, DLX3 and SMAD6 were localized to the nucleus of placental trophoblasts independent of apparent TGFβ/BMP signaling. Smad6 has been shown to serve as a transcriptional co-repressor following interaction with another homeodomain transcription factor, *Hox* c-8 [35,36]. In these studies, Smad6 complexed with *Hox* c-8 appeared to be sufficient to recruit histone deacetylase activities to *Hox* c-8-dependent genes thus repressing transcription via altered organization of chromatin structure. Our studies suggest that the interaction between DLX3 and SMAD6 may utilize an entirely different mechanism for transcriptional repression in human placental cells. SMAD6 interaction clearly resulted in a reduction of DLX3 DNA binding activity, probably via steric interference. Our results demonstrate that the SMAD6 interaction interface includes the first two α helices of the homeodomain. SMAD6 interaction would then potentially interfere with DLX3 DNA binding, since these two α helices are central to DNA binding as well. This mechanism potentially alleviates a need for recruitment of transcriptional co-repressor activities, since a DLX3-SMAD6 complex association may preclude association of DLX3 with specific target gene promoter elements. Increased SMAD6 protein levels using overexpression inhibited DLX3-dependent gene expression. Conversely, reductions in the expression of endogenous SMAD6 using siRNA knockdown provides important evidence that DLX3-dependent gene expression may be particularly sensitive to relatively modest changes in SMAD6 protein levels in placental cells. These complementary approaches underscore the potential importance and sensitivity of DLX3-dependent genes to SMAD6 regulation. This may be largely true of Dlx3 target genes with binding sites that have low relative binding affinity, like *Esx1*.

The Dlx3 homeodomain is centrally located and serves as a DNA binding domain, one of the defining characteristics of all homeobox transcription factors [37,38]. The domain structure of Dlx3 has been examined in studies defining a bipartite nuclear localization signal (residues 124-150) in a region adjacent to and including a portion of the homeodomain; transcriptional activation domains have been ascribed to residues 1-43 and 189-220; and Ser^{138} within the homeodomain is an apparent substrate for protein kinase C isozymes [20,21,24]. The deletion mutagenesis carried out in the present studies defined residues 80-163 within DLX3 as the SMAD6 interaction domain *in vitro*. This region of DLX3 contains the first full α helix and approximately two-thirds of helix 2 within the homeodomain. In addition, this interaction interface contains Ser^{138}, a substrate for PKC activity. Several possibilities exist for how DLX3-SMAD6 association may alter DNA binding. Perhaps the most obvious is a steric interference model, since the interaction interface includes a portion of the homeodomain. In addition, the presence of Ser^{138} in this interaction domain lends itself to potentially interesting speculation. The equivalent of this serine residue is conserved in all six Dlx family members [1], consistent with the observation that, like DLX3, DLX4 is also a SMAD6 interacting protein. Using recombinant Dlx3, Morasso and co-workers demonstrated that phosphorylation at Ser^{138} by PKC (most strongly by PKCα) resulted in partial inhibition of Dlx3 DNA binding [21], consistent with the potential effects of SMAD6 on DNA binding. This supports speculation that phosphorylation of Dlx3 at Ser^{138} may alter or increase Smad6 binding leading to reduced DNA binding at Dlx3 target genes. Studies are currently underway to address this possibility.

R- and C-Smads appear to be constitutively expressed in most cell types whereas I-Smads are subject to regulation by a number of growth factors, such as EGF, TGFβ and BMPs. In many cases the effects of these growth factors are mediated through R-

and C-Smad-dependent transcriptional mechanisms. This has led to a hypothesis implicating an intracellular negative feedback loop, whereby positive TGFβ/BMP signals are modulated over time by accumulation of induced I-Smads (reviewed in Ref. [39]). Interestingly, Dlx3 expression patterns during Xenopus development depend in part upon BMP signaling gradients [40,41]. Inhibition of these gradients using the BMP receptor antagonist chordin resulted in a dose-sensitive inhibition of Dlx3, Dlx5 and Dlx6 mRNA expression. Dlx3 expression in mouse keratinocytes was also reported to be subject to regulation by BMPs [42] in a manner potentially coordinate with I-Smad expression. This supports speculation that not only might BMP-regulated Smad6 expression serve as a negative feedback mechanism controlling the duration of Smad signaling but increased BMP-dependent Smad6 expression may lead to important modulation of Dlx3-dependent gene expression. BMPs have been shown to regulate early embryogenesis during the perimplantation period, such that these types of ligands are probably present and important during placental morphogenesis [43].

REFERENCES

1. Bendall,A.J. & Abate-Shen,C. Roles for Msx and Dlx homeoproteins in vertebrate development. *Gene* **247**, 17-31 (2000).

2. Beanan,M.J. & Sargent,T.D. Regulation and function of Dlx3 in vertebrate development. *Dev. Dyn.* **218**, 545-553 (2000).

3. Morasso,M.I., Mahon,K.A. & Sargent,T.D. A Xenopus distal-less gene in transgenic mice: conserved regulation in distal limb epidermis and other sites of epithelial-mesenchymal interaction. *Proc. Natl. Acad. Sci. U. S. A* **92**, 3968-3972 (1995).

4. Price,J.A., Bowden,D.W., Wright,J.T., Pettenati,M.J. & Hart,T.C. Identification of a mutation in DLX3 associated with tricho-dento-osseous (TDO) syndrome. *Hum. Mol. Genet.* **7**, 563-569 (1998).

5. Price,J.A., Wright,J.T., Kula,K., Bowden,D.W. & Hart,T.C. A common DLX3 gene mutation is responsible for tricho-dento-osseous syndrome in Virginia and North Carolina families. *J. Med. Genet.* **35**, 825-828 (1998).

6. Haldeman,R.J. *et al.* Increased bone density associated with DLX3 mutation in the tricho-dento-osseous syndrome. *Bone* **35**, 988-997 (2004).

7. Dong,J. *et al.* DLX3 mutation associated with autosomal dominant amelogenesis imperfecta with taurodontism. *Am. J. Med. Genet. A* **133**, 138-141 (2005).

8. Juriloff,D.M., Harris,M.J. & Brown,C.J. Unravelling the complex genetics of cleft lip in the mouse model. *Mamm. Genome* **12**, 426-435 (2001).

9. Clouthier,D.E. *et al.* Signaling pathways crucial for craniofacial development revealed by endothelin-A receptor-deficient mice. *Dev. Biol.* **217**, 10-24 (2000).

10. Clouthier,D.E., Williams,S.C., Hammer,R.E., Richardson,J.A. & Yanagisawa,M. Cell-autonomous and nonautonomous actions of endothelin-A receptor signaling in craniofacial and cardiovascular development. *Dev. Biol.* **261**, 506-519 (2003).

11. Clouthier,D.E. & Schilling,T.F. Understanding endothelin-1 function during craniofacial development in the mouse and zebrafish. *Birth Defects Res. C. Embryo. Today* **72**, 190-199 (2004).

12. Ivey,K. *et al.* Galphaq and Galpha11 proteins mediate endothelin-1 signaling in neural crest-derived pharyngeal arch mesenchyme. *Dev. Biol.* **255**, 230-237 (2003).

13. Morasso,M.I., Grinberg,A., Robinson,G., Sargent,T.D. & Mahon,K.A. Placental failure in mice lacking the homeobox gene Dlx3. *Proc. Natl. Acad. Sci. U. S. A* **96**, 162-167 (1999).

14. Roberson,M.S., Meermann,S., Morasso,M.I., Mulvaney-Musa,J.M. & Zhang,T. A role for the homeobox protein Distal-less 3 in the activation of the

glycoprotein hormone alpha subunit gene in choriocarcinoma cells. *J. Biol. Chem.* **276**, 10016-10024 (2001).

15. France,J.T. *et al.* Serum concentrations of human chorionic gonadotrophin and immunoreactive inhibin in early pregnancy and recurrent miscarriage: a longitudinal study. *Aust. N. Z. J. Obstet. Gynaecol.* **36**, 325-330 (1996).

16. Acevedo,H.F. Human chorionic gonadotropin (hCG), the hormone of life and death: a review. *J. Exp. Ther. Oncol.* **2**, 133-145 (2002).

17. Keay,S.D., Vatish,M., Karteris,E., Hillhouse,E.W. & Randeva,H.S. The role of hCG in reproductive medicine. *BJOG.* **111**, 1218-1228 (2004).

18. Holland,M.P., Bliss,S.P., Berghorn,K.A. & Roberson,M.S. A role for CCAAT/enhancer-binding protein beta in the basal regulation of the distal-less 3 gene promoter in placental cells. *Endocrinology* **145**, 1096-1105 (2004).

19. Roberson,M.S., Ban,M., Zhang,T. & Mulvaney,J.M. Role of the cyclic AMP response element binding complex and activation of mitogen-activated protein kinases in synergistic activation of the glycoprotein hormone alpha subunit gene by epidermal growth factor and forskolin. *Mol. Cell Biol.* **20**, 3331-3344 (2000).

20. Bryan,J.T. & Morasso,M.I. The Dlx3 protein harbors basic residues required for nuclear localization, transcriptional activity and binding to Msx1. *J. Cell Sci.* **113 (Pt 22)**, 4013-4023 (2000).

21. Park,G.T., Denning,M.F. & Morasso,M.I. Phosphorylation of murine homeodomain protein Dlx3 by protein kinase C. *FEBS Lett.* **496**, 60-65 (2001).

22. Quinn,L.M., Johnson,B.V., Nicholl,J., Sutherland,G.R. & Kalionis,B. Isolation and identification of homeobox genes from the human placenta including a novel member of the Distal-less family, DLX4. *Gene* **187**, 55-61 (1997).

23. Li,Y., Lemaire,P. & Behringer,R.R. Esx1, a novel X chromosome-linked homeobox gene expressed in mouse extraembryonic tissues and male germ cells. *Dev. Biol.* **188**, 85-95 (1997).

24. Feledy,J.A., Morasso,M.I., Jang,S.I. & Sargent,T.D. Transcriptional activation by the homeodomain protein distal-less 3. *Nucleic Acids Res.* **27**, 764-770 (1999).

25. MacLean,J.A., Roberts,R.M. & Green,J.A. Atypical Kunitz-type serine proteinase inhibitors produced by the ruminant placenta. *Biol. Reprod.* **71**, 455-463 (2004).

26. MacLean,J.A. *et al.* Family of Kunitz proteins from trophoblast: expression of the trophoblast Kunitz domain proteins (TKDP) in cattle and sheep. *Mol. Reprod. Dev.* **65**, 30-40 (2003).

27. Hassan,M.Q. *et al.* Dlx3 transcriptional regulation of osteoblast differentiation: temporal recruitment of Msx2, Dlx3, and Dlx5 homeodomain proteins to chromatin of the osteocalcin gene. *Mol. Cell Biol.* **24**, 9248-9261 (2004).

28. ten Dijke,P., Miyazono,K. & Heldin,C.H. Signaling inputs converge on nuclear effectors in TGF-beta signaling. *Trends Biochem. Sci.* **25**, 64-70 (2000).

29. ten Dijke,P. & Hill,C.S. New insights into TGF-beta-Smad signalling. *Trends Biochem. Sci.* **29**, 265-273 (2004).

30. Chen,D., Zhao,M. & Mundy,G.R. Bone morphogenetic proteins. *Growth Factors* **22**, 233-241 (2004).

31. Chiba,S. *et al.* Homeoprotein DLX-1 interacts with Smad4 and blocks a signaling pathway from activin A in hematopoietic cells. *Proc. Natl. Acad. Sci. U. S. A* **100**, 15577-15582 (2003).

32. Shi,Y. & Massague,J. Mechanisms of TGF-beta signaling from cell membrane to the nucleus. *Cell* **113**, 685-700 (2003).

33. Hata,A., Lagna,G., Massague,J. & Hemmati-Brivanlou,A. Smad6 inhibits BMP/Smad1 signaling by specifically competing with the Smad4 tumor suppressor. *Genes Dev.* **12**, 186-197 (1998).

34. Lin,X. *et al.* Smad6 recruits transcription corepressor CtBP to repress bone morphogenetic protein-induced transcription. *Mol. Cell Biol.* **23**, 9081-9093 (2003).

35. Bai,S., Shi,X., Yang,X. & Cao,X. Smad6 as a transcriptional corepressor. *J. Biol. Chem.* **275**, 8267-8270 (2000).

36. Bai,S. & Cao,X. A nuclear antagonistic mechanism of inhibitory Smads in transforming growth factor-beta signaling. *J. Biol. Chem.* **277**, 4176-4182 (2002).

37. Gehring,W.J. Exploring the homeobox. *Gene* **135**, 215-221 (1993).

38. Wright,C.V., Cho,K.W., Oliver,G. & De Robertis,E.M. Vertebrate homeodomain proteins: families of region-specific transcription factors. *Trends Biochem. Sci.* **14**, 52-56 (1989).

39. Miyazono,K. A new partner for inhibitory Smads. *Cytokine Growth Factor Rev.* **13**, 7-9 (2002).

40. Feledy,J.A. *et al.* Inhibitory patterning of the anterior neural plate in Xenopus by homeodomain factors Dlx3 and Msx1. *Dev. Biol.* **212**, 455-464 (1999).

41. Luo,T., Matsuo-Takasaki,M., Lim,J.H. & Sargent,T.D. Differential regulation of Dlx gene expression by a BMP morphogenetic gradient. *Int. J. Dev. Biol.* **45**, 681-684 (2001).

42. Park,G.T. & Morasso,M.I. Bone morphogenetic protein-2 (BMP-2) transactivates Dlx3 through Smad1 and Smad4: alternative mode for Dlx3 induction in mouse keratinocytes. *Nucleic Acids Res.* **30**, 515-522 (2002).

43. Paria,B.C. *et al.* Cellular and molecular responses of the uterus to embryo implantation can be elicited by locally applied growth factors. *Proc. Natl. Acad. Sci. U. S. A* **98**, 1047-1052 (2001).

CHAPTER THREE

MATRIX METALLOPROTEINASE 9 IS A DLX3 TARGET-GENE IN PLACENTAL CELLS

Clark PA[1], Woods AK[1], Han L[1], Xie, J[1], Navratil AM[1], Zhang X[3], Coonrod SA[1,3], Davisson RL[1,2], and Roberson MS[1]

[1] Department of Biomedical Sciences, Cornell University, Ithaca NY
[2] Cell and Developmental Biology, Weill Cornell Medical College, New York, NY
[3] The James A. Baker Institute for Animal Health, Cornell University, Ithaca, NY

Abstract

Matrix metalloproteinases (MMPs) are a large group of proteolytic enzymes that regulate extracellular matrix composition during normal biological processes such as during placental morphogenesis. Previous microarray studies in mouse placenta suggested that at E9.5, MMP-9 transcript abundance was dependent upon Distal-less 3 (Dlx3), a homeodomain-containing placental-specific transcriptional regulator. Here we investigate putative mechanism(s) for Dlx3-dependent MMP-9 gene transcription and activity in placental trophoblasts and examine the hypothesis that Dlx3 and MMP-9 may be involved in genetic mechanism(s) underlying preeclampsia (PE) using the murine model of PE, the BPH/5 mouse. Initial studies confirmed array data, demonstrating that MMP-9 secretion and catalytic activity were reduced in placental explants from $Dlx3^{-/-}$ mice compared to controls. To investigate mechanisms of gene transcription, 1.9 kb of the murine MMP-9 5' flanking sequence was cloned for use in luciferase-based reporter gene assays. Bioinformatic analysis of this promoter fragment identified two near-consensus Dlx3 binding sites and MMP-9 promoter-luciferase reporter activity was increased 3-5 fold by overexpression of Dlx3 in a human trophoblast cell line (JEG3). Recombinant Dlx3 was able to bind to both putative Dlx3 binding sites *in vitro*. Using JEG3 cell nuclear extracts, DNA affinity chromatography revealed a Dlx3-containing complex formed specifically at both Dlx3 binding sites. Mutations in both elements resulted in a reduction of basal expression of the MMP-9 gene promoter and abolished regulation by overexpression of Dlx3. Chromatin immunoprecipitation studies in JEG3 cells also demonstrated that Dlx3 binds to the human MMP-9 promoter in cells and siRNA-mediated knockdown of human Dlx3 resulted in marked reduction in endogenous human MMP-9 transcript levels and secreted MMP-9 protease activity. Since MMP-9 has been shown to be mis-regulated in term human placentas during PE, we sought to determine if Dlx3 and

MMP-9 transcript levels were altered during early and late gestation in the BPH/5 model of PE. Quantitative PCR revealed that MMP-9 mRNA level was reduced in early gestation (E9.5) and increased during late gestation (E18.5) in placentas of BPH/5 mice. Further, MMP-9 transcript mis-regulation was correlated with changes in Dlx3 mRNA levels in this study. These studies provide novel evidence that Dlx3 may be involved in the transcriptional regulation of mouse and human MMP-9 gene expression in placental trophoblasts. Further, MMP-9 and Dlx3 are coordinately mis-regulated in the BPH/5 mouse model suggesting these two genes may be involved in the gene network underlying placental pathologies in PE.

Introduction

During pregnancy, the placenta forms the critical fetal-maternal interface to support fetal nutrient supply and exchange of gases and waste products that underlie the coordinated growth and development of the mammalian fetus *in utero*. In the mouse, the primary site of exchange occurs within the placental labyrinth. The labyrinth layer is formed by distinct inter-digitations between fetal blood vessels and maternal blood spaces that are paramount for nutrient exchange to meet the metabolic demands of the growing fetus [1]. Accurate morphogenesis and function of the labyrinth compartment depends upon a number of dynamic cellular processes such as controlled proliferation, differentiation, cell migration, and (re)organization of the extracellular matrix (ECM) environment. Any genetic or environmental insult(s) that interferes with these dynamic processes can potentially disrupt the morphogenesis of the labyrinth and result in placental insufficiency, intrauterine growth restriction (IUGR) of the fetus and ultimately embryonic lethality.

Placental cell migration is critical for normal placental morphogenesis. For example, cytotrophoblasts migrate through the extracellular matrix (ECM) of the

maternal decidua and engage in remodeling of the maternal spiral arteries [2,3]. This vascular remodeling leads to enlargement of vessel diameter, decreased vascular resistance and sustained blood flow into the intervillious space and ultimately appropriate perfusion of the placental vascular bed [4]. Inadequate maternal spiral artery remodeling has been detected in the placentas of women with fetal IUGR and/or symptoms consistent with preeclampsia (PE) [5,6]. These observations suggest that the dynamic process of cytotrophoblast invasion and maternal spiral artery remodeling is required for successful placental perfusion and a productive pregnancy [7]. Matrix metalloproteinases or MMPs appear to play a key role in ECM breakdown and remodeling at several levels. For example, MMP-1 and 9 have been found in normal human decidual samples collected as biopsies from term pregnancies and MMP-1 specifically was demonstrated to be reduced in deciduas collected from patients with PE [4]. In these same studies, MMP-9 expression was clearly inducible in decidual cells following activation of protein kinase C; however, PE did not appear to alter this response in the maternal tissues examined. Additionally, Campbell and colleagues used a bilayer co-culture model to examine the effect of decidual endothelial cells on MMP secretion and cytotrophoblast migration from PE pregnancies [8]. These studies provide evidence that cytotrophoblasts from PE pregnancies secreted significantly less MMP-2 and MMP-9 compared to control. These observations were supported by other studies demonstrating decreased MMP-9 mRNA expression [9,10] and histological staining [11,12] in human PE placentas. Collectively, these results suggest that abnormal trophoblast invasion of the maternal vasculature in PE may be due in part to mis-regulation of specific MMPs, including MMP-9; however, these observations remain controversial since others have been unable to identify a specific role for MMPs during trophoblast invasion. One such study examined chorionic villous biopsies taken from pregnancies complicated by PE, HELLP syndrome, or IUGR compared to

matched control patients. A specific immuno-capture assay revealed the presence of both MMP-2 and 9 (but not MMPs-1, 3 8 or 13) activity in these tissues; however, total MMP-2 and MMP-9 activity was not different in complicated and uncomplicated pregnancies. The authors concluded that misregulation of MMP-2 and -9 early in pregnancy were not correlated with maternal pregnancy complications [13]. Additionally, human pregnancies complicated by gestational hypertension found circulating levels of pro-MMP-9 and its inhibitor, tissue inhibitor of metalloproteinase-1 (TIMP-1), to be higher in hypertensive patients compared to control women; however, pregnancies complicated by PE did not reveal such differences indicating differences in the pathophysiological gene profiles characteristic of PE and gestational hypertension [14]. Yet, another study indicated significantly higher immunohistochemical MMP-9 levels in decidual cells and adjacent interstitial trophoblasts in preeclamptic placental sections verses gestational age-match control women [15]. While difficult to reconcile, these studies may collectively support the conclusion that the MMP-9 gene profile may be misregulated in at least a subset of PE patients potentially reflecting an abnormal trophoblast invasive phenotype.

Dlx3 is one of six Distal-less family members characterized as homeobox-containing transcription factors necessary for the development of numerous tissues including the mouse placenta [16,17]. Targeted deletion of Dlx3 results in midgestation embryonic lethality (~E9.5-10) due to placental labyrinth defects suggesting the Dlx3 and Dlx3-dependent gene targets play a critical role in labyrinth development [1,17]. Microarray analysis of Dlx3 null placentas collected at embryonic day (E) 9.5 linked Dlx3 to aberrant expression of a number of genes critical to placental function, including reduced expression of placental growth factor, a key marker of PE and MMP-9 [18]. The present studies examined the hypothesis that Dlx3 may regulate MMP-9 directly at the transcriptional level in placental cells. Data presented here

demonstrates that Dlx3 is a key regulator of MMP-9 transcript levels and secreted MMP-9 catalytic activity in mouse placental explants and human choriocarcinoma cells. Dlx3-dependent regulation of the MMP-9 gene promoter occurred through near consensus cis regulatory elements within the mouse and human MMP-9 gene promoters suggesting the effects of Dlx3 on the MMP-9 gene promoter were direct. In an attempt to reconcile the role of MMP-9 during PE, we examined expression levels of Dlx3 and MMP-9 early and late in gestation in a new model of PE, the BPH/5 mouse. These studies provide novel evidence of mis-regulation MMP-9 transcript levels in BPH/5 mouse placentas early in gestation, correlated with Dlx3 transcript expression. These studies support the conclusion that Dlx3 is a critical transcriptional regulator of mouse and human MMP-9 gene expression. Further, mis-expression of Dlx3 and MMP-9 in the BPH/5 mouse model during gestation suggests that these genes may be important markers of early disease progression during PE in this model.

Materials and Methods

Animals- Dlx3$^{-/-}$ mice were a generous gift from the laboratory of Dr. Maria Morasso at the National Institutes of Health. BPH/5 mice have been developed in the laboratory of Dr. Robin Davisson here at Cornell University and described in some detail elsewhere [19]. All mice used in these studies were maintained and used in full compliance with protocols approved by the Cornell University Institutional Animal Care and Use Committee. All animals had free access to food and water; qualified Cornell University lab animal veterinarians were responsible for all animal care.

Culture of Placental Explants, JEG3 cells and Gel Zymography- Mouse placental explants were harvested at E9.5 from Dlx3$^{+/-}$ females that were mated with Dlx3$^{+/-}$

males. At the time of dissection, embryos were dissected free of uterine and placental tissues and used for genotyping as described [18,20]. Placental explants (essentially the placental disk with minimal maternal deciduas; n = 4-6 explants/genotype) were washed 3 times in Dulbecco's Phosphate Buffered Saline (DPBS) and then cultured in Dulbecco's Modified Eagle's medium (DMEM) supplemented with fetal bovine serum (10%) at 37˚C in 5% CO_2 as previously described [18,20]. Following a two hour equilibration period, media was removed and replaced with fresh media. Media was collected four hours later (6 hours following the start of culture) and all media samples were snap frozen and stored at -80˚C until zymography studies could be completed. In some studies using siRNA-mediate Dlx3 knockdown (described below), stably transfected JEG3 cells were split to new culture dishes and cultured to 50-80% confluence. Cells were washed with DPBS and placed in fresh media. Media was collected from these cultures in a manner identical to the placental explants and media samples were again stored at -80˚C until subsequent assays.

Zymography studies were carried out as previously described [21]. Briefly for zymography studies, equal volumes of conditioned culture media from the placenta explant study and the siRNA knockdown cell lines were resolved in 10% gelatin Zymogram gels (Bio-Rad Laboratories, Hercules, CA). Following electrophoresis, proteins within these gels were allowed to renature in 2.5% Triton X-100 for 30 minutes at room temperature and incubated in Developing Buffer (Millipore, Billerica, MA), containing 50mM Tris-HCl, 0.2M NaCl, 5mM $CaCl_2$ and 0.02% Brij35, for 30 minutes at room temperature and then placed in fresh Developing Buffer overnight at 37˚C. The gels were then stained with 0.5% Coomassie Brilliant Blue (Sigma, St. Louis, MO) in methanol/acetic acid/water (40:10:50 v/v) for 30 minutes at room temperature followed by destaining with methanol/acetic acid/water (50:10:40) for 4 hours at room temperature. The presence of clear bands in the gels at 92kDa and

105kDa reflected the gelatinase activity of human MMP-9 and mouse MMP-9, respectively. Bands were visualized using BioRad Gel Imaging system and gelatinase activity was quantified using densitometry analysis.

Western Blotting Analysis- Conditioned media from placental explants was suspended in SDS-PAGE loading buffer (100mM Tris (pH6.8), 4% SDS, 20% glycerol, and 200mM DTT), boiled for 3 minutes and incubated on ice for 5 minutes. Complexes were resolved by SDS-PAGE and transferred to polyvinylidine difluoride membranes by electroblotting. Membranes were blocked in 2x casein (Vector laboratories, Burlingame, CA) in Tris-buffered saline (10mM Tris (pH 7.6), 150mM sodium chloride) containing 0.1% Tween 20 (TBST) for 1 hour at room temperature. The following antibodies were used at a 1:1000 dilution in western blotting: MMP-9 (Abcam, Cambridge, UK), thrombospondin 2 (BD Transduction Labs, San Jose, CA) and the Dlx3 [20] antibody. Actin antibody (Santa Cruz, Santa Cruz, CA) was used at 1:500 dilution. All protein bands were visualized by chemiluminesence reagents. All Western blotting studies were carried out on at least 3 separate occasions with similar results.

Plasmids and cDNA- All plasmids used in these studies were purified using two cycles through cesium chloride. 1.9kb portion of the mouse MMP-9 promoter was obtained by PCR using mouse genomic DNA and subsequently cloned into a luciferase reporter vector using the following primers: MMP-9 forward primer, 5'-ggtaccgtcagagcattcattgtagaag-3'; MMP-9 reverse primer, 5'-ggatccgagattttaaagaggcagtaaa-3'. Cloning of this promoter fragment was facilitated by adding restriction sites Kpn1 and Bam H1 to the forward and reverse primers, respectively. The fidelity of MMP-9 luciferase reporter was verified by nucleotide

sequence analysis. PCR-based site-directed mutagenesis was used to disrupt the two Dlx3 binding sites located at -1498 and -825 within the mouse MMP-9 promoter luciferase reporter. These mutations substituted a Not-1 restriction site for the near consensus Dlx3 binding sites. These mutations were confirmed using nucleotide sequence analysis. The pKH3-Dlx3 expression construct has been previously reported [20] and encodes mouse Dlx3 with the addition of three HA epitopes at the amino terminal end of the protein. Additionally, both the human glycoprotein hormone α subunit gene promoter luciferase construct and the PGF gene promoter luciferase construct have been previously reported [18,22].

Cell Culture and Transient Transfection Studies- JEG3 cells were cultured in monolayer using DMEM supplemented with fetal bovine serum (10%). Before transfection studies, cells were split into 6-well tissue culture dishes and grown to 50-80% confluence. To compare relative gene promoter activity, JEG3 cells were transiently transfected with a luciferase reporter vector that did not contain a promoter fragment (empty), the MMP-9 promoter-luciferase construct, the human -204 α subunit gene promoter-luciferase construct or the placental growth factor (PGF) promoter-luciferase construct, the latter two known to be expressed in human trophoblasts. Additionally in some studies, the MMP-9 promoter-luciferase construct was transiently co-transfected with increasing doses of pKH3-Dlx3 expression vector, a constant dose of Smad6 (2μg) or a combined constant dose of pKH3-Dlx3 expression vector (2μg) in combination with Smad6 (2μg). All transfections were carried out utilizing Genejuice transfection reagent (EMD4Biosciences, Gibbstown, NJ) and a constant amount of total DNA by supplementing reactions with the empty expression vector, pKH3. Luciferase activity was determined after 24 h of transfection using reagents from a luciferase reporter assay system (Promega

Corporation, Madison, WI). Luciferase activity levels were standardized using total cellular protein as determined by a Bradford assay. All transfections were conducted in triplicate on at least 3 separate occasions. Data are shown as means (n=3) ± standard error of the mean for a representative experiment.

Recombinant protein synthesis and electrophorectic mobility shift assay- Recombinant Dlx3 protein was prepared using a coupled transcription and translation Wheat Germ Extract system (Promega Corporation, Madison, WI) following the prescribed protocol. Electrophoretic mobility shift assays (EMSAs) were carried out as described previously [20,22]. Briefly, binding reactions (without radiolabeled probe) containing non-specific DNA were maintained at room temperature for 20 minutes followed by the addition of ^{32}P-labeled oligonucleotide Dlx3 binding site probes from the two putative Dlx3 binding sites indentified within the mouse MMP-9 promoter. The binding reactions were incubated another 20 minutes at room temperature and resolved on native polyacrylamide gels. Following electrophoresis, the gels were dried, and DNA-protein complexes were visualized by autoradiography. All DNA binding studies were conducted at least 3 times with similar results. The nucleotide sequences for the probes were as follows (only the top strand is represented): MMP-9 -1498 binding site, 5'-ctaaaacaaattaacaaacaa-3' and; MMP-9 -825 binding site, 5'-cagtctcctaatttccaatca-3'.

Preparation of JEG3 Cell Nuclear Extracts- Near confluent JEG3 cells were washed twice with ice-cold DPBS and collected by scraping in ice-cold DPBS supplemented with a 1:1000 dilution of protease inhibitor mixture (Sigma-Aldrich, St. Louis, MO), 5mM benzamidine, and 0.2mM phenylmethylsulfonyl fluoride. Cells were pelleted by centrifugation and resuspended in a hypotonic buffer consisting of 120mM potassium

chloride, 30mM sodium chloride, 30mM Hepes (pH8.0), 0.3M sucrose, protease inhibitor mix supplemented with 5mM benzamidine, and 0.2 mM phenylmethylsulfonyl fluoride and allowed to swell for 15 minutes on ice. Cells were lysed by dounce homogenization and nuclei were isolated by layering the broken cell lysates over a sucrose cushion (0.9M sucrose), then centrifuging at 2000 x *g* for 30 minutes at 4˚C. The nuclear pellet was resuspended in buffer containing 10mM Tris (pH 7.5), 50 mM NaCl, 5% glycerol, 1mM ethylenediaminetetraacetic acid (EDTA), protease inhibitor mixture, 5mM benzamidine, and 0.2 mM phenylmethylsulfonyl fluoride. Additional sodium chloride was added to a final concentration of 450mM and nuclear proteins were extracted at 4˚C for 30 minutes with constant agitation. Nuclear extracts were clarified by centrifugation (85,000x g for 60 minutes), and the nuclear extracts were stored in aliquots at -80˚C until later use. The protein concentration of each nuclear extract was determined by Bradford assay.

DNA affinity chromatography- M-280 streptavidin Dynabeads® (Invitrogen, Carlsbad, CA) were washed 3 times in wash buffer, 10mM Tris pH7.5, 1mM EDTA, 2M NaCl. The nucleotide sequences for the two putative Dlx3 binding sites on the MMP-9 promoter (-1498 and -825) were biotinylated on the 5' end. The biotinylated DNA binding sites were incubated with washed Dynabeads for 15 minutes at room temperature with constant shaking. Dynabeads-DNA mixture was washed in wash buffer twice followed by one wash in 50mM Tris pH 7.5, 1mM EDTA, 100mM KCl, 5% glycerol, 0.1% Trition X-100, and 1mM dithiothreitol (incubation buffer) to equilibrate the affinity matrix to incubation conditions. JEG3 cell nuclear extracts (60ug) were added to the Dynabeads-DNA mixture plus 100ul incubation buffer and incubated at room temperature 30 minutes with gentle shaking every 2 minutes. In some cases, these binding reactions also included 50 or 100 fold molar excess of

unbiotinylated competitor oligonucleotides. Following this incubation, the Dynabeads-DNA-protein mixture was washed 3 times in incubation buffer. Complexes were suspended in 2XSDS loading buffer (100mM Tris (pH6.8), 4% SDS, 20% glycerol, and 200mM DTT). Samples were boiled for 3 minutes and chilled on ice for 5 minutes, resolved by SDS-PAGE and immunoblotted using the Dlx3 antibody as described above.

Chromatin Immunoprecipitation Assay- Protein A/G beads (Invitrogen, Carlsbad, CA) were blocked overnight with 1mg/ml sonicated salmon sperm DNA and 1mg/ml bovine serum albumin (BSA) at 4˚C with gentle agitation then washed in TE buffer several times. JEG3 cells were transiently transfected with either the pKH3-Dlx3 expression vector or a mock transfection containing only the pKH3 expression vector, using Genejuice (EMD4Biosciences, Gibbstown, NJ) as described above. Twenty-four hours following transfection, cells were fixed in 1% formaldehyde in PBS for 10 minutes at 37˚C. Glycine (125mM) was added to quench the crosslinking and cells were incubated on ice for 5 minutes. Cells were rinsed with DPBS and collected in 1ml DPBS containing 1 Complete Mini Protease Inhibitor tablet (Roche, Indianapolis, IN). Cells were centrifuged at 4000 RPM for 5 minutes and resuspended in 1% SDS, 10mM EDTA, 50mM Tris (pH7.9), 1mM DTT containing 1 Complete Mini Protease Inhibitor tablet (Roche, Indianapolis, IN). Cells were incubated on ice for 10 minutes and sonicated using a Diagenode Bioruptor UCD-200 sonicator at 27% amplitude 20 times, 10 seconds per round with 1 minute between sonications. Lysed cells were centrifuged for 10 minutes at 13,000 RPM at 4˚C and the supernatant was collected. Chromatin was pre-cleared with blocked agarose beads for 3 hours at 4˚C with gentle agitation. After centrifugation, 10% of each sample was removed for analysis of input controls and 100µl of each sample was mixed with 900µl of a buffer containing 0.5%

Trition X-100, 2mM EDTA, and 10mM Tris pH 7.5, 150mM NaCl, 1mM DTT and 1 Complete Mini Protease Inhibitor tablet (Roche, Indianapolis, IN). Complexes were incubated with the anti-HA (1:500; Sigma-Aldrich, St. Louis, MO) or Acetyl-Histone H3 (1:1000; Abcam, Cambridge, UK) antibodies overnight at 4˚C with gentle agitation. Blocked agarose beads were added to each reaction and incubated at 4˚C for an additional 2 hours. Complexes were washed four times in a buffer containing 0.25% Tergitol-type NP-40, 0.5% SDS, 2mM EDTA, 20mM Tris (pH8.0), 250mM NaCl, 0.2µl/ml leupeptin, and 0.2µl/ml aprotinin. Complexes were then resuspended in 100mM $NaHCO_3$, 1% SDS and incubated at 65˚C overnight followed by a phenol-cholorform extraction. Real time PCR was performed using appropriate primers MMP-9 forward primer 5'-gattacaggaatgagccacca-3', MMP-9 reverse primer 5'-ctgtaggttgtaagtccgcaac-3', human glycoprotein hormone α subunit gene (h α JRE) forward 5'-tgacctaagggttgaaacaagataag-3', h α JRE reverse 5'-ggaaattccatccaatgattga-3', distal h α JRE forward 5'-agtttctttgtggatgaagagatagacg-3' and distal hα JRE reverse 5'-tttccgaacttcaaaggccctg-3'. The distal site on the human glycoprotein hormone α subunit gene served as a negative control. A standard curve was generated with the appropriate sample inputs, representing a 1:2, 1:20, and a 1:200 dilution.

Preparation of Stable Cell Lines Expressing Small Interference RNA's (siRNAs)- The mammalian expression vector, pSUPER-retro-neo (OligoEngine, Seattle, WA) was used for preparation and expression of specific siRNAs. Each gene-specific insert targeted a 19-nucleotide sequence within the human Dlx3 mRNA. The Dlx3 siRNA sequence was as follows: 5'-gtagaagactgtagctata-3'. A control siRNA vector was also prepared in pSUPER-retro-neo vector using a non-specific 19-nuclotide mammalian gene sequence (5'-ttctccgaacgtgtcacgt-3'), which served as a negative control for all studies (Applied Biosystems, Foster City, CA). To create stable cell populations of

siRNA expressing cells, JEG3 cells were cultured and transfected as outlined above. Twenty four hours following transfection, stable cell lines were selected for using 500 μg/ml neomycin in the culture media.

Immunocytochemistry- Control and stably transfected JEG3 cells were cultured on glass bottom culture dishes (MatTek Corporation, Ashland, MA) for 24 hours, rinsed with DPBS and fixed with 4% paraformaldehyde for 20 minutes on ice. Cells were then washed twice with cold DPBS and permeabilized in 0.3% Triton X-100 for 20 minutes at room temperature. Cells were then washed twice in DPBS and blocked in 3% bovine serum albumin (BSA) for 1 hour at room temperature. Primary Dlx3 antibody (1:500) was then delivered to the cells in 3% BSA overnight at 4˚C. Cells were washed twice in 0.3%Triton X-100 followed by incubation with a fluorescence-conjugated secondary antibody (Alexa 488, Molecular Probes Inc., Eugene, OR) for 1 hour at room temperature. Finally, cells were washed twice in DPBS and stained with DAPI glue (Vector labs, Burlingame, CA).

Quantitative (q)PCR- siRNA knockout cell lines were grown to ~80% confluence and RNA was harvested using TRIzol® (Invitrogen, Carlsbad, CA). Additionally, placental RNA was harvested and prepared using TRIzol® (Invitrogen, Carlsbad, CA) from the BPH/5 and C57 mice at E9.5 and E18.5. RNA was subjected to q-PCR using TaqMan® probes (Applied BioSystems, Foster City, CA) for MMP-9 and Dlx3, respectively. Analysis of the qPCR data has been previously described [18].

Statistical Analysis-Data were subjected to analysis of variance and differences between treatment groups using a Student's T-Test. Probability of less than 0.05 ($p<0.05$) was considered statistically significant.

Results

Dlx3$^{-/-}$ mouse placentas have reduced levels of MMP-9 protein and gelatinase activity- The Dlx3 knockout mouse dies at midgestation (~E9.5-10.5) due to placental dysfunction [17,18,20]. Further, placental microarray studies revealed that MMP-9 transcript levels were markedly reduced in the placentas of Dlx3$^{-/-}$ mice at E9.5 suggesting that MMP-9 may be an important target of Dlx3-dependent gene regulation [18]. Given the critical role MMPs and in particular, MMP-9 plays in the remodeling of placental ECM during trophoblast cell invasion and maternal spiral artery remodeling, we sought to investigate the activity levels of MMP-9 in the Dlx3$^{-/-}$ mouse model. Using Dlx3$^{+/+}$, $^{+/-}$, $^{-/-}$ mouse placental explants; we initially examined relative levels of secreted MMP-9 assayed in culture media (Figure 3.1A). Western analysis revealed that loss of both Dlx3 alleles resulted in a marked reduction in secreted MMP-9 in these cultures. This was corroborated by zymography studies of gelatinase activity using the same media collected 4 hours after culture (Figure 3.1B). Gelatinase activity associated with MMP-9 was again markedly reduced ($p<0.05$) in the Dlx3$^{-/-}$ placentas in culture. Similar observations were made examining media samples collected at the 6 hour time point (data not shown). The reduction in secreted MMP-9 activity was not attributable to an overall reduction in secretion from these explants since secretion of the anti-angiogenic glycoprotein, thrombospondin 2 [23,24] was increased markedly in a gene dosage-dependent manner where the highest thrombospondin 2 secretion occurred in the Dlx3 null placentas. These observations were consistent with changes in thrombospondin 2 transcript levels in the Dlx3$^{-/-}$ placenta in our previous array studies [18]. Interestingly in the Dlx3$^{+/-}$ placentas, MMP-9 protein levels and gelatinase activity was increased compared to the wildtype controls ($p<0.05$; Figure 3.1A and B). On potential interpretation of this observation is that haploinsufficiency at the Dlx3 loci induces an apparent compensatory mechanism associated with elevated MMP-9

protein and gelatinase activity; however, a more complete understanding of this mechanism(s) awaits further investigation.

MMP-9 gene promoter is active in placental cells and responsive to Dlx3 overexpression- To further investigate the mechanisms associated with Dlx3 regulation of the mouse MMP-9 gene, we cloned a 1.9kb portion of the 5'-flanking region of the mouse MMP-9 promoter and incorporated this promoter fragment into a luciferase reporter gene. Initially, we compared the expression level of the MMP-9 promoter fragment to other promoters known to be expressed in JEG3 choriocarcinoma cells as a model for placental trophoblasts. In transient transfection studies, MMP-9 promoter activity was observed to be ~175 fold greater ($p<0.05$) than the empty luciferase reporter (Figure 3.2A). Using equal amounts of reporter plasmid for transfection, MMP-9 promoter activity was similar to another placental-specific gene promoter, 5.2kb portion of the 5'-flanking region of mouse placental growth factor (PGF) gene promoter (Figure 3.2A)[18]; however, both MMP-9 and PGF promoter activity was markedly less ($p<0.05$) than the transcriptional activity associated with the human glycoprotein hormone α subunit gene promoter [25].

Transient co-tranfection studies with the MMP-9 gene promoter and increasing doses of pKH3-Dlx3 expression vector revealed the MMP-9 gene promoter was responsive to Dlx3 overexpression in a dose dependent manner (Figure 3.2B). Overexpression of Dlx3 was confirmed using Western blot analysis making use of the HA epitope on the overexpressed Dlx3 in cell lysates used to analyze luciferase activity. These studies provide important evidence that Dlx3 was overexpressed in a dose-dependent manner; further, additional western analysis examining Dlx3 (rather than the HA epitope) revealed that overexpression was evident at 2-3 fold over

Figure 3.1. MMP-9 protein and gelatinase activity is reduced in the Dlx3$^{-/-}$ mouse placenta. A. Wildtype (Dlx3$^{+/+}$), Dlx3 heterozygous (Dlx3$^{+/-}$), and Dx3 null (Dlx3$^{-/-}$) placental explants (n=4-6/genotype) were cultured for four hours and media was collected. Western blot analysis was used to determine secreted MMP-9 and thrombospondin 2 protein abundance in the Dlx3$^{-/-}$ compared with Dlx3$^{+/+}$. **B.** Zymography studies were performed to determine the amount of secreted MMP-9 gelatinase activity from the explant study. Gels were scanned and densiotometry measurements were obtained to determine the level of gelatinase activity corresponding to a band consistent with the molecular weight of MMP-9. All studies were replicated on at least three separate occasions with equivalent results.

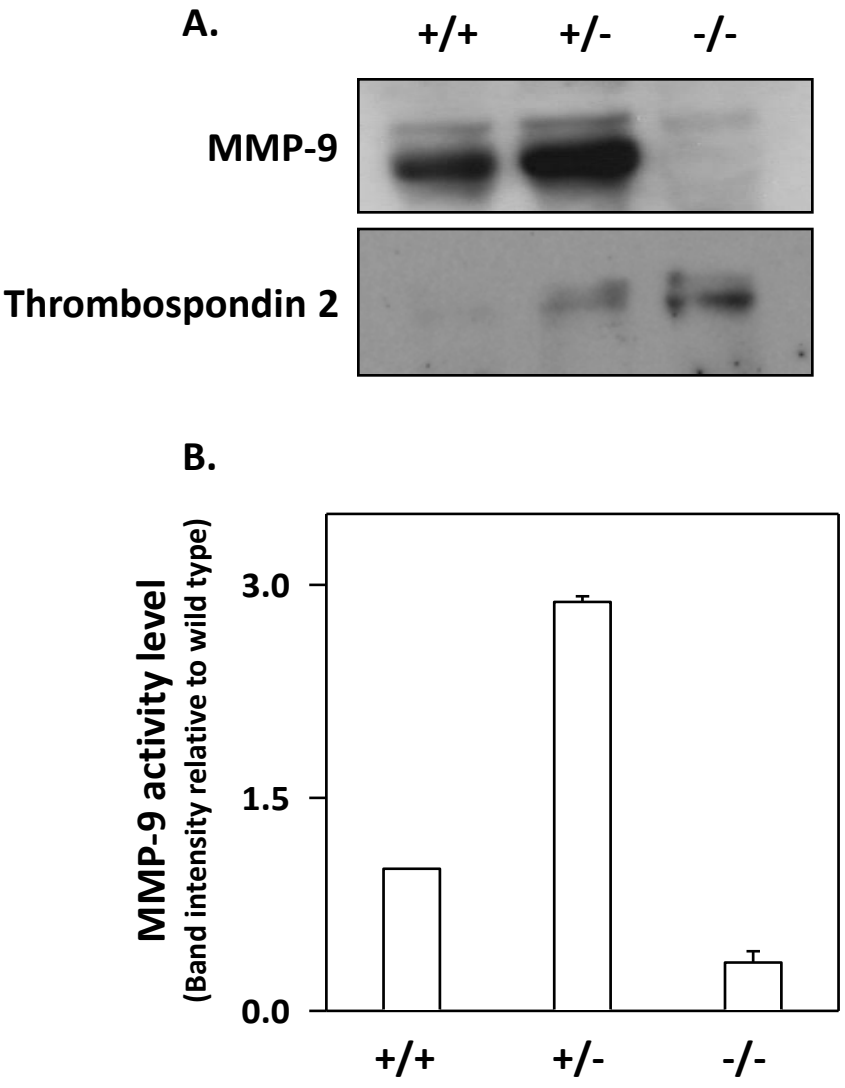
A.
+/+
+/-
-/-
MMP-9
Thrombospondin 2
B.
MMP-9 activity level
(Band intensity relative to wild type)
3.0
1.5
0.0
+/+
+/-
-/-

endogenous levels of Dlx3 (data not shown) suggesting that these overexpression studies did not reflect supra-physiological conditions.

Upon examination of 1.9kb portion of the mouse MMP-9 gene promoter, two Dlx3 near-consensus binding sites were identified; one near the proximal end of the MMP-9 gene promoter at -825 and one near the distal portion of the promoter at -1498 relative to the transcription start site [26]. Although both sites contain the core TAATT motif, the flanking nucleotides from each site varied from the Dlx3 consensus site (A/C/G) TAATT (G/A)(C/G) (Figure 3.3A). Electrophoretic mobility shift assays (EMSA) compared relative DNA binding of both the distal (-1498) and proximal (-825) sites using recombinant Dlx3 (rDlx3). Addition of rDlx3 resulted in dose-dependent DNA binding (Figure 3.3B). These studies were corroborated with studies using DNA affinity chromatography (Figure 3.3C). Using JEG3 nuclear extracts as a source of Dlx3, the distal (-1498) Dlx3 binding site was able to bind Dlx3 in this assay and Dlx3 binding was competed for using 50 and 100 fold molar excess of unbiotinylated oligonucleotides for the -1498 and -825 binding sites. These studies support the conclusion that recombinant and endogenous Dlx3 can bind these sites *in vitro*.

Dlx3 binding sites within the mouse MMP-9 gene promoter are required for basal and Dlx3-induced transactivation- In order to evaluate the importance of these near consensus Dlx3 binding sites within the mouse MMP-9 gene promoter, both the distal (MMP-9 Δ-1498) and proximal (MMP-9 Δ-825) sites were mutated alone and in combination in the context of the luciferase reporter. Each construct was transiently co-transfected into JEG3 cells with control vector or pKH3-Dlx3 to facilitate Dlx3 overexpression. Both of the individual mutants resulted in marked reduction ($p<0.05$) in basal expression of the MMP-9 luciferase reporter ($p<0.05$); however, neither

Figure 3.2. An MMP-9 promoter fragment coupled to a luciferase reporter is active in placental cells and responsive to Dlx3 overexpression. A. Transient transfection studies in JEG3 choriocarcinoma cells were used to compare the relative promoter activity of the 1.9kb portion of the MMP-9 gene promoter-luciferase reporter (MMP-9) to the luciferase reporter construct without a functional promoter (Empty), a 0.2kb portion of the glycoprotein hormone α-subunit (Ha-204), and 5.2kb placental growth factor (PGF) gene promoter luciferase reporter. **B.** Dlx3 overexpression was used to test the inducible activity of the MMP-9 luciferase reporter in JEG3 cells. Cotransfection of the MMP-9 luciferase reporter with a control vector (2.0μg) or increasing doses of an expression vector encoding hemaglutinin (HA) epitope-tagged Dlx3 (0.5, 1.0, and 2.0μg) were carried out. Data are reported as relative luciferase activity standardized by total cellular protein content from representative studies (n=3/treatment). Western analysis was used to confirm HA-tagged Dlx3 overexpression (inset). Lane 1 is control; Lanes 2 through 4 are HA-Dlx3 expression vector doses of 0.5, 1.0 and 2.0 mg, respectively. Actin was used as a lane loading control. All studies were replicated on at least three separate occasions with equivalent results.

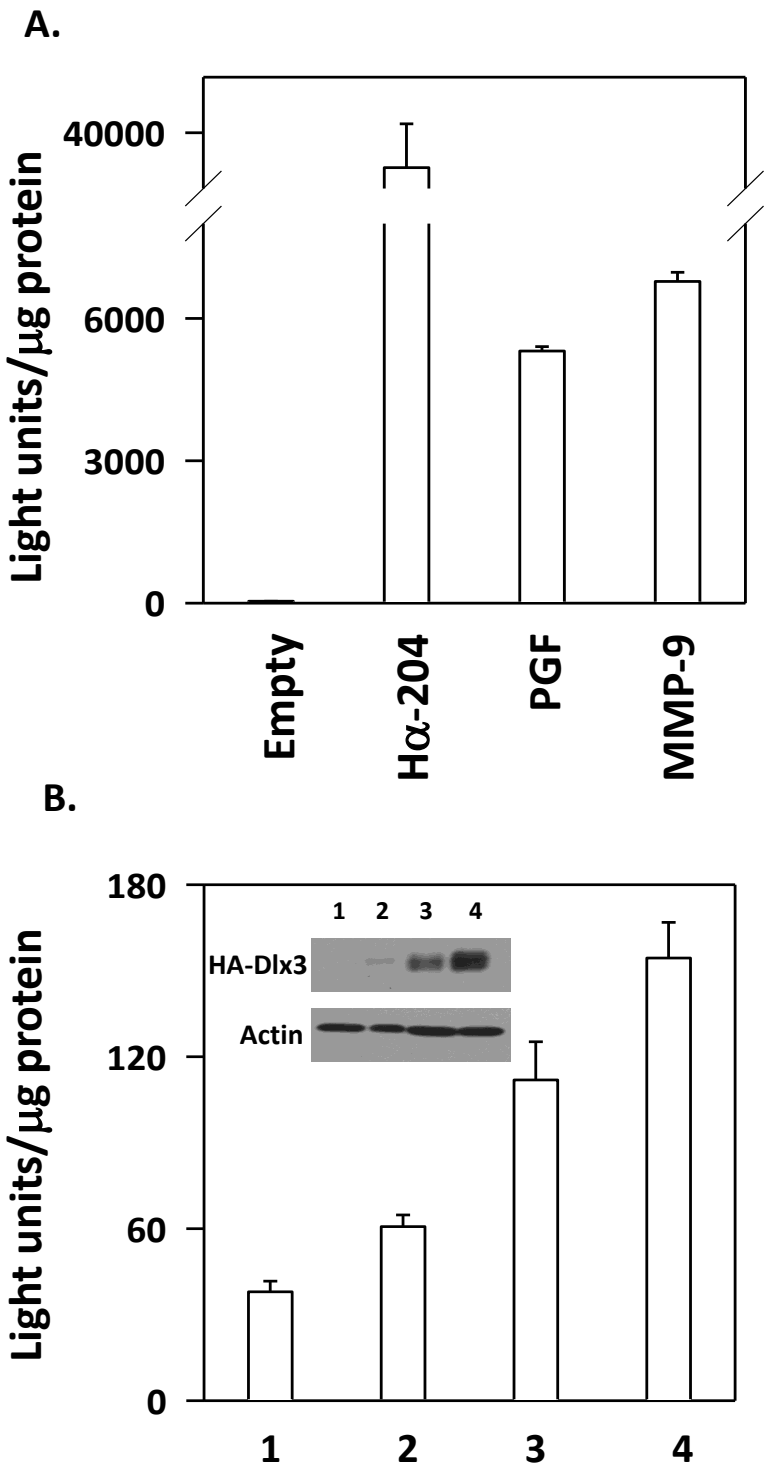
A.
Light units/μg protein
40000
6000
3000
0
Empty
Hα-204
PGF
MMP-9
B.
Light units/μg protein
180
120
60
0
1 2 3 4
HA-Dlx3
Actin
1
2
3
4

Figure 3.3. Dlx3 binds to two cis elements within the MMP-9 promoter fragment. **A.** Bioinformatic investigation of the MMP-9 gene promoter identified two near-consensus Dlx3 binding sites based upon homology to a consensus Dlx3 site. The positions of these sites (designated as probes) were at -1498 and -825 relative to the start site of transcription. **B.** Using electrophoretic mobility shift assay (EMSA), both binding sites were found to bind recombinant (r) Dlx3 with differing relative affinity. Dlx3 complexes as well as free probe are identified by arrows to the left of the panel. **C.** Using JEG3 nuclear extracts as a source of Dlx3 binding activity, DNA affinity chromatography followed by Western Blot studies revealed Dlx3 bound the -1498 site consistent with EMSA. Competition studies using the -1498 and -825 binding sites at 50 and 100 fold molar excess of unbiotinylated oligonucleotides were used to demonstrate specificity of binding. The same experiment was performed on the -825 site with similar results (data not shown). All studies were replicated on at least three separate occasions with equivalent results.

A.

Dlx3 consensus site	(A/C/G)	TAATT	(G/A)	(C/G)
-1498	T	TAATT	T	G
-825	C	TAATT	T	C

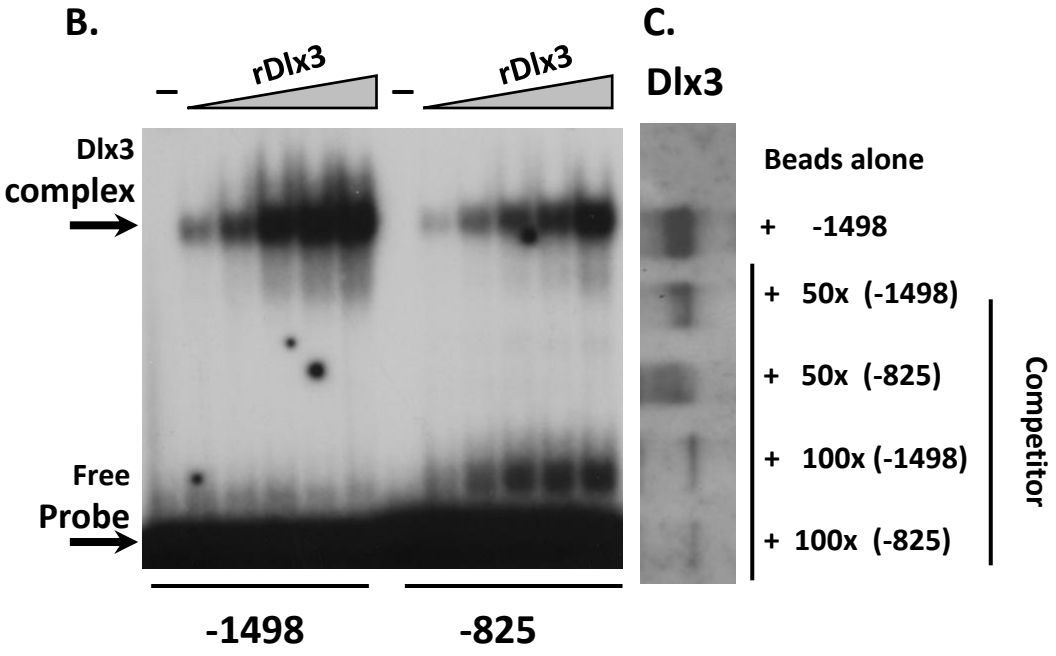

mutation blunted the response to Dlx3 overexpression (Figure 3.4). Only the combined mutations (MMP-9 Δ-1498+825) abolished ($p<0.05$) responsiveness of this promoter to Dlx3 overexpression (Figure 3.4). These findings indicate the interaction between Dlx3 and the cis-elements within the MMP-9 gene promoter are necessary for full transcriptional activation in placental trophoblasts.

Smad6 blocks the effects of Dlx3 on the MMP-9 gene promoter- As previously reported, Smad6 (an inhibitory or iSmad) has the ability to physically interact with and repress Dlx3 transcriptional activity on the human glycoprotein hormone α subunit and Esx-1 gene promoters in JEG3 cells [20]. This repression is thought to be due to Dlx3-Smad6 interactions leading to allosteric interference of Dlx3 DNA binding to target genes. We sought to investigate the transcriptional regulation of Smad6 on MMP-9 gene promoter activity in JEG3 cells. Co-transfection of pKH3-Dlx3 expression vector with the MMP-9 luciferase reporter resulted in a predictable ~four fold increase ($p<0.05$) in luciferase expression. Smad6 overexpression alone did not have an impact on the MMP-9 promoter luciferase reporter; however, when co-transfected together, Smad6 expression effectively blocked Dlx3-dependent induction of the MMP-9 reporter (Figure 3.5). These results are entirely consistent with previous studies of other dlx3 target genes and provide additional evidence that Dlx3 engagement on the MMP-9 gene promoter is necessary for full transcriptional regulation of this gene.

Dlx3 binds to the human MMP-9 gene promoter and is required for full MMP-9 expression in JEG3 cells- Studies thus far focused on the regulation of the mouse MMP-9 gene promoter consistent with our previous microarray studies of the $Dlx3^{-/-}$ mouse placenta [18]. We next sought to examine the putative binding of Dlx3 on the

Figure 3.4. Mutations within the two Dlx3 binding sites reduce basal MMP-9 promoter activity and abolish response to overexpression of Dlx3. Dlx3 binding sites within the MMP-9 gene promoter were mutated using a PCR-based site-directed mutagenesis. The 1.9kb portion of the MMP-9 gene promoter (wildtype), the mutation at the distal -1498 site (MMP-9 Δ-1498), proximal -825 site (MMP-9 Δ-825) and the combined mutations (MMP-9 Δ-1498+825) were cloned into a luciferase reporter. Transient transfection studies were performed in JEG3 cells with MMP-9 gene promoter-luciferase reporter constructs cotransfected with a control pKH3 vector (2.0μg) or 2.0μg of pKH3-Dlx3 expression vector. Data are reported as relative luciferase activity standardized by total cellular protein content from representative studies (n=3/treatment). All studies were replicated on at least three separate occasions with equivalent results.

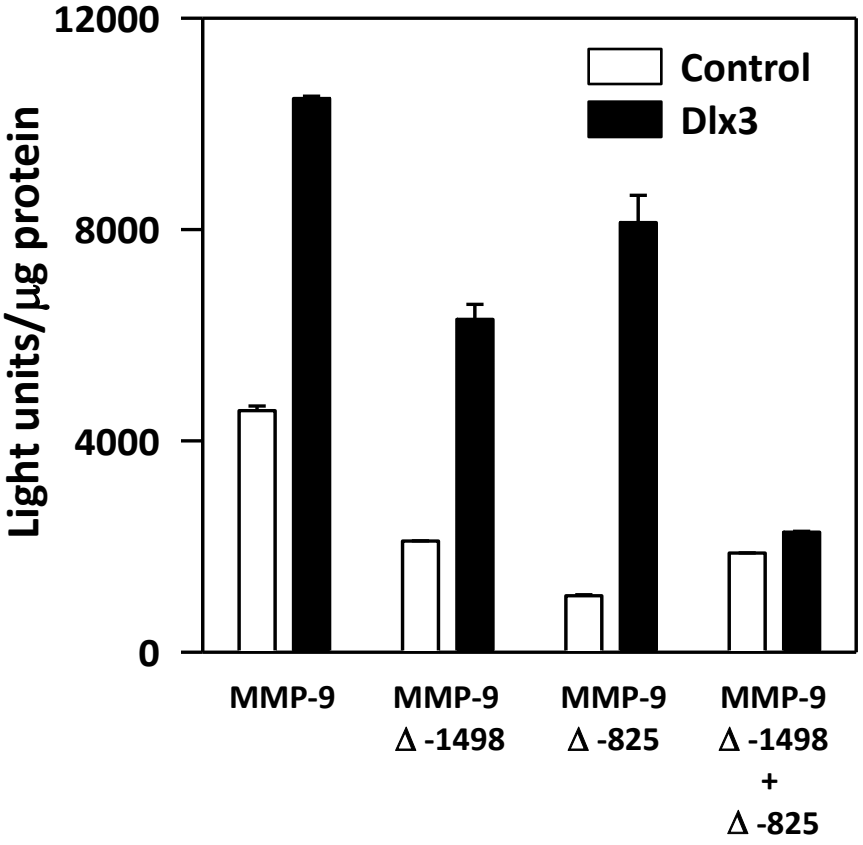
12000
8000
4000
0
Light units/μg protein
Control
Dlx3
MMP-9
MMP-9 Δ -1498
MMP-9 Δ -825
MMP-9 Δ -1498 + Δ -825

Figure 3.5. Smad6 blocks Dlx3-induced MMP-9 promoter activity. Transient co-transfection studies were carried out in JEG3 cells with the MMP-9 luciferase reporter, and Dlx3 and Smad6 expression constructs. Control cells were transfected with the reporter and control expression plasmids. Some cells were cotransfected pKH3-Dlx3 (2 mg), or CMV-Smad6 (500 ng) or the combination Dlx3 and Smad6. Data are reported as relative luciferase activity standardized by total cellular protein content from representative studies (n=3/treatment). All studies were replicated on two separate occasions with equivalent results.

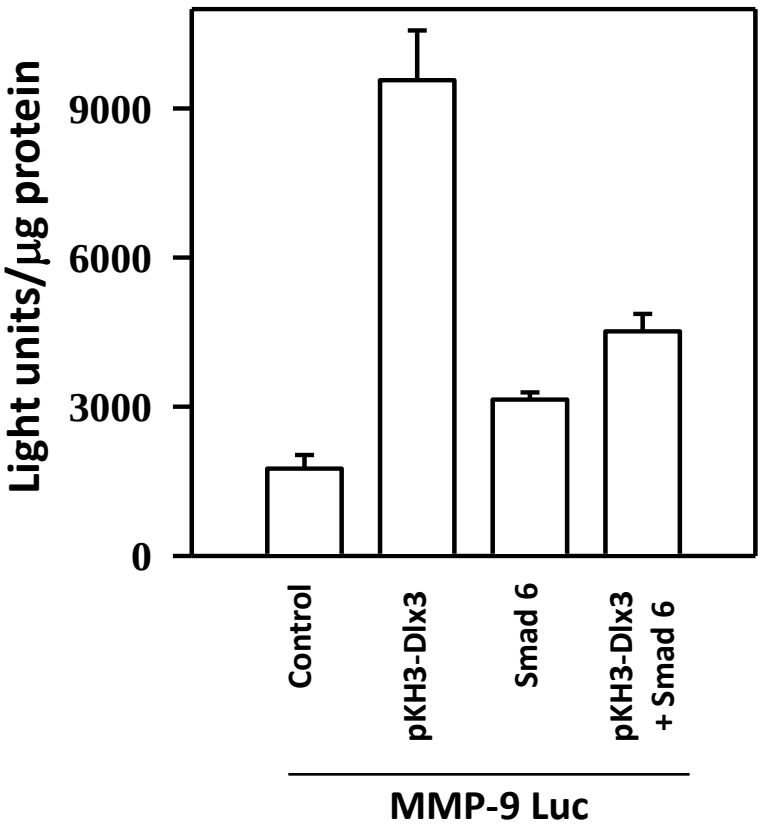
Light units/μg protein
9000
6000
3000
0
Control
pKH3-Dlx3
Smad 6
pKH3-Dlx3
+ Smad 6
MMP-9 Luc

human MMP-9 gene promoter using chromatin immunoprecipitation assay (ChIP). Boinformatic analysis of the human MMP-9 gene promoter revealed three near consensus Dlx3 binding sites containing the core TAATT motif within 2kb portion of the 5' flanking region specifically located at -1812, -1268 and -889 relative to the transcriptional start site of this gene (Figure 3.6A). Preliminary ChIP studies using our Dlx3 polyclonal antibody clearly demonstrated that this antibody was not of ChIP qualified and could not be used reliably for ChIP studies. As an alternative, pKH3-Dlx3 expression vector was transiently transfected in JEG3 cells and subsequent ChIP studies made use of the three HA epitopes engineered into this overexpressed protein. The HA ChIP studies revealed specific Dlx3 binding on the MMP-9 gene promoter at or near the -889 element ($p<0.05$; Figure 3.6B). Negative and positive controls for this ChIP study included examining a no antibody IP control, ChIP of the human glycoprotein hormone α subunit gene promoter at the junctional regulatory element (JRE) and a ChIP target ~2 kb upstream from the JRE on the same segment of DNA. Dlx3 engaged the JRE robustly in this assay ($p<0.05$) while the distal portion of the α subunit gene promoter served as a negative control. Lastly, all three targets were identified by ChIP using an acetylated-histone H3 (Ac-H3 IP) immunoprecipitation (Figure 3.6C). These ChIP studies provide strong evidence that the human MMP-9 gene promoter binds Dlx3 in placental trophoblasts.

siRNA mediated knockdown of human Dlx3 resulted in decreased endogenous MMP-9 transcript levels and gelatinase activity- To examine a requirement for Dlx3 on the human MMP-9 gene promoter, we sought to investigate endogenous MMP-9 transcript and protein abundance in an environment where Dlx3 was reduced in JEG3 cells. To create such an environment, we developed JEG3 cell lines stably expressing a specific Dlx3 siRNA hairpin. The siRNA Dlx3 cell line was

Figure 3.6. Human Dlx3 occupies the MMP-9 gene promoter endogenously. A. Analyses of the human MMP-9 gene promoter revealed three near consensus Dlx3 binding sites containing the core TAATT motif within a 2kb portion of the 5' flanking region specifically located at -1812, -1268 and -889 relative to the transcriptional start site of this gene. **B.** Chromatin immunoprecipitation (ChIP) studies were carried out in cells overexpressing HA-tagged Dlx3. Three separate targets were assayed by PCR following ChIP. As a positive control, the junctional regulatory element from the human a subunit gene promoter (h a JRE) was used; a target approximately 2 kb downstream of the JRE within the a subunit gene was used as a negative control; the putative Dlx3 binding at position -889 was arbitrarily selected within the human MMP-9 gene promoter. Mock transfections include transfection with en empty pKH3 plasmid. For each condition, a ChIP reaction was carried out without the primary antibody as a control. Acetylated-histone H3 (Ac-H3 IP) ChIP was used on all three targets as an additional positive control for the ChIP assay. This ChIP study was carried out on two separate occasions, each in triplicate, with similar results.

A.

Dlx3 consensus site	(A/C/G)	TAATT	(G/A)	(C/G)
Human -1812	T	TAATT	T	A
Human -1268	A	TAATT	G	G
Human -889	G	TAATT	A	A

B.

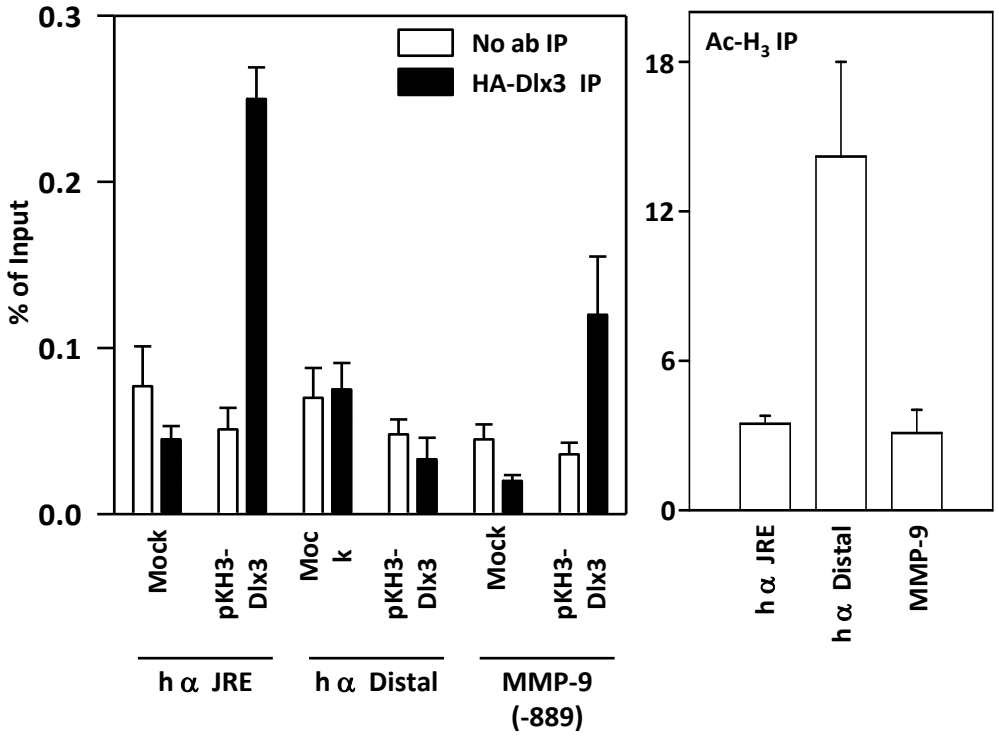

characterized by reduction of ~60-70% of MMP-9 transcript abundance relative to the control siRNA cell line (Figure 3.7A). Consistent with the transcript data, Dlx3 protein levels were markedly reduced and this correlated well with reduced MMP-9 protein levels as measured by Western blot analysis (Figure 3.7B) and immunocytochemistry (Figure 3.7C). To evaluate a relationship between reduced Dlx3 protein levels and MMP-9 gelatinase activity, media from siRNA knockout cell lines was collected and subjected to zymography to investigate gelatinase activity associated with MMP-9. Results indicated ~50% reduction ($p<0.05$) in MMP-9 activity in the siRNA Dlx3 cell line compared to the siRNA control cell line (Figure 3.8). Combined these data support our working hypothesis that in human trophoblasts, Dlx3 engages the MMP-9 gene promoter and is necessary for MMP-9 expression and gelatinase activity.

Dlx3 and MMP-9 transcript levels during gestation in the BPH/5 mouse- As indicated earlier, misregulation of MMP-9 transcript and activity levels in the placenta has been associated with at least a subset of human patients experiencing PE [8,11,27]; however, these finding have not been consistently observed across PE studies in the literature [13,14]. In an attempt to reconcile these disparities, we examined Dlx3 and MMP-9 transcript levels at two time points during gestation in a novel mouse model of PE, the BPH/5 mouse. The advantage of this animal model of PE is that these mice develop maternal disease (hypertension and proteinuria) in a manner consistent with human disease. These mice are characterized by altered placental morphogenesis, failed maternal spiral artery remodeling and intrauterine growth retardation again consistent with PE in women [28]. Moreover, this mouse model provides the unique opportunity to examine specific gestational ages that are simply not possible in human patients. In this study, we isolated placental RNA from both BPH/5 and C57control

Figure 3.7. Knockdown of human Dlx3 using siRNA results in reduced expression of MMP-9 in JEGS cells. A. Knockdown of Dlx3 was accomplished in stably transfected JEG3 cells using specific siRNAs (siRNA control or Dlx3). In the siRNA Dlx3 cell lines, mRNA levels of endogenous MMP-9 were decreased ~60% compared to control cells or the control siRNA cell line as measured by qPCR. **B.** Dlx3 protein levels were reduced by ~70% in the siRNA Dlx3 cell line as detected by immunoblot. This result was correlated with reductions in MMP-9 protein levels in the same cell line. Actin was used as a lane loading control. **C.** Immunocytochemistry was also used to demonstrate reduced levels of Dlx3 in the siRNA Dlx3 cell line compared to the control. All studies were replicated on at least three separate occasions with equivalent results.

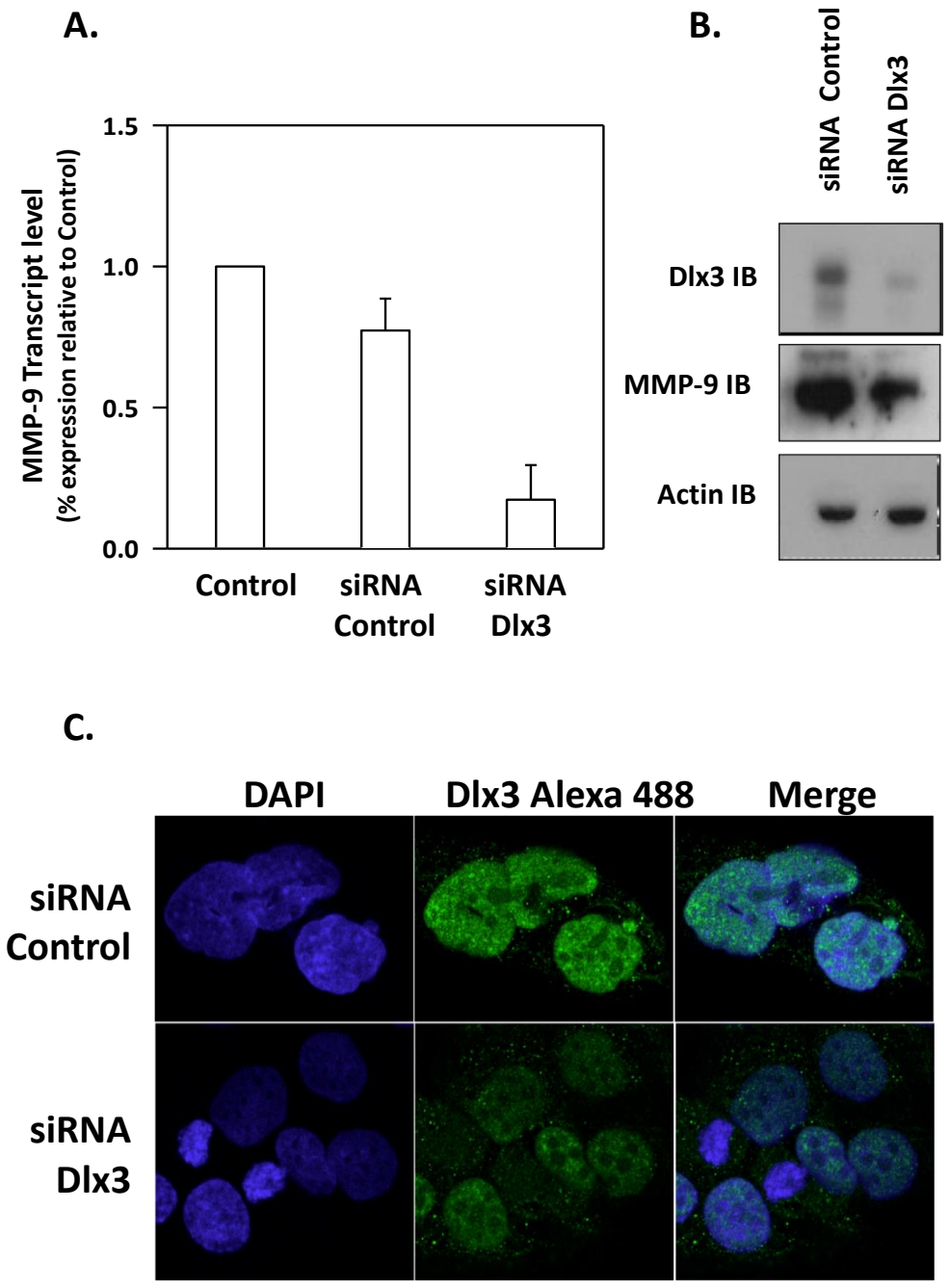
A.
B.
MMP-9 Transcript level
(% expression relative to Control)
1.5
1.0
0.5
0.0
Control
siRNA Control
siRNA Dlx3
siRNA Control
siRNA Dlx3
Dlx3 IB
MMP-9 IB
Actin IB
C.
DAPI
Dlx3 Alexa 488
Merge
siRNA Control
siRNA Dlx3

Figure 3.8. Secreted MMP-9 gelatinase activity is reduced in the siRNA Dlx3 cell line. Media collected from control siRNA and siRNA Dlx3 cell lines following four hours of culture was used in zymography assays to determine secreted gelatinase activity. Gels were scanned and densiotometry measurements were obtained to determine the level of gelatinase activity corresponding to a band consistent with the molecular weight of MMP-9. All studies were replicated on three separate occasions with equivalent results.

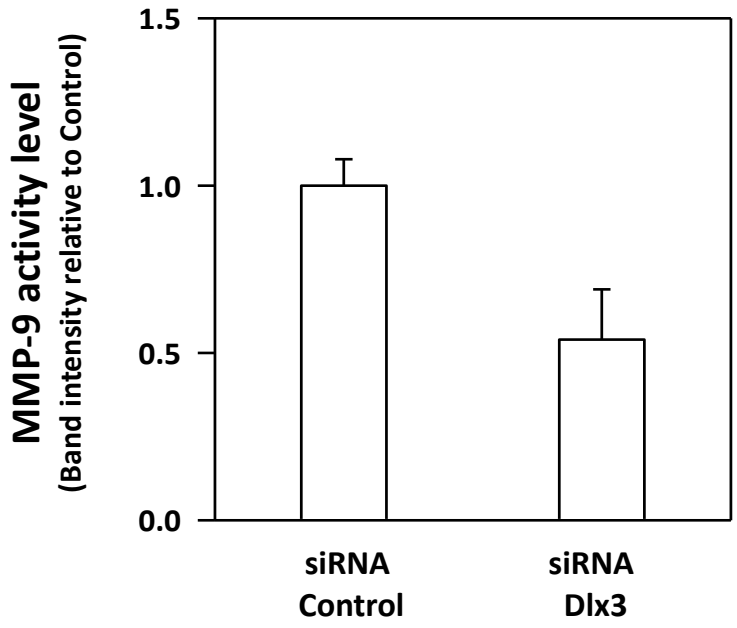
MMP-9 activity level
(Band intensity relative to Control)
1.5
1.0
0.5
0.0
siRNA
Control
siRNA
Dlx3

mice at 2 different gestational time points, E9.5 and 18.5. Figure 3.9 depicts steady-state Dlx3 and MMP-9 mRNA levels as determined by q-PCR. For each transcript within gestational age, the C57 transcript abundance was standardized to 1.0 and BPH/5 transcript levels are reported relative to the C57 value. At the early gestational time point (E9.5) transcript levels of both Dlx3 and MMP-9 were markedly reduced ($p<0.05$). At near term (E18.5), both transcripts were found to be upregulated compared to the C57 control. These data provide the first report of altered Dlx3 mRNA expression during early stages of PE in this model, well prior to onset of maternal disease in these mice. Further, the correlation between altered Dlx3 and MMP-9 transcript levels was completely consistent with a role for Dlx3 in the regulation of MMP-9 gene expression in this model.

Figure 3.9. Dlx3 and MMP-9 transcripts are misregulated in a mouse model of preeclampsia. Placental RNA was collected from both BPH/5 and control C57 mice (n=3/genotype) at 2 different gestational time points, E9.5 and 18.5. Quantitative PCR (q-PCR) was used to determine abundance of Dlx3 and MMP-9 transcripts using b actin as an internal standard. For each transcript within gestational age, the C57 control levels were set to 1.0 and Dlx3 and MMP-9 transcript levels are reported relative to this standardization.

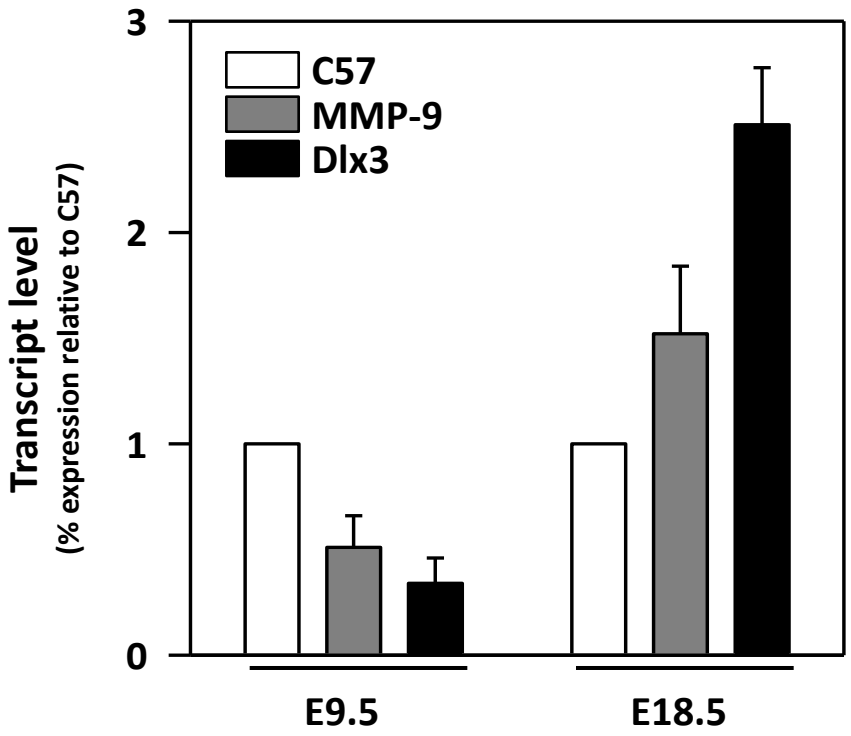
3
2
1
0
C57
MMP-9
Dlx3
Transcript level
(% expression relative to C57)
E9.5
E18.5

Discussion

Loss of Dlx3 has been linked to placental insufficiency and midgestation lethality in the $Dlx3^{-/-}$ mouse model [17]. These findings suggest a dynamic role for Dlx3 and putatively the Dlx3 gene network in facilitating proper placentation necessary for adequate fetal fitness and successful pregnancy in the mouse. The current studies demonstrate the ability of this homeodomain-containing placental specific transcriptional regulator to bind to and regulate the mouse and likely human MMP-9 gene promoters in trophoblasts. Our working model suggests that within populations of placental trophoblasts, Dlx3-dependent regulation of MMP-9 expression and activity may underlie aspect of altered ECM remodeling potential leading to alterations in trophoblast invasive properties and placental morphogenesis in the mouse. More broadly, the mechanistic relationship between Dlx3 and its gene target, MMP-9 may also contribute to early determinants related to the onset of maternal disease in the BPH/5 mouse model of preeclampsia.

MMPs are a complex family of proteolytic enzymes linked to various developmental processes including cell invasion, migration and ECM/tissue remodeling. This complexity is underscored by multiple levels of regulation of MMPs including changes in gene transcription and transcript abundance, requirements for zinc for MMP endopeptidase activity, post-translational cleavage of some of these enzymes for activity, subcellular localization (membrane associated versus secreted) and control of MMP activity by tissue inhibitors of MMP or TIMPs[29]. The current studies provide important evidence for the role of Dlx3 in the regulation of MMP-9 gene transcription and activity in placental trophoblasts. MMP-9 proteolytic activity has been shown to degrade denatured collagens and basement membrane components [30], cleave fibrin [31], serpin α_1-proteinase inhibitor [32], interleukin-1β (IL-1β) [33], and

transforming growth factor-β (TGF-β) [34] revealing the involvement of MMP-9 in many processes including tissue remodeling, inflammatory responses, and metastasis in the progression of cancer. As there are currently 20 recognized MMP family members in humans, it is difficult at present to ascribe specific functions to discrete members of this family without careful consideration of potential redundancies in activity. In the placenta, it would appear that MMP-2 and MMP-9 may be playing central roles based on several published studies [8,9,11]. One of the primary steps for proper placentation includes invasion of extravillous trophoblasts into maternal deciduas where extensive ECM remodeling appears to take place. In the normal placenta, this includes extensive maternal spiral artery remodeling by trophoblasts to facilitate appropriate perfusion of the placental vascular bed [2]. When this fails to occur in a spatially and temporally restricted manner, placental dysfunction can occur, potentially leading to health complications. For example in placental tissues examined from patients experiencing preeclampsia, shallow trophoblast invasion impairs spiral artery and arteriole remodeling causing reduced uteroplacental blood flow and compromised fetal fitness [6,35]. Similar observations of inadequate maternal spiral artery remodeling have also been made using the BPH/5 mouse model [36]. Currently the role of MMP-2 and MMP-9 during placental morphogenesis is controversial since only a subset of studies provide strong evidence of a role for these MMPs during placental development and possible complications such as those seen with preeclampsia [8,11,14,15]. The present studies extend our understanding of the specific role of Dlx3 and MMP-9 on placental morphogenesis in mouse and human trophoblast models.

Our studies suggest that the $Dlx3^{-/-}$ mouse placenta is largely deficient in its ability to secrete MMP-9 and as such displays diminished MMP-9 gelatinase activity *in vitro* (Figure 3.1). Since Dlx3 is expressed earlier in the etoplacental cone and

chorionic plate and later predominantly within trophoblast populations in the labyrinth [17], it is reasonable to assume MMP-9 activity is playing a fundamental role in the ECM remodeling that occurs within these compartments to establish implantation and fetal/maternal vascular relationships. Surprisingly, MMP-9 secretion and activity in the $Dlx3^{+/-}$ placenta was seen to be increased, appreciably higher than anticipated; this is perhaps suggestive of some compensatory mechanism. Additional studies of this phenomenon will be necessary to fully understand the importance of this observation. Equally interesting was the observation that, unlike diminished secretion of MMP-9, thrombospondin 2 secretion was markedly elevated in the $Dlx3^{-/-}$ placenta. These observations were consistent with predictions made from the microarray data comparing $Dlx3^{+/+}$ and $^{-/-}$ placentas [18]. In those studies, thrombospondin 2 transcript levels were upregulated ~2-3 fold in $Dlx3^{-/-}$ placentas and this array data was validated using qPCR. Thrombospondin 2 is a secreted glycoprotein known to inhibit angiogenesis, particularly in cancer models [23]. It is presently unclear if Dlx3 may be playing a direct role in transcriptional repression of the thrombospondin 2 gene promoter or if the apparent elevation of thrombospondin 2 transcript levels and secretion observed in the current studies reflects a more complex and potentially indirect mechanism(s). The reciprocal relationship between loss of MMP-9 secretion concurrent with elevated thrombospondin 2 secretion from the E9.5 mouse placenta raised the intriguing possibility that Dlx3 may regulate both the invasive properties of placental trophoblasts to establish fetal/maternal vascular relationships through regulation of MMP-9 (and potentially other ECM remodeling factors) and modulate angiogenic tone within the developing placenta through control of thrombospondin 2. While entirely speculative, alterations in the combined actions of these two secreted protein likely contributes to placental failure of the $Dlx3^{-/-}$ mouse at multiple levels.

Perhaps the most exciting finding of the current studies is the characterization of mis-expression of Dlx3 and Dlx3 target genes such as MMP-9 in the BPH/5 mouse model of preeclampsia. The BPH/5 mouse exhibits a number of important characteristics of preeclampsia such as maternal hypertension and proteinuria late in gestation; BPH/5 mice display abnormal maternal spiral artery remodeling and placental insufficiency characterized by a decrease in branching morphogenesis and overall decreased labyrinth layer by E12.5; intrauterine growth retardation is also evident in this animal model [28,36]. These defects during pregnancy were shown recently to be largely ameliorated by feeding a superoxide dismutase mimetic suggesting that oxidative stress is playing an important role in progression of preeclampsia [28]. Collectively, these observations provide exciting support that this mouse model may reflect an important resource in our understanding of the basic determinants that underlie this complex disease.

The current studies examining transcript profiling of Dlx3 and MMP-9 during early and late gestation in the BPH/5 mouse support the conclusion that at both gestational ages transcript misexpression occurs, likely for different reasons. One of the important early observations that lead to the identification of this model was that BPH/5 mice had reduced litter sizes [19]. This simple observation actually reflected important phenotypic variability during gestation associated with this model. Specifically, BPH/5 fetuses decline in number as gestation progresses suggesting that subsets of BPH/5 fetuses experience differing levels of intrauterine stresses. Our current studies suggest that early in gestation, Dlx3 and MMP-9 transcript abundance is markedly reduced compared to the C57 control mice. Although speculative, there is a strong likelihood that at this gestational age, the complete spectrum of fetal/placental phenotypic variation exists within the BPH/5 uterus and changes at this time likely reflect important changes associated with determinants of preeclampsia prior to the

onset of maternal disease. Interestingly, loss of MMP-9 in the MMP-9 knockout mouse resulted in a compensatory mechanism in the cyclooxygenase (COX) 1 pathway leading to enhanced production of prostaglandin E_2 involved in increased vascular permeability in neutrophils [37]. While these studies did not consider the placenta, similar mechanisms may contribute to placental vascular (dys)function beyond an invasive phenotype. Conversely, at late gestational age (E18.5), the positive correlation between Dlx3 and MMP-9 remains; however, both transcripts are essentially overexpressed. This result reflects the subset of fetuses that remain viable at term in the BPH/5 mice and are clearly a phenotypically different population than those present at E9.5. Nonetheless, these observations late in gestation may reflect important contributions to disease progression. Equally plausible is the possibility that that at E18.5, changes in Dlx3 and MMP-9 transcript abundance in the BPH/5 mouse are a result (rather than a cause) of disease progression. Future studies will focus on these possibilities.

In conclusion, the present studies highlight the important interplay between Dlx3 and MMP-9 in the placenta suggesting a role for both of these genes in proper placentation. The MMP-9 gene promoter appears to be a target of Dlx3 transcriptional regulation in both mouse and human trophoblasts. The finding that thrombospondin 2 expression is also coordinately regulated within this gene network provides compelling evidence that Dlx3 may be controlling placental labyrinth development at multiple levels; controlling an invasive phenotype and modulating the angiogenic environment. Finally, Dlx3 and MMP-9 may reflect important early genetic determinants in the BPH/5 mouse model of preeclampsia and represent important biomarkers for future studies focusing the pathophysiology of this disease.

REFERENCES

[1] Rossant, J. and Cross, J. C., Placental development: lessons from mouse mutants. *Nat Rev Genet* **2** (7), 538 (2001).

[2] Pijnenborg, R., Bland, J. M., Robertson, W. B., and Brosens, I., Uteroplacental arterial changes related to interstitial trophoblast migration in early human pregnancy. *Placenta* **4** (4), 397 (1983).

[3] Harris, L. K. et al., BeWo cells stimulate smooth muscle cell apoptosis and elastin breakdown in a model of spiral artery transformation. *Hum Reprod* **22** (11), 2834 (2007).

[4] Gallery, E. D. et al., Preeclamptic decidual microvascular endothelial cells express lower levels of matrix metalloproteinase-1 than normals. *Microvasc Res* **57** (3), 340 (1999).

[5] Khong, T. Y., Lane, E. B., and Robertson, W. B., An immunocytochemical study of fetal cells at the maternal-placental interface using monoclonal antibodies to keratins, vimentin and desmin. *Cell Tissue Res* **246** (1), 189 (1986); McFadyen, I. R., Price, A. B., and Geirsson, R. T., The relation of birthweight to histological appearances in vessels of the placental bed. *Br J Obstet Gynaecol* **93** (5), 476 (1986).

[6] Pijnenborg, R. et al., Placental bed spiral arteries in the hypertensive disorders of pregnancy. *Br J Obstet Gynaecol* **98** (7), 648 (1991).

[7] Paiva, P., Salamonsen, L. A., Manuelpillai, U., and Dimitriadis, E., Interleukin 11 inhibits human trophoblast invasion indicating a likely role in the decidual restraint of trophoblast invasion during placentation. *Biol Reprod* **80** (2), 302 (2009).

[8] Campbell, S., Rowe, J., Jackson, C. J., and Gallery, E. D., Interaction of cocultured decidual endothelial cells and cytotrophoblasts in preeclampsia. *Biol Reprod* **71** (1), 244 (2004).

[9] Li, J. K., Xiong, Q., Zhou, S., and Yang, P. F., [Differences between the expression of matrix metalloproteinase-2, 9 in preeclampsia and normal placental tissues]. *Zhonghua Fu Chan Ke Za Zhi* **42** (2), 73 (2007).

[10] Qiao, C., Wang, C. H., Shang, T., and Lin, Q. D., [Clinical significance of KiSS-1 and matrix metalloproteinase-9 expression in trophoblasts of women with preeclampsia and their relation to perinatal outcome of neonates]. *Zhonghua Fu Chan Ke Za Zhi* **40** (9), 585 (2005).

[11] Shokry, M. et al., Expression of matrix metalloproteinases 2 and 9 in human trophoblasts of normal and preeclamptic placentas: preliminary findings. *Exp Mol Pathol* **87** (3), 219 (2009).

[12] Zhang, H., Lin, Q. D., and Qiao, C., [Expression of trophoblast invasion related genes mRNA and protein in human placenta in preeclampsia]. *Zhonghua Fu Chan Ke Za Zhi* **41** (8), 509 (2006).

[13] Huisman, M. A. et al., Matrix-metalloproteinase activity in first trimester placental bed biopsies in further complicated and uncomplicated pregnancies. *Placenta* **25** (4), 253 (2004).

[14] Palei, A. C., Sandrim, V. C., Cavalli, R. C., and Tanus-Santos, J. E., Comparative assessment of matrix metalloproteinase (MMP)-2 and MMP-9, and their inhibitors, tissue inhibitors of metalloproteinase (TIMP)-1 and TIMP-2 in preeclampsia and gestational hypertension. *Clin Biochem* **41** (10-11), 875 (2008).

[15] Lockwood, C. J. et al., Matrix metalloproteinase 9 (MMP9) expression in preeclamptic decidua and MMP9 induction by tumor necrosis factor alpha and

interleukin 1 beta in human first trimester decidual cells. *Biol Reprod* **78** (6), 1064 (2008).

[16] Morasso, M. I., Markova, N. G., and Sargent, T. D., Regulation of epidermal differentiation by a Distal-less homeodomain gene. *J Cell Biol* **135** (6 Pt 2), 1879 (1996); Berghorn, K. A. et al., Developmental expression of the homeobox protein Distal-less 3 and its relationship to progesterone production in mouse placenta. *J Endocrinol* **186** (2), 315 (2005); Depew, M. J., Simpson, C. A., Morasso, M., and Rubenstein, J. L., Reassessing the Dlx code: the genetic regulation of branchial arch skeletal pattern and development. *J Anat* **207** (5), 501 (2005).

[17] Morasso, M. I. et al., Placental failure in mice lacking the homeobox gene Dlx3. *Proc Natl Acad Sci U S A* **96** (1), 162 (1999).

[18] Han, L. et al., Analysis of the gene regulatory program induced by the homeobox transcription factor distal-less 3 in mouse placenta. *Endocrinology* **148** (3), 1246 (2007).

[19] Davisson, R. L. et al., Discovery of a spontaneous genetic mouse model of preeclampsia. *Hypertension* **39** (2 Pt 2), 337 (2002).

[20] Berghorn, K. A. et al., Smad6 represses Dlx3 transcriptional activity through inhibition of DNA binding. *J Biol Chem* **281** (29), 20357 (2006).

[21] Herron, G. S., Werb, Z., Dwyer, K., and Banda, M. J., Secretion of metalloproteinases by stimulated capillary endothelial cells. I. Production of procollagenase and prostromelysin exceeds expression of proteolytic activity. *J Biol Chem* **261** (6), 2810 (1986).

[22] Roberson, M. S. et al., A role for the homeobox protein Distal-less 3 in the activation of the glycoprotein hormone alpha subunit gene in choriocarcinoma cells. *J Biol Chem* **276** (13), 10016 (2001).

[23] Krady, M. M. et al., Thrombospondin-2 modulates extracellular matrix remodeling during physiological angiogenesis. *Am J Pathol* **173** (3), 879 (2008).

[24] De Stefano, D. et al., NF-kappaB blockade upregulates Bax, TSP-1, and TSP-2 expression in rat granulation tissue. *J Mol Med* **87** (5), 481 (2009).

[25] Roberson, M. S. et al., A role for mitogen-activated protein kinase in mediating activation of the glycoprotein hormone alpha-subunit promoter by gonadotropin-releasing hormone. *Mol Cell Biol* **15** (7), 3531 (1995).

[26] Backstrom, J. R. and Tokes, Z. A., The 84-kDa form of human matrix metalloproteinase-9 degrades substance P and gelatin. *J Neurochem* **64** (3), 1312 (1995).

[27] Campbell, S., Rowe, J., Jackson, C. J., and Gallery, E. D., In vitro migration of cytotrophoblasts through a decidual endothelial cell monolayer: the role of matrix metalloproteinases. *Placenta* **24** (4), 306 (2003).

[28] Hoffmann, D. S. et al., Chronic tempol prevents hypertension, proteinuria, and poor feto-placental outcomes in BPH/5 mouse model of preeclampsia. *Hypertension* **51** (4), 1058 (2008).

[29] Stetler-Stevenson, W. G., The tumor microenvironment: regulation by MMP-independent effects of tissue inhibitor of metalloproteinases-2. *Cancer Metastasis Rev* **27** (1), 57 (2008).

[30] Hibbs, M. S., Hoidal, J. R., and Kang, A. H., Expression of a metalloproteinase that degrades native type V collagen and denatured collagens by cultured human alveolar macrophages. *J Clin Invest* **80** (6), 1644 (1987).

[31] Lelongt, B. et al., Matrix metalloproteinase 9 protects mice from anti-glomerular basement membrane nephritis through its fibrinolytic activity. *J Exp Med* **193** (7), 793 (2001).

[32] Liu, Z. et al., The serpin alpha1-proteinase inhibitor is a critical substrate for gelatinase B/MMP-9 in vivo. *Cell* **102** (5), 647 (2000).

[33] Ito, A. et al., Degradation of interleukin 1beta by matrix metalloproteinases. *J Biol Chem* **271** (25), 14657 (1996).

[34] Yu, Q. and Stamenkovic, I., Cell surface-localized matrix metalloproteinase-9 proteolytically activates TGF-beta and promotes tumor invasion and angiogenesis. *Genes Dev* **14** (2), 163 (2000).

[35] Pijnenborg, R., Vercruysse, L., and Hanssens, M., The uterine spiral arteries in human pregnancy: facts and controversies. *Placenta* **27** (9-10), 939 (2006).

[36] Dokras, A. et al., Severe feto-placental abnormalities precede the onset of hypertension and proteinuria in a mouse model of preeclampsia. *Biol Reprod* **75** (6), 899 (2006).

[37] Kolaczkowska, E. et al., Enhanced early vascular permeability in gelatinase B (MMP-9)-deficient mice: putative contribution of COX-1-derived PGE2 of macrophage origin. *J Leukoc Biol* **80** (1), 125 (2006).

CHAPTER FOUR

DISTAL-LESS (DLX) 3 HAPLOINSUFFICIENCY RESULTS IN PLACENTAL OXIDATIVE STRESS AND INTRAUTERINE GROWTH RETARDATION IN THE MOUSE

Clark PA[1], Woods AK[1], Riccio ML[1,2], Han L[1], Brown JL[1], Southard TL[1], Davisson RL[1,3], and Roberson MS[1]

[1] Department of Biomedical Sciences, Cornell University, Ithaca NY
[2] Micro-Computed Tomography Imaging Facility, Cornell University, Ithaca, NY
[3] Cell and Developmental Biology, Weill Cornell Medical College, New York, NY

Abstract

Distal-less 3 (Dlx3), a homeodomain-containing placental-specific transcription factor, is required for normal placentation and fetal development in the mouse. $Dlx3^{-/-}$ mice die at embryonic day (E) 9.5 putatively due to placental insufficiency. Initially, to test the hypothesis that loss of Dlx3 within the placenta caused embryonic lethality in the $Dlx3^{-/-}$ mouse, Dlx3 conditional knockout mice were generated using an epiblast-specific $Meox2^{CreSor}$. A subpopulation of the $Dlx3^{-/flox}$ x $Meox2^{CreSor}$ animals survived to weaning and beyond indicating loss of Dlx3 in the placenta likely is a primary cause of embryonic lethality associated with the $Dlx3^{-/-}$ mouse model. Intrauterine growth retardation (IUGR), along with improper placentation, are hallmarks of preeclampsia in the BPH/5 mouse model and in women. Although the underlying genetic mechanism(s) for the BPH/5 phenotype has not been elucidated, studies reported in Chapter 3 of this dissertation reveal a reduction of Dlx3 transcript levels in the placentas of BPH/5 mice at E9.5. These studies support for the hypothesis that early genetic determinants of preeclampsia in this model may include mis-regulation of the Dlx3 gene program. The aim of the current studies was to determine if loss of a single Dlx3 allele would affect fetal growth in mice. $Dlx3^{+/-}$ mice were characterized by a marked reduction in fetal weight and crown rump length compared to control fetuses beginning at E12.5 ($p<0.05$), which was compensated for by E18.5. This delay in fetal growth was correlated to increased oxidative stress and elevated apoptosis within $Dlx3^{+/-}$ placentas. Consistent with these findings, supplementation $Dlx3^{+/-}$ mice with the superoxide dismutase mimetic, Tempol, throughout gestation effectively rescued the IUGR phenotype. Perhaps more interesting, supplementation of Tempol rescued a small proportion of $Dlx3^{-/-}$ animals to E12.5, fully 3 days beyond the timeframe of normal fetal demise. $Dlx3^{+/-}$ mice were also characterized by reduced VEGF in maternal serum at E12.5. This putative loss in

angiogenic potential was correlated with reduced maternal spiral artery cross-sectional area ($p<0.05$). Administration of Tempol restored maternal spiral artery area in the $Dlx3^{+/-}$ mice consistent with the observed rescue of fetal growth. Collectively, these data support the conclusion that haploinsufficiency at the Dlx3 locus results in reduced fetal fitness in midgestation corresponding with elevated oxidative stress and reduced maternal spiral artery cross-sectional area within the mouse placenta. Administration of antioxidant therapy throughout gestation effectively reduced oxidative stress and ameliorated this fetal/placental phenotype.

Introduction

Dlx3 is a homeodomain-containing transcription factor that has been known to play a role in many developing tissues. Dlx3 is expressed in hair follicles, tooth germ cells, branchial arch mesenchme, interfollicular epidermis, and the developing placenta [1-3]. In general, Dlx3 appears to play a key role in the differentiation of epithelial compartments including epidermis. Ectopic expression of Dlx3 in the basal layer of mouse epidermis resulted in cessation of proliferation of the basal cells and the activation of profilaggin, a late differentiation marker of keratinocytes [4]. Deletion of Dlx3 in mice results in mid-gestational lethality due putatively to placental insufficiency; however $Dlx3^{+/-}$ mice are viable and fertile [2]. In the primate placenta, Dlx3 was identified as a key transcriptional regulator of the α subunit of chorionic gonadotropin (CG), through its binding to the junctional regulatory elements within the promoter of this gene. Consistent with these findings, loss of Dlx3 function in JEG3 choriocarcinoma cells results in diminished expression of the α subunit gene [5]. Studies of human placental sections obtained from pregnancies terminated at 8 weeks gestation suggest that in humans, Dlx3 is expressed in trophoblasts cell populations at a time when CG production is highest[5,6]. These studies support the conclusion that Dlx3 may be playing an important role in the regulation of expression of CG subunits,

thus aiding in maintenance of luteal function early in pregnancy in women. Despite these important findings related to Dlx3 function in mice and humans, a number of questions remain regarding the significance of this homeodomain-containing transcription factor in the developing placenta.

The placenta is the main site of exchange of gases, nutrients and hormones between mother and fetus throughout mammalian gestation. Proper placentation is necessary to achieve the metabolic needs of the fetus for normal growth. There are many examples in the literature linking improper placentation to intrauterine growth retardation (IUGR), placental insufficiency, embryonic death and preeclampsia [7 8]. The cause of placental insufficiency stems from numerous factors including abberant gene expression, endothelial cell dysfunction, abnormalities in growth factor production, improper placental vascularization, all of which can lead to reduced placental perfusion and thus, nutrient delivery to the fetus. $Dlx3^{-/-}$ animals die at ~E9.5 [2] likely due to abnormal placentation [6]. Interestingly, the Dlx3 mouse model shares placental phenotypic qualities observed in the preeclamptic mouse model, BPH/5 [9]. Both the Dlx3 and BPH/5 mouse models display a lack in vascularization of the labyrinth layer, which in mice is the main site of fetal-maternal exchange [1,9]. In Chapter 3 of this dissertation, our studies demonstrate that both Dlx3 and the matrix metalloproteinase MMP-9 are misregulated early in gestation in the BPH/5 mouse model. The shared placental phenotype and gene expression patterns of these mouse models suggest aberrant Dlx3 gene expression may be associated with a molecular gene program leading to placental insufficiency.

The studies presented in Chapter 4 examine the role of Dlx3 in the developing placenta in greater detail. Results from these studies provide indirect evidence that loss of Dlx3 specifically in the placenta (rather than the placenta and fetus) is the likely cause of fetal lethality in the $Dlx3^{-/-}$ mouse model since animals engineered to

have an epiblast-restricted gene deletion of Dlx3 survive to weaning and beyond. Further, we demonstrate loss of a single Dlx3 allele has marked effects on fetal growth patterns correlated with oxidative stress and vascular dysfunction in the placentas of these animals. These defects are largely reversed with chronic administration of antioxidants prior to conception and throughout gestation.

Materials and Methods

Animals- Generation of the $Dlx3^{-/flox}$ x Meox2 Cre^{+} animals. B6 $Dlx3^{+/-}$ females were mated with $Meox2^{CreSor}$ males (Jackson Laboratories, Bar Harbor, ME) to generate $Dlx3^{+/-}$ Meox2 Cre^{+} males. $Dlx3^{+/-}$ Meox2 Cre^{+} males were then mated with $Dlx3^{flox/flox}$ females [10] to generate the $Dlx3^{-/flox}$ x Meox2 Cre^{+} animals on a B6 background. $Meox2^{CreSor}$ expression is detected at embryonic day (E) 6 and is expressed in a mosaic pattern.

Genotype for the $Dlx3^{-/flox}$ Meox2 Cre^{+} animals was determined by PCR. In order to determine heterozygosity of Dlx3 gene we used a line that had been previously characterized including PCR methods were used that were previously described [2]. To assess for presence of the $Dlx3^{Flox}$ allele we again used a line and PCR methods were used that were previously described [10]. The Cre mediated deletion of Dlx3 was determined by PCR using the following 3 primers. Primer oIMR1542 (5' GGGACCACCTCCTTTTGG CTTC 3'), Primer oIMR 1871 (5'AAGATGTGGAGAGTTCGGGGTAG 3'), and Primer oIMR 3671 (5' CCAGATCCTCCTCAGAAATCAGC 3'). Generation of 410bp band resulted in a $Cre^{+/+}$ mouse, a 300bp band was equivalent to a $Cre^{-/-}$ mouse and a combination of a 400bp band and a 300bp band was a $Cre^{+/-}$ animal. The PCR cycling times were 94˚C

for 3 minutes followed by 35 cycles of 94˚C for 30 seconds, 69˚C for 1 minute, 72˚C for 1 minute and 72˚C for 2 minutes.

All mice used in these studies were maintained and used in full compliance with protocols approved by the Cornell University Institutional Animal Care and Use Committee. All animals had free access to food and water; qualified Cornell University lab animal veterinarians were responsible for all animal care.

Analysis of Dlx3$^{-/f}$ Meox2 Cre^{+} animals- Male and female Dlx3$^{-/flox}$ x Meox2 Cre^{+} animals along with gender matched, littermate controls were sacrificed at approximately 6 weeks of age and subjected to a complete small animal pathology diagnostic workup at Cornell University, College of Veterinary Science Pathology Department. Tissue sections of liver, kidney, heart, lungs, skeletal muscle, ovary and testis, skin and teeth were fixed in 10% formalin and paraffin embedded. Histological sections (10μm) were cut and stained with Hematoxylin and Eosin (H&E). Sections were photographed on a Nikon Eclipse E400 microscope**,** using a 20x objective and SPOT Imaging Software (Diagnostic Instruments, Sterling Heights, MI).

Embryos Weights and Crown Rump Measurements- Embryo weights for the Dlx3$^{+/-}$ matings were assessed at five different gestational time points: E9.5, E10.5, E12.5, E15.5 and E18.5. The yolk sac from each animal was used for genotyping. Average embryo weights were assigned based on genotyping. Embryos were weighed and photographed using a Nikon dissecting microscope, model SMZ-U, at a magnification of 1.4x. Crown rump measurements of each animal were obtained using the Image J Analysis Software (NIH) line tool and measuring each animal from the top of the crown to the edge of the rump.

Tempol Administration and Vascular Endothelial Growth Factor (VEGF) assessment- Tempol ($C_9H_{18}NO_2$-4-hydroxy tetramethylpiperidinyloxyl, Sigma, St. Louis MO) was administered in the drinking water of the $Dlx3^{+/-}$ female mice in light sensitive containers. Tempol was given at a concentration of 2mM, 5 days prior to mating with $Dlx3^{+/-}$ male mice and continued throughout gestation until the animals were sacrificed at E12.5. Sterile water was used as the control for Tempol. The experimental design was a 2x2 factorial comparing $Dlx3^{+/+}$ receiving water, $Dlx3^{+/+}$ receiving Tempol, $Dlx3^{+/-}$ receiving water and $Dlx3^{+/-}$ receiving Tempol. This study was carried out on two occasions with n=4-6 animals per cell in the factorial study. At the time of sacrifice, maternal whole blood was collected from $Dlx3^{+/-}$ females from all treatment groups at E12.5 using cardiac puncture. Maternal serum was collected by centrifugation at 2,000rpm for 10minutes at 4˚C. Maternal vascular endothelial growth factor (VEGF) concentrations were assessed by ELISA (Invitrogen, Carlsbad, CA) as per manufacturer's instructions.

Oxidative Stress Analysis and Western Blot analysis- Placental samples from $Dlx3^{+/+}$ and $Dlx3^{+/-}$ animals were collected at E10.5, E12.5, and E15.5. All samples were subjected to the protein Oxidation Detection Kit, Oxybot™ (Millipore, Billerica, MA). Complexes were resolved on SDS-polyacrylamide gel electrophoresis and transferred to polyvinylidine difluoride membranes by electroblotting. Membranes were blocked in 2x casein (Vector laboratories, Burlingame, CA) in Tris-buffered saline (10mM Tris (pH 7.6), 150mM sodium chloride) containing 0.1% Tween 20 (TBST) for 1 hour at room temperature. For Oxyblot™, primary and secondary antibodies were provided in the protein Oxidation Detection Kit. An additional Western blot used an Actin antibody at 1:500 (Santa Cruz Biotechnology, Inc., Santa Cruz, CA) in TBST-1X casein. Protein bands were visualized by chemiluminesence reagents.

Assessment of placental reactive oxidative species- Placental tissues were collected from both genotypes in the Tempol and water treated groups. These dissections were characterized as full thickness section from the uterine wall through the chorionic plate. Yolk sac from the corresponding embryo was collected and used for genotyping. Placental tissues were frozen on dry ice in Optical Cutting Temperature Compound (OCT) (Fisher Scientific, Pittsburg, PA) and sectioned on a microtome at 16µm. Sections were washed twice in Dulbecco's phosphate-buffered saline (DPBS; Invitrogen, Carlsbad, CA) and stained with dihydroethidium (DHE; Sigma, St. Louis, MO) for 10 minutes at room temperature in the dark. Following the staining, samples were washed twice in DPBS. Sections were assessed for DHE stain using a spinning disc confocal imaging system (CSU-10) mounted on a Nikon Eclipse TE2000-U inverted microscope at 60x. Background was subtracted for each section to calculate the DHE.

Assessment of Placental Apoptosis- Placental tissues were collected from both genotypes in the Tempol and water treated groups. As described above, yolk sac from the corresponding embryos was collected and used for genotyping. For these studies, placental tissues were fixed in 10% formalin and paraffin embedded. Sections were cut at 10µm and subjected to apoptosis analysis using a terminal deoxynucleotidyl transferase dUTP nick end labeling (TUNEL) Apoptosis Detection kit (Millipore, Billerica, MA). Stained sections were analyzed using a Nikon Eclipse E400 microscope, 10X objective and SPOT Imaging Software (Diagnostic Instruments, Sterling Heights, MI). Positively stained cells were visualized and counted in a 10x relative field of view for each sample.

Micro-Computed Tomography (micro-CT) Analysis- $Dlx3^{+/-}$ female mice mated with $Dlx3^{+/-}$ male mice were assigned to either the Tempol or water treated group. Treatments of groups were carried out as described above and animals were sacrificed at E12.5. Pregnant $Dlx3^{+/-}$ females were prepped for imaging with a cardiac injection of micro-CT compound, Microfil (Flow Tech, Carver, MA), to fill placental vasculature and imaged as described previously [11]. The scans were performed using the GE CT120 micro-CT scanner (GE Heathcare, London, Ontario, Canada). For each dataset, 1200 projections were obtained at 0.3° intervals over 360° using 80keV, 32ma, 100ms exposure time and 25µm x-y-z resolution. Prior to each scan, 10 bright-field images were acquired with no objects in the field of view, providing a correction for detector non-uniformity. Proper placement of the subject will be done with the assistance of X-ray fluoroscopy to ensure that the entire specimen was included within the scanning field of view. Each image dataset collected was transferred from the CT120 system to an image-processing workstation (HP xw8400 with 8 CPU cores and 16GB RAM). The projection views were used to reconstruct a CT image using a convolution back-projection approach implemented in 3D, giving a 80×80×50 mm^3 volume of image data with .25µm isotropic voxels in analog-to-digital units. Analysis was carried out utilizing Microview software (GE Healthcare, Piscataway, NJ) measuring volumes of maternal blood spaces associated with the maternal contribution to the implantation site, maternal spiral artery, and overall branching number of maternal spiral arteries. Volume measurements for maternal contribution to the implantation site and maternal spiral artery were calculated as previously described [11]; maternal spiral artery branching numbers were observed and counted in 3D rendered images in Microview software (GE Healthcare, Piscataway, NJ). A branch point was defined as any deviation from the initial maternal artery vessel flowing from the uterine artery into the placental vasculature.

Assessment of Placental labyrinth, artery and vein area- $Dlx3^{+/-}$ female mice mated with $Dlx3^{+/-}$ male mice were assigned to either the Tempol or water treated group. Treatments of groups were carried out as described above and animals were sacrificed at E12.5. For these studies, placental tissues were fixed in 10% formalin and paraffin embedded. Placental sections were cut at 10μm and stained with Masson's Trichrome followed by staining with H&E. Stained placental sections were imaged on Aperio Scanscope and images stored for later analysis. Sections representing the widest portion of the placental disk were evaluated further. The labyrinth compartment was easily discernable with H&E staining and the presence of nucleated fetal red blood cells. Full placental area and the area of the labyrinth defined manually and quantitated using Aperio software. Maternal arteries (n=12 or 13/treatment group) were identified as cross-sectional areas containing non-nucleated maternal red blood cells surrounded by a layer of smooth muscle. Maternal veins (n=12 or 13/treatment group) were identified as vessels containing maternal red blood cells without associated smooth muscle. The areas of these vessels were defined manually and quantitated using Aperio software. Data are presented as relative measures of areas of the labyrinth, maternal arteries or maternal veins as a ratio of the total placental area.
Statistical Analysis- All data are expressed as means ± SE. Comparisons were made by Student's *t*-test or by Mann-Whitney *U* test, where appropriate. A *P* value of <0.05 was considered statistically significant; a *P* value of <0.1 was considered a trend.

Results

Mice with conditional epiblast-restricted deletion of the Dlx3 gene survive to weaning- Our initial studies sought to examine the effects conditional deletion of Dlx3 within the epiblast to determine if embryonic loss of Dlx3 resulted in embryonic lethality consistent with the $Dlx3^{-/-}$ mouse model. Surprisingly, $Dlx3^{-/flox}$ x

Meox2^{CreSor} animals survived to weaning and beyond albeit with substantial defects at several levels. Dlx3$^{-/flox}$ x Meox2^{CreSor} mice were smaller at birth than gender matched littermate controls and clearly displayed abnormal hair growth (Figure 4.1A). The Dlx3$^{-/flox}$ x Meox2^{CreSor} females were observed as much smaller in stature than the male littermates.

Histological examination of numerous tissues revealed marked and predictable differences between the Dlx3$^{-/flox}$ x Meox2^{CreSor} animals and their littermate controls. Figure 4.1B depicts immature gonads of both the male and female Dlx3$^{-/flox}$ x Meox2^{CreSor} compared to the littermate controls. Dlx3$^{-/flox}$ x Meox2^{CreSor} testis have fewer mature spermatozoa in the seminiferous tubules as well as a lower number of interstitial cells. Dlx3$^{-/flox}$ x Meox2^{CreSor} ovaries contained primary and secondary follicles, but no preovulatory follicles or corpora lutea, as seen in the littermate control. In the skin of the Dlx3$^{-/flox}$ x Meox2^{CreSor} mice, the epidermis was characterized by acanthosis (Figure 4.1B); scattered hair follicles are observed which contained normal hairs, but most hair follicles are mildly distended by the presence of amorphous keratin. The structure and distribution of the hair follicles, as well as the percentage of follicles in each stage of the hair cycle, are comparable between the Dlx3$^{-/flox}$ x Meox2^{CreSor} mice and littermate controls. In the Dlx3$^{-/flox}$ x Meox2^{CreSor} mice, both the enamel and dentin layers of the teeth were found to be irregular in thickness compared to littermate controls. The pulp cavity in the Dlx3$^{-/flox}$ x Meox2^{CreSor} teeth is often narrowed and there are infiltrates of neutrophils and macrophages, along with areas of hemorrhage in the surrounding periodontal tissue and gingiva. The ameloblasts are similar in both groups of mice, but the odontoblast layer is thinner and more disorganized in the Dlx3$^{-/flox}$ x Meox2^{CreSor} mice. Altogether these results indicate the impact of loss of Dlx3 in the developing embryo was substantial in many tissue types that have been shown to express Dlx3 as part of a

developmental program. Importantly, when Dlx3 deficient embryos develop in the presence of a $Dlx3^{+/-}$ placenta, the potential survival rate of that embryo increases dramatically. This provides indirect evidence that the placental lesions within the $Dlx3^{-/-}$ embryo likely are the primary cause of embryonic lethality in this knockout model.

Loss of one Dlx3 allele results in altered growth kinetics in the embryo- Complete Dlx3 deletion in mice leads to midgestational embryonic lethality due to abnormal placentation [1,2]. This outcome hinders assessment of the role of Dlx3 later in pregnancy. We sought to examine the impact of haploinsufficiency at the Dlx3 loci on fetal growth and placental viability during gestation. Embryos from $Dlx3^{+/-}$ matings were genotyped and weighed at five different gestational time points, embryonic days (E) 9.5, 10.5, 12.5, 15.5, and 18.5 Figure 4.2 illustrates growth kinetics in the $Dlx3^{+/-}$ mouse embryo compared to the wildtype littermate controls. Similar embryonic weights were observed at the E9.5 and E10.5 time points for the $Dlx3^{+/-}$ embryos and wildtype littermate controls. However, at E12.5, $Dlx3^{+/-}$ fetal weight was reduced ($p<0.05$) compared to the controls. By E15.5 the difference in weight between genotypes appeared to be less; and at E18.5, the fetal weights were indistinguishable between genotypes (data not shown). These results indicate that haploinsufficiency at the Dlx3 loci may be involved in creating an intrauterine environment that is detrimental to normal patterns of fetal growth. Interestingly, $Dlx3^{+/-}$ embryos appear

Figure 4.1. Dlx3 epiblast-conditional knockout survives to parturition with growth abnormalities. A. $Dlx3^{-/flox}$ x $Meox2^{CreSor}$ female animals are considerable smaller in stature at 6 weeks of age and display visible abnormal hair growth patterns in contrast to wildtype gender matched control littermates. Male $Dlx3^{-/flox}$ x $Meox2^{CreSor}$ mice display a similar growth and hair pattern phenotype compared to littermate controls (Data not shown). **B.** Hemotoxylin and Eosin (H&E) stained sections of gonads, bone and teeth from $Dlx3^{-/flox}$ x $Meox2^{CreSor}$ animals indicate structural and developmental irregularities compared to wildtype littermate controls.

A.


♀
Wildtype
Dlx3 -/flox Meox2Cre +

B.

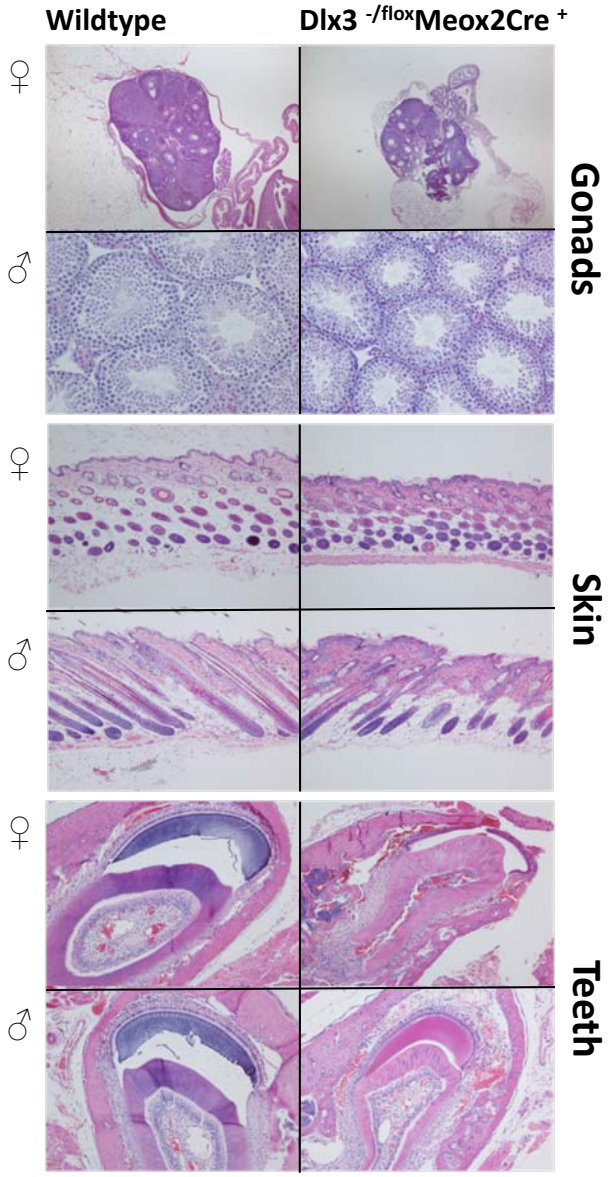
Wildtype
Dlx3 -/flox Meox2Cre +
♀
♂
Gonads
Skin
Teeth

to compensate for this IUGR phenotype later in gestation via mechanisms that are currently unknown.

Loss of one Dlx3 allele results in placental oxidative stress- Placental tissues were collected from $Dlx3^{+/-}$ and wildtype animals at 3 different gestational time points E10.5, E12.5 and E15.5, around the time of altered fetal growth kinetics observed above. Tissues were subjected to an Oxyblot™ (Millipore, Billerica, MA) and investigated for increased carbonyl side chains in protein. Protein carbonyl groups are a direct result of oxidative reactions with ozone or oxides of nitrogen or by metal catalyzed oxidation thereby serving as a marker of oxidative stress. Figure 4.3 reveals an increased overall abundance of protein carbonyl modifications in the $Dlx3^{+/-}$ mouse placentas compared to wildtype controls. Additionally, the degree of oxidative stress increased to a higher degree throughout gestation in the $Dlx3^{+/-}$ placentas. Increased accumulation of protein carbonyl groups observed at E12.5 in the $Dlx3^{+/-}$ placentas correlates with the IUGR phenotype at the same gestational time point (Figure 4.2).

Antioxidant therapy prior to and during gestation rescues the IUGR $Dlx3^{+/-}$ phenotype- Studies described above suggest increase oxidative stress in the $Dlx3^{+/-}$ placenta correlated with the IUGR phenotype. Based on this correlation, we sought to examine the effects of antioxidant therapy on fetal and placental well-being in the $Dlx3^{+/-}$ mouse. The superoxide disumutase mimetic, $C_9H_{18}NO_2$-4-hydroxy tetramethylpiperidinyloxyl (Tempol) has been used as an antioxidant in many experimental settings including the prevention of symptoms of neurodegenerative disease in IRP2 knockout mice [12], reducing renal dysfunction and injury associated with ischemia in the kidney [13], and most significant to our studies, oral administration of Tempol normalized embryo birth weights and placental development in the BPH/5

Figure 4.2. Dlx3$^{+/-}$ matings reveal a potential intrauterine growth (IUGR) phenotype. Dlx3 heterozygous (Dlx3$^{+/-}$) animals were mated and sacrificed at four different gestations ages, E9.5, E10.5, E12.5, E15.5 (n≥4/timepoint). Dlx3$^{+/-}$ and $^{+/+}$ embryos display similar growth patterns at E9.5 and E10.5. By E12.5 Dlx3$^{+/-}$ embryos weights (mg) are significantly less ($p<0.05$) than Dlx3$^{+/+}$ littermates and the same growth pattern is maintained at E15.5.

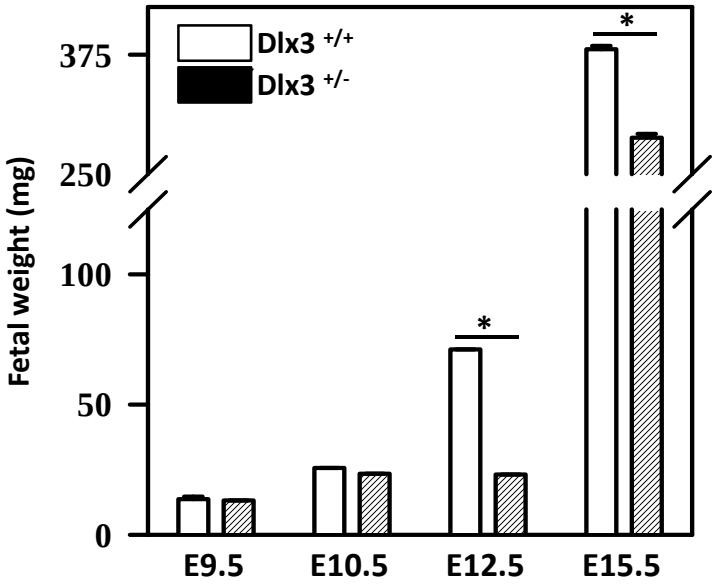
Dlx3 +/+
Dlx3 +/-
Fetal weight (mg)
375
250
100
50
0
*
*
E9.5
E10.5
E12.5
E15.5

Figure 4.3. Oxyblot indicates increased relative abundance of protein carbonyl groups in Dlx3$^{+/-}$ placentas throughout gestation. Wildtype (Dlx3$^{+/+}$) and Dlx3 heterozygous (Dlx3$^{+/-}$) placentas were harvested at 3 different gestational time points, E10.5, E12.5, and E15.5. Placental tissues were subjected to an Oxyblot assay to determine the abundance of protein carbonyl side chains which are indicative of oxidative stress. Dlx3$^{+/-}$ placental tissues reveal an increased abundance of protein carbonyl groups throughout gestation in contrast to Dlx3$^{+/+}$ (n=3/genotype and timepoint). Actin was used as a lane loading control.

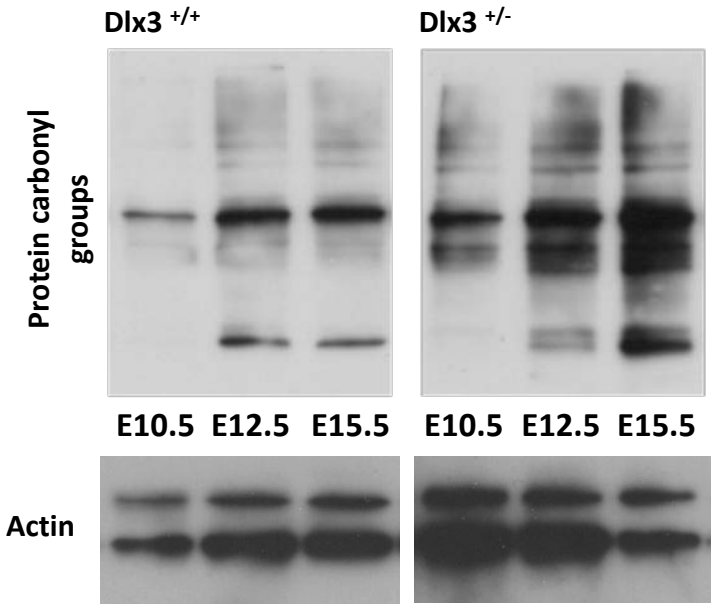
Dlx3 +/+
Dlx3 +/-
Protein carbonyl groups
E10.5 E12.5 E15.5
E10.5 E12.5 E15.5
Actin

mouse model of preeclampsia [14]. Based on these findings, we chose to examine the potential effects of Tempol administration in our $Dlx3^{+/-}$ mouse model. Beginning 5 days prior to mating and throughout gestation, $Dlx3^{+/-}$ females (mated to $Dlx3^{+/-}$ males) received Tempol in their drinking water; control animals received water. Tempol was routinely accepted and well-tolerated by these animals with no evidence of dehydration seen in these animals during the experimental period. Based upon these timed matings, animals were sacrificed at E12.5 and embryos and placental disks removed for analysis (Figure 4.4A-C). Consistent with our initial studies, $Dlx3^{+/-}$ fetuses had reduced fetal weight and crown rump measurements ($p<0.05$) compared to wildtype littermates. The addition of Tempol in the drinking water effectively rescued this IUGR phenotype. Surprisingly, oral administration of Tempol revealed a subset of small but viable $Dlx^{-/-}$ animals at E12.5, fully 3 days beyond the normal timing of fetal demise of these animals (Figure 4.4A) [2]. These initial results using Tempol indicate the potential benefits of antioxidant therapy in rescuing the IUGR phenotype associated with a single allelic loss of Dlx3.

These studies supported the hypothesis that fetal growth retardation in this model was a result of oxidative stress. To examine this hypothesis further, we examined ROS abundance and apoptosis within the placentas from our Tempol study. ROS abundance in $Dlx3^{+/+}$and $Dlx3^{+/-}$ placental sections from both treatment groups was assessed by staining these sections with superoxide probe, DHE. Our results reveal an increase ($p<0.05$) in the abundance of DHE stain observed in placental sections comparing $Dlx3^{+/+}$ with $Dlx3^{-/-}$ receiving water, again correlated with the IUGR phenotype (Figure 4.5A). The elevated level of ROS detected by this method in the $Dlx3^{+/-}$ placentas was rescued by administration of Tempol. Tempol administration did not appear to reduce DHE staining in $Dlx3^{+/+}$ placentas. Similar results were obtained using TUNEL staining to detect apoptotic cells (Figure 4.5B).

Figure 4.4. Antioxidant therapy rescues the IUGR phenotype in Dlx3$^{+/-}$ mice. Dlx3 heterozygous (Dlx3$^{+/-}$) females were pretreated with the superoxide dismutase mimetic, Tempol (2mM), in their drinking water five days prior to mating with Dlx3$^{+/-}$ males and continue throughout gestation. Control Dlx3$^{+/-}$ were given control drinking water before mating and during gestation. All animals were sacrificed at E12.5. **A.** No gross morphological differences other than size were noted for the E12.5 Dlx3$^{+/+}$ and $^{+/-}$ embryos ($n \geq 10$/genotype and treatment) between the control group (top row) and Tempol treated group (bottom row). Tempol administration did reveal a subset of Dlx3$^{-/-}$ embryos at E12.5. **B.** Fetal weights (mg) indicate an IUGR phenotype with single allelic loss of Dlx3 in the water group ($p<0.05$). Tempol supplementation ameliorates the IUGR phenotype in the Dlx3$^{+/-}$ animal. No significant changes in fetal weight are observed in the Dlx3$^{+/+}$ mouse despite antioxidant therapy. **C.** Embryo crown-rump measurements (mm) correlate with the IUGR phenotype displayed in the Dlx3$^{+/-}$ animals indicating decreased ($p<0.05$) embryo length measurements with loss of one Dlx3 allele. Chronic Tempol administration increased ($p<0.05$) crown rump measurements in Dlx3$^{+/-}$ embryos. No significant alterations were found in Dlx3$^{+/+}$ animals with antioxidant therapy.

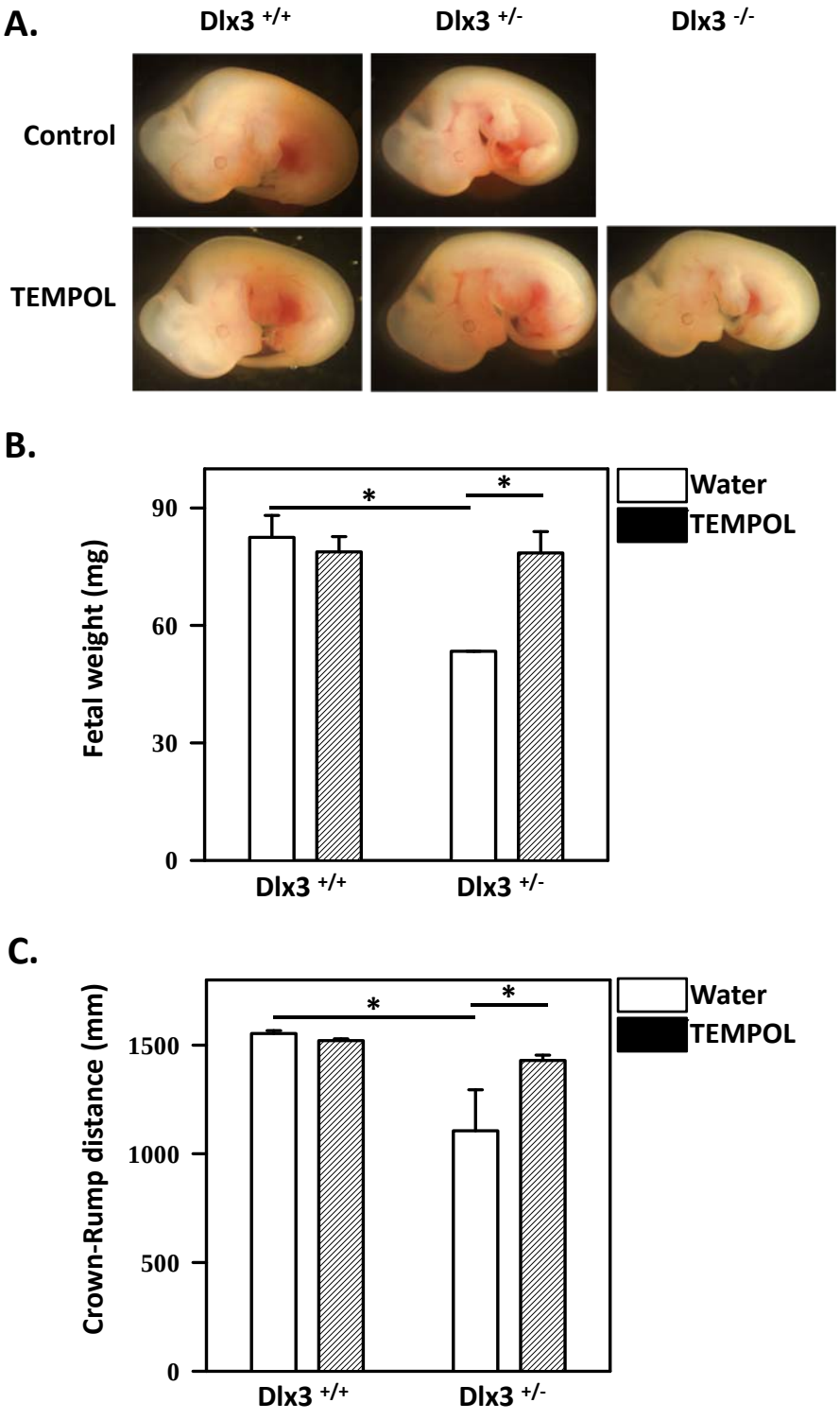
A.
Dlx3 +/+
Dlx3 +/-
Dlx3 -/-
Control
TEMPOL
B.
Fetal weight (mg)
90
60
30
0
*
*
Water
TEMPOL
Dlx3 +/+
Dlx3 +/-
C.
Crown-Rump distance (mm)
1500
1000
500
0
*
*
Water
TEMPOL
Dlx3 +/+
Dlx3 +/-

Increased TUNEL positive cells were detected ($p<0.05$) in the $Dlx3^{+/-}$ placentas compared to $Dlx3^{+/+}$ animals receiving water. This effect was again reversed in the $Dlx3^{+/-}$ animals receiving Tempol. Addition of Tempol also reduced the number of apoptotic cells in placentas from $Dlx3^{+/+}$ animals. These results support the conclusion that loss of a single Dlx3 allele results in increased placental ROS accumulation and apoptosis, correlated with the IUGR phenotype. These measures of oxidative stress were effectively reversed by antioxidant treatment.

Loss of one Dlx3 allele results in vascular dysfunction within the placenta- One potential cause of oxidative stress within the developing placenta is altered vascularization and placental perfusion. For example, in the BPH/5 mouse model of preeclampsia, maternal hypertension was associated with increased placental ROS accumulation, reduced fetal weights and defects in maternal spiral artery remodeling [9,14,15]. We initially examined circulating concentration VEGF in maternal serum collected from $Dlx3^{+/-}$ and wildtype mice at E12.5. Figure 4.6 depicts decreased ($p<0.05$) circulating VEGF in maternal serum in $Dlx3^{+/-}$ animal compared to wildtype control. These findings suggest a shift in angiogenic potential in $Dlx3^{+/-}$ mice may be effecting vascularization of the mouse placenta.

To examine this possibility, we took two approaches; 1) assessment of maternal placental vasculature using microCT imaging; and 2) assessment of maternal vascular volume using standard histological techniques augmented by the use of an Aperio Scanscope. To examine placental vascularization using micro-CT imaging, we injected a micro-CT compound, Microfil (Flow Tech, Carver, MA) into pregnant $Dlx3^{+/+}$ and $Dlx3^{+/-}$ mice at E12.5. Further, to investigate the potential role of ROS stress on placental vascularization, we included our Tempol administration paradigm as outlined above. Gravid uteri were harvested, injected with Mircofil and subjected

Figure 4.5. Chronic Tempol administration ameliorates ROS insult. A. A single loss of a Dlx3 allele resulted in significant ($p<0.05$) ROS accumulation in placental tissue as measured by dihydroethidum (DHE) stain. Antioxidant therapy with Tempol effectively resolved ($p<0.05$) ROS abundance in the $Dlx3^{+/-}$ placenta. No significant difference was noted in the $Dlx3^{+/+}$ placentas with chronic Tempol supplementation. (n=6-8/genotype/treatment) **B.** Terminal deoxynucleotidyl transferase dUTP nick end labeling (TUNEL) indicated an abundance of TUNEL positive cells in the placentas lacking one Dlx3 allele compared to littermate controls. Tempol administration resulted in significantly less ($p<0.05$) TUNEL positive cells in the $Dlx3^{+/+}$ and $Dlx3^{+/-}$ placentas. (n=6/genotype/treatment)

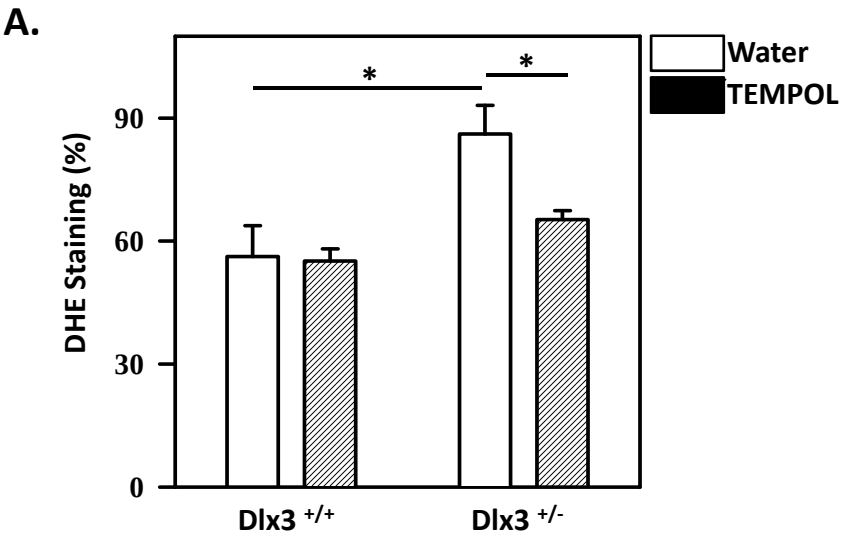
A.
Water
TEMPOL
DHE Staining (%)
90
60
30
0
*
*
Dlx3 +/+
Dlx3 +/-

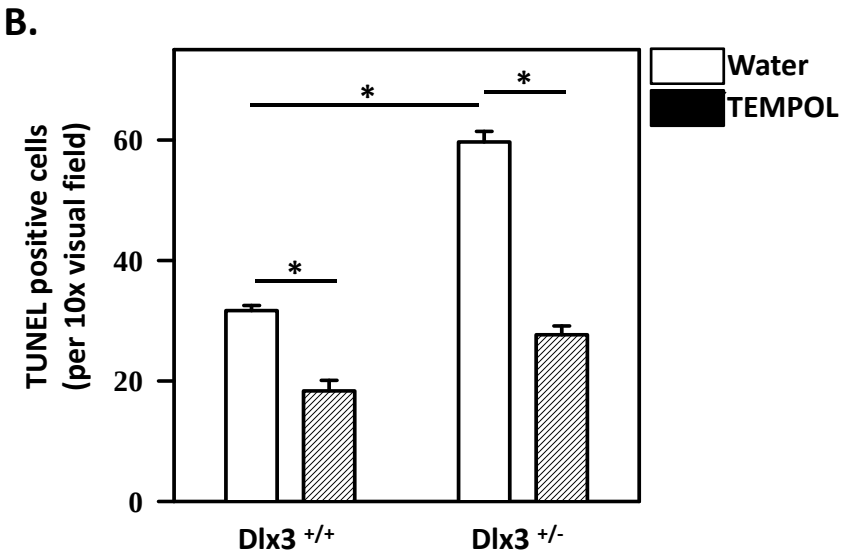
B.
Water
TEMPOL
TUNEL positive cells
(per 10x visual field)
60
40
20
0
*
*
*
Dlx3 +/+
Dlx3 +/-

Figure 4.6. Vascular endothelial growth factor (VEGF) is misregulated in the maternal serum of Dlx3$^{+/-}$ mice. Loss of a single Dlx3 allele resulted in lower ($p<0.05$) maternal serum concentrations of VEGF compared to Dlx3$^{+/+}$ mothers. VEGF was measured by a commercially available ELISA.

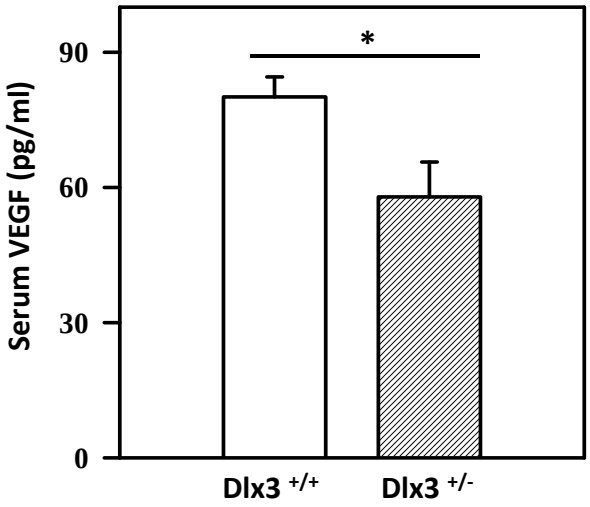
*
90
60
30
0
Serum VEGF (pg/ml)
Dlx3 +/+
Dlx3 +/-

to micro-CT analysis. Rendered images of placental vasculature were obtained and volume measurements were assessed using Microview (GE Healthcare, Piscataway, NJ) software. Results revealed significant insights into Tempol antioxidant therapy effects on placental vasculature. First, the volume of total placental Microfil tended ($P<0.1$) to be lower in $Dlx3^{+/-}$ mice compared to $Dlx3^{+/+}$ animals treated with water. Further, administration of Tempol to the $Dlx3^{+/-}$ mice increased ($p<0.05$) total microfil volume; however, this same increase did not appear to be evident in the $Dlx3^{+/+}$ mice (Figure 4.7A). These differences were paralleled in the specific Microfil volume measurements associated with maternal spiral arteries (Figure 4.7B). Maternal spiral artery branch points did not differ remarkably among treatments (Figure 4.7C). It is important to note that these micro-CT imaging studies are considered preliminary at present since the sample size for the $Dlx3^{+/+}$ mice is limited to four placentas in each treatment group. We continue to collect and analyze these data as this project moves forward.

In parallel, we used more traditional histological assessment of vascular parameters in these tissues using Masson's trichrome staining (Figure 4.8). Identification of discrete compartments within the mouse placenta was discernable with H&E staining in these sections. Initially, we quantitated total placental and labyrinth area in the $Dlx3^{+/+}$ and $Dlx3^{+/-}$ mice receiving water or Tempol. The proportion of labyrinth area (as a percent of total placental area) was not affected by genotype or antioxidant treatment (Figure 4.8A). In contrast, maternal spiral artery cross-sectional area (as a percentage of total placental area) was reduced ($p<0.05$) in the $Dlx3^{+/-}$ mice compared to $Dlx3^{+/+}$ mice receiving water (Figure 4.8B). Addition of Tempol tended ($p<0.1$) to increase maternal spiral artery cross-sectional area in both genotypes. Cross-sectional area of maternal veins within these placentas were unaffected by genotype or antioxidant treatment in this study (Figure 4.8C). These

Figure 4.7. Micro-CT analysis indicates alterations in placental vascularization of the Dlx3$^{+/-}$ mouse model. A. Quantitation of placental microfil volume following microCT imaging indicates a trend ($p<0.1$) in decreased placental vascular volume with a single loss of a Dlx3 allele. Chronic antioxidant supplementation resulted in resolution of the placental vascular volume in Dlx3$^{+/-}$ mice ($p<0.05$). No significant change was observed in Dlx3$^{+/+}$ placental volumes with antioxidant administration. **B.** Volumetric measurements of the maternal spiral arteries indicate a tendency toward reduction ($p<0.1$) in total volume in the Dlx3$^{+/-}$ placentas compared with Dlx3$^{+/+}$ placentas. Antioxidant administration eliminates this difference ($p<0.05$) in maternal spiral artery volumes across Dlx3 genotypes. No statistical difference was detected for maternal spiral artery volume measurements between treatment groups for the Dlx3$^{+/+}$ placentas. **C.** Maternal spiral artery branch points in Dlx3$^{+/+}$ and Dlx3$^{+/-}$ placentas were not different across genotype and antioxidant treatment.

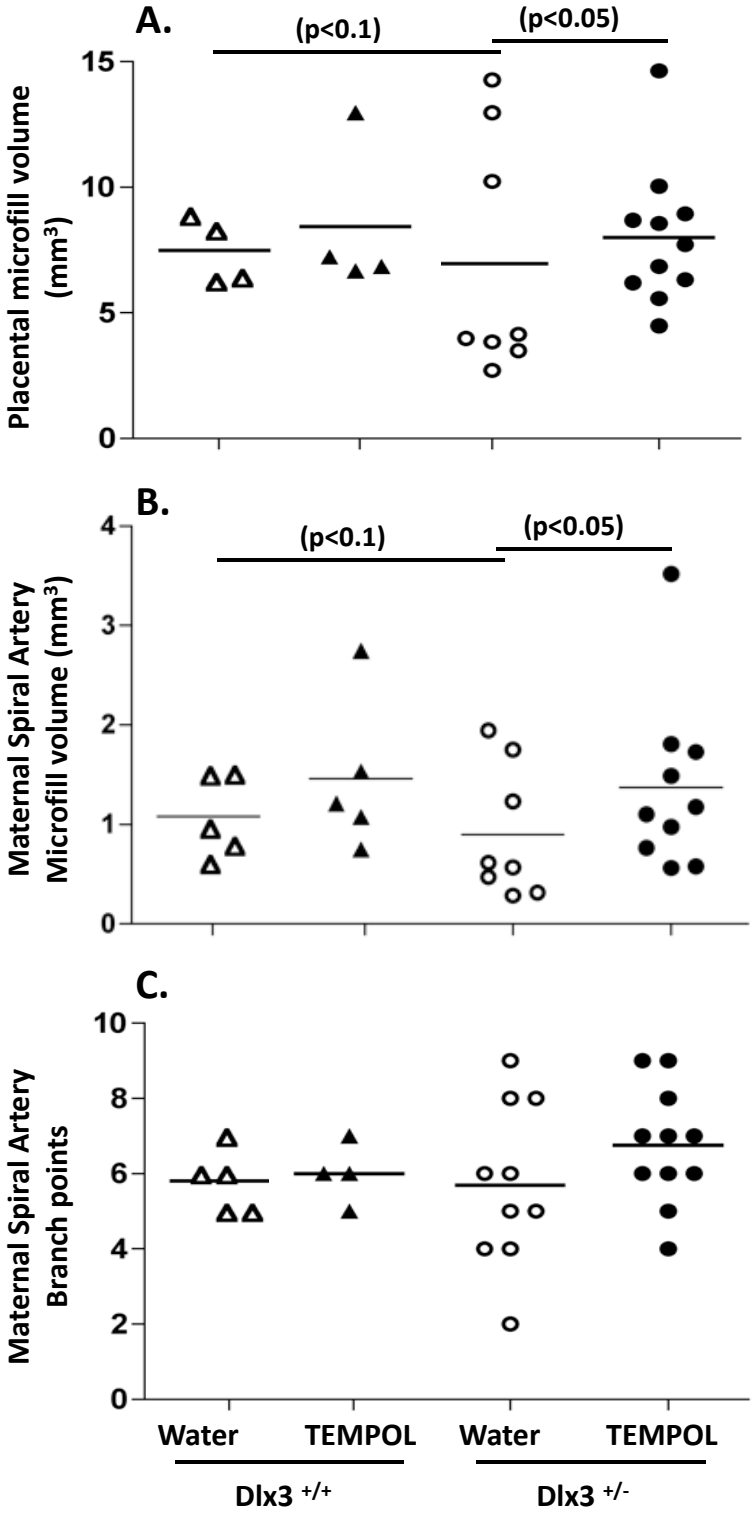
A.
(p<0.1)
(p<0.05)
Placental microfill volume (mm³)
15
10
5
0
B.
(p<0.1)
(p<0.05)
Maternal Spiral Artery Microfill volume (mm³)
4
3
2
1
0
C.
Maternal Spiral Artery Branch points
10
8
6
4
2
0
Water
TEMPOL
Water
TEMPOL
Dlx3 +/+
Dlx3 +/-

Studies support the preliminary conclusion that loss of one Dlx3 allele clearly impacts maternal VEGF serum concentrations and this is correlated with alterations in maternal spiral artery volume as measured by micro-CT imaging and histological analysis. These data support our working hypothesis that these changes in placental vasculature may underlie mechanisms regulating the ability of the $Dlx3^{+/-}$ placenta to manage oxidative stress during gestation leading to IURG in this model. We continue to expand our histological analyses to include a number of new vascular markers to assess (for example) smooth muscle actin and expand our timeframe to beyond E12.5 to better assess maternal spiral artery remodeling.

Figure 4.8. Loss of a single Dlx3 allele results in a reduction in cross-sectional area in maternal arteries. Standard histological analysis using Masson's trichrome and H&E staining was used to examine placental labyrinth and vasculature. **A.** Total placental labyrinth area was not different between in the wildtype ($Dlx3^{+/+}$) and Dlx3 heterozygous ($Dlx3^{+/-}$) with and without chronic antioxidant supplementation. **B.** Measurements of the total placental artery area indicated a decrease ($p<0.05$) in the $Dlx3^{+/-}$ placenta compared to $Dlx3^{+/+}$. Chronic supplementation of antioxidant during gestation increased the arterial area in both $Dlx3^{+/-}$ and $Dlx3^{+/+}$ placentas. **C.** Calculations of total placental venous area indicate no statistical difference between $Dlx3^{+/-}$ and $Dlx3^{+/+}$ placentas. Administration of antioxidant demonstrates no change in placental venous area in the Dlx3 mouse model.

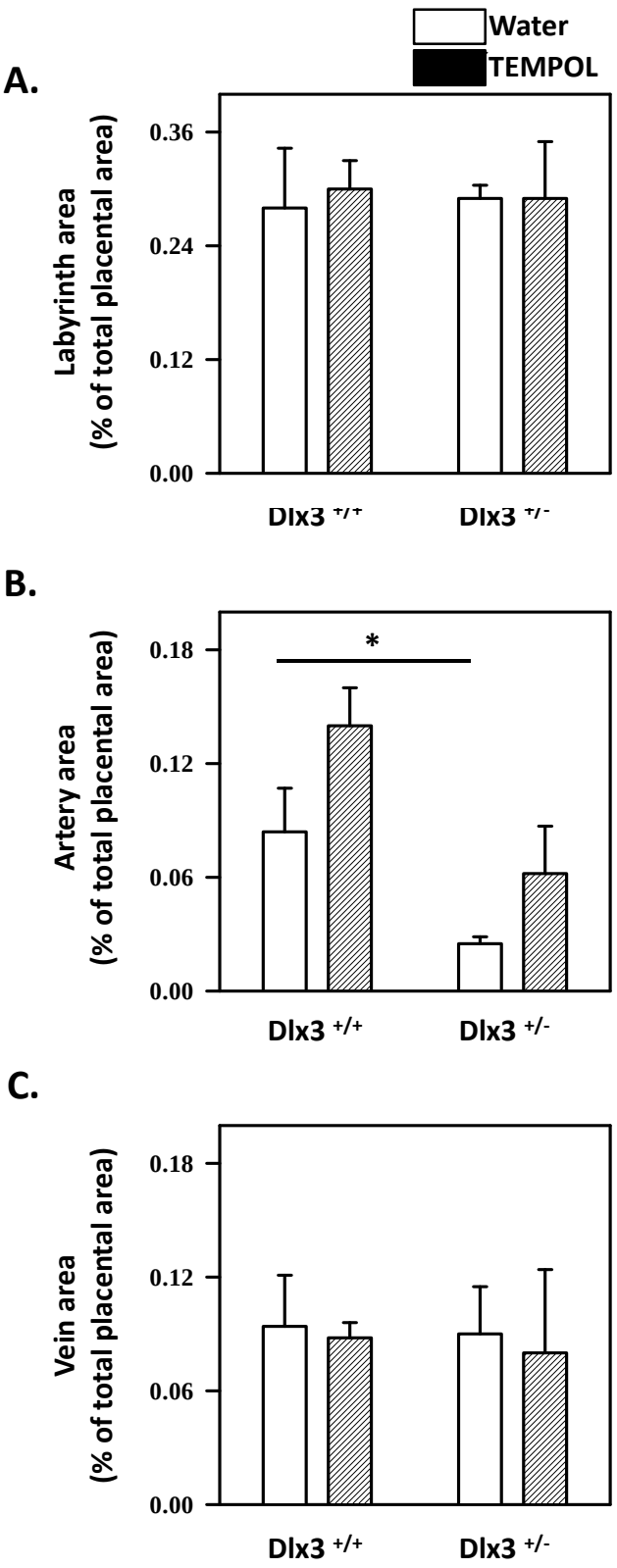
A.
Water
TEMPOL
Labyrinth area
(% of total placental area)
0.36
0.24
0.12
0.00
Dlx3 +/+
Dlx3 +/-
B.
Artery area
(% of total placental area)
*
0.18
0.12
0.06
0.00
Dlx3 +/+
Dlx3 +/-
C.
Vein area
(% of total placental area)
0.18
0.12
0.06
0.00
Dlx3 +/+
Dlx3 +/-

Discussion

The role of Dlx3 in the developing placenta has a clear impact on not only fetal fitness [2], but also suitable placentation necessary for proper blood flow and nutrient exchange [1]. Our studies indicate conditional loss of Dlx3 in the epiblast of the developing embryo does not affect the ability of $Dlx3^{-/flox}$ x $Meox2^{CreSor}$ to be born (Figure 4.1A). Closer examination of histological sections of several $Dlx3^{-/flox}$ x $Meox2^{CreSor}$ embryonic tissues including gonads, skin, and teeth, suggest abnormal patterns of growth and development compared to wildtype littermate controls (Figure 4.1B). More specifically, both male and female $Dlx3^{-/flox}$ x $Meox2^{CreSor}$ mice display immature gonadal structure, acanthosis of the epidermis, and irregular enamel and dental layers in tooth structure. However, there are important limitations to this study that need to be carefully considered. Unlike the $Dlx3^{-/-}$ animal, $Meox2^{CreSor}$ animals do not display epiblast-specific Cre expression until ~ embryonic day (E) 6.0. Thus, key developmental events associated with Dlx3 expression may have occurred prior to gene excision in the embryo. Additionally, Cre expression in $Meox2^{CreSor}$ animals has been largely characterized as a mosaic, limiting the probability of Dlx3 excision in every cell within the epiblast. The frequency of Dlx3 excision within the epiblast is increased in our studies based on the use of one floxed allele and one null allele. Despite these caveats, the $Dlx3^{-/flox}$ x $Meox2^{CreSor}$ embryos display a predictable phenotype in hair, skin and teeth as have been previously described in patients with tricho-dento-osseus syndrome and during mouse development in many tissues that are known to express Dlx3 [2]. More importantly, these studies indicate the midgestational embryonic lethality associated with $Dlx3^{-/-}$ mice may be associated with a maternal Dlx3 placental lesion despite defects within the embryo proper.

This cohort of studies implies loss of one Dlx3 allele results in problems associated with fetal fitness and placental disruptions. Analysis of Dlx3 heterozygous

($Dlx3^{+/-}$) embryos from matings between $Dlx3^{+/-}$ male and females mice resulted in altered growth kinetics in contrast to wildtype littermate controls (Figure 4.2). Specifically, at E12.5 $Dlx3^{+/-}$ embryos lag behind in embryonic weight gain compared to controls. By E15.5 there is a decreased difference between embryonic weights of $Dlx3^{+/-}$ and wildtype littermate controls. By E18.5, fetal weight is similar between the two genotypes (Data not shown). In accord with these findings, assessment of $Dlx3^{+/-}$ placentas revealed an increase in protein carbonyl groups at E12.5, in contrast to wildtype placental controls (Figure 4.3). Additional assessment of $Dlx3^{+/-}$ placentas found a statistically significant ($p<0.05$) increase in reactive oxygen species (ROS) (Figure 4.5A) and apoptotic cell types (Figure 4.5B), as measured by DHE and TUNEL assays, respectively. Analysis of $Dlx3^{+/-}$maternal serum revealed decreased ($p<0.05$) concentrations of a potent placental angiogenic factor, vascular endothelial growth factor (VEGF), in contrast to controls. Together these findings imply reactive oxygen species stress within the $Dlx3^{+/-}$ placental development may have implications on placental cell types, placental angiogenic factors, and a potential direct correlation to embryo growth kinetics.

Further investigation of $Dlx3^{+/-}$ placental vasculature using micro-CT analysis revealed loss of a single Dlx3 allele resulted in trends ($p<0.1$) toward decreased maternal spiral arteries volume (Figure 4.7B) in contrast to control placental vasculature. In corroboration with these findings, Masson's Trichrome staining revealed a decrease placental maternal artery area ($p<0.05$) in $Dlx3^{+/-}$ placentas compared to wildtype controls (Figure 4.8B). Chronic administration of the superoxide dismutase mimetic Tempol, ameliorates the observed adverse effects in the $Dlx3^{+/-}$ mouse including altered embryonic growth kinetics (Figure 4.4A-C), abundance of ROS (Figure 4.5A), abundance of apoptotic cell types (Figure 4.5B), and decreased placental and maternal spiral artery volumes (Figure 4.7A, B).

Importantly, antioxidant therapy rescued a subset of $Dlx3^{-/-}$ embryos at E12.5, 3 days beyond their normal fetal demise [2]. The statistical trends observed in both the micro-CT analysis and the Masson's Trichrome staining are currently representations of preliminary evidence. Further studies are necessary to add to the statistical relevance of each data set. However even at this preliminary stage of data collection, these data indicate $Dlx3^{+/-}$ mice are sensitive to ROS stresses resulting in detrimental structural implications in the $Dlx3^{+/-}$ placenta and ultimately altered fetal growth kinetics. Moreover antioxidant therapy in the Dlx3 mouse has the ability to rescue the placental and embryonic phenotypes found in the $Dlx3^{+/-}$.

The Dlx3 mouse is not the only model of altered embryo growth kinetics and abnormal placentation. The BPH/5 mouse model of preeclampsia also displays an intrauterine growth retardation (IUGR) phenotype and placental insufficiency. More specifically, neonatal weights of BPH/5 embryos are significantly less than that of control mice [15]; as early as E10.5, BPH/5 decidual vessels have narrowed lumens and a thickened arterial wall; by E12.5 BPH/5 placental labyrinth exhibits decreased vascularization compared to controls [9]. Moreover, BPH/5 and $Dlx3^{+/-}$ placentas indicate a similar susceptibility to ROS accumulation. Similar to the Dlx3 mouse model, antioxidant therapy normalizes ROS levels in the BPH/5 placenta and increases fetal growth and survival rates [14]. However, antioxidant therapy in the BPH/5 model does not reveal the same extent of IUGR rescue as indicated by our studies in the Dlx3 mouse model, suggesting some portion of variable phenotype in these models as gestation progresses.

The condition of pregnancy is deemed to be a state of oxidative stress arising from increased metabolic activity in placental mitochondria and reduced ROS scavenging potential by antioxidants [16]. Measurements of markers of oxidative stress in maternal blood and urine show that pregnancy is a condition of high oxidative stress due to the

high metabolic activity of the placenta and maternal metabolism[17]. This condition is exacerbated in pregnancies complicated by preeclampsia, intrauterine growth restriction (IUGR), and diabetes as measured by increased markers of ROS and a decrease in antioxidant defense mechanisms [18]. For example, immunostaining of placental vascular endothelium revealed an increase in ROS production in pregnancies complicated by preeclampsia compared to control pregnancies [19]. Although an exact mechanism of increased placental ROS generation associated with preeclampsia has not been elucidated, one particular hypothesis arises from the placental vasculature associated with preeclampsia. Pregnancies complicated by preeclampsia exhibit a failed remodeling of maternal spiral arteries [20] resulting in impaired placental perfusion leading to potential harmful effects on fetal growth kinetics [21].

A mounting body of evidence points to a disrupted secretion and/or sequestering of proangiogenic growth factors, such as VEGF and placental growth factor (PGF), in abnormal placentation such as observed in preeclampsia. VEGF is an endothelial-specific mitogen that promotes angiogenesis. The activities of VEGF are primarily mediated by two high-affinity cell surface receptor tyrosine kinases: kinase insert domain region (KDR) and fms-like tyrosine kindase-1 [22,23]. Soluble fms-like tyrosine kindase-1 (sFlt-1) is a naturally occurring antagonist of both VEGF and PGF, which is formed by alternative splicing of the pre-mRNA encoding VEGF-R1 (Flt-1). sFlt-1 lacks both the cytoplasmic and transmembrane domain and can bind to both circulating VEGF and PGF preventing interactions with endogenous receptors. Increased expression of sFlt-1 has been found in both the maternal serum [23] and placenta [24] of preeclamptic patients implicating altered expression of placental growth factors may one cause of impaired placentation observed in preeclampsia. The BPH/5 mouse model of preeclampsia also shows abnormal secretion of angiogenic factors such as VEGF and PGF, in addition to abnormal placental endothelial cell

morphology, as mentioned above [14]. Our studies indicate a similar disruption in relative VEGF concentration in maternal serum of $Dlx3^{+/-}$ animals compared to controls (Figure 4.6). This current set of studies supports previous findings indicating altered vasculature in the $Dlx3^{+/-}$ placentas [1]. Together these studies indicate altered placental angiogenic secretion may correlate with abnormal placental vasculature.

Antioxidants represent a potentially powerful defense from the onslaught of ROS-mediated placental effects. Antioxidant therapy has been used as a way to combat ROS assault on placental vasculature. Results from studies of supplementation of vitamin C and E during the second trimester of pregnancy decreased the biochemical incidence of ROS [25]. Further, gestational supplementation of vitamins C and E indicate a significant reduction in syncytiotrophoblast apoptosis associated with placental hypoxia-reoxygenation [26]. Recent evidence points to a critical gestational time frame for antioxidant therapy to effectively treat ROS stress in the placenta. Myatt and colleagues have indicated antioxidant therapy is most effective when administered before conception and during early gestation [18]. The placenta is in a dynamic state of growth and differentiation throughout gestation with development of the placental vasculature and fetal development occurring in a highly regulated manner. Stressors, particularly from ROS, to the placental at these key growth periods may impact placental development and augment the fetal growth trajectory. Our studies corroborate previous findings in the BPH/5 mouse model, indicating administration of antioxidant therapy prior to and during presumptively critical periods of placental establishment and growth has positive outcomes. Chronic supplementation of Tempol not only ameliorated the observed IUGR phentoype in the $Dlx3^{+/-}$ mouse model (Figure 4.4A-C), but also normalized placental ROS levels (Figure 4.5A, B) and vascularization defects (Figure 4.7A, B). Altogether, these studies add to the beneficial theory of gestational antioxidant therapy.

Proper placental perfusion is critical for fetal growth and development. Impaired placental angiogenic function in combination with placental endothelial cell dysfunction leads to placental insufficiency as observed in both the BPH/5 and $Dlx3^{+/-}$ mouse models. Both models indicate an impaired fetal growth curve that maybe a direct repercussion of ROS mediated effects resulting in placental insufficiency. Our studies clearly point to the possible benefits of antioxidant therapy on not only placental development but also fetal fitness throughout gestation.

REFERENCES

[1] Berghorn, K. A. et al., Smad6 represses Dlx3 transcriptional activity through inhibition of DNA binding. *J Biol Chem* **281** (29), 20357 (2006).

[2] Morasso, M. I. et al., Placental failure in mice lacking the homeobox gene Dlx3. *Proc Natl Acad Sci U S A* **96** (1), 162 (1999).

[3] Robinson, G. W. and Mahon, K. A., Differential and overlapping expression domains of Dlx-2 and Dlx-3 suggest distinct roles for Distal-less homeobox genes in craniofacial development. *Mech Dev* **48** (3), 199 (1994).

[4] Morasso, M. I., Markova, N. G., and Sargent, T. D., Regulation of epidermal differentiation by a Distal-less homeodomain gene. *J Cell Biol* **135** (6 Pt 2), 1879 (1996).

[5] Roberson, M. S. et al., A role for the homeobox protein Distal-less 3 in the activation of the glycoprotein hormone alpha subunit gene in choriocarcinoma cells. *J Biol Chem* **276** (13), 10016 (2001).

[6] Berghorn, K. A. et al., Developmental expression of the homeobox protein Distal-less 3 and its relationship to progesterone production in mouse placenta. *J Endocrinol* **186** (2), 315 (2005).

[7] Hill, J. R. et al., Evidence for placental abnormality as the major cause of mortality in first-trimester somatic cell cloned bovine fetuses. *Biol Reprod* **63** (6), 1787 (2000); Regnault, T. R. et al., Placental expression of VEGF, PlGF and their receptors in a model of placental insufficiency-intrauterine growth restriction (PI-IUGR). *Placenta* **23** (2-3), 132 (2002); Levine, R. J. and Karumanchi, S. A., Circulating angiogenic factors in preeclampsia. *Clin Obstet Gynecol* **48** (2), 372 (2005).

[8] Cheng, M. H. and Wang, P. H., Placentation abnormalities in the pathophysiology of preeclampsia. *Expert Rev Mol Diagn* **9** (1), 37 (2009).

[9] Dokras, A. et al., Severe feto-placental abnormalities precede the onset of hypertension and proteinuria in a mouse model of preeclampsia. *Biol Reprod* **75** (6), 899 (2006).

[10] Hwang, J., Mehrani, T., Millar, S. E., and Morasso, M. I., Dlx3 is a crucial regulator of hair follicle differentiation and cycling. *Development* **135** (18), 3149 (2008).

[11] Rennie, M. Y. et al., 3D visualisation and quantification by microcomputed tomography of late gestational changes in the arterial and venous feto-placental vasculature of the mouse. *Placenta* **28** (8-9), 833 (2007).

[12] Ghosh, M. C. et al., Tempol-mediated activation of latent iron regulatory protein activity prevents symptoms of neurodegenerative disease in IRP2 knockout mice. *Proc Natl Acad Sci U S A* **105** (33), 12028 (2008).

[13] Chatterjee, P. K. et al., Tempol, a membrane-permeable radical scavenger, reduces oxidant stress-mediated renal dysfunction and injury in the rat. *Kidney Int* **58** (2), 658 (2000).

[14] Hoffmann, D. S. et al., Chronic tempol prevents hypertension, proteinuria, and poor feto-placental outcomes in BPH/5 mouse model of preeclampsia. *Hypertension* **51** (4), 1058 (2008).

[15] Davisson, R. L. et al., Discovery of a spontaneous genetic mouse model of preeclampsia. *Hypertension* **39** (2 Pt 2), 337 (2002).

[16] Wisdom, S. J., Wilson, R., McKillop, J. H., and Walker, J. J., Antioxidant systems in normal pregnancy and in pregnancy-induced hypertension. *Am J Obstet Gynecol* **165** (6 Pt 1), 1701 (1991).

[17] Palm, M., Axelsson, O., Wernroth, L., and Basu, S., F(2)-isoprostanes, tocopherols and normal pregnancy. *Free Radic Res* **43** (6), 546 (2009); Morris, J. M. et al., Circulating markers of oxidative stress are raised in normal pregnancy and pre-eclampsia. *Br J Obstet Gynaecol* **105** (11), 1195 (1998); Toescu, V. et al., Oxidative stress and normal pregnancy. *Clin Endocrinol (Oxf)* **57** (5), 609 (2002).

[18] Myatt, L., Review: Reactive oxygen and nitrogen species and functional adaptation of the placenta. *Placenta* **31 Suppl**, S66.

[19] Myatt, L. et al., Nitrotyrosine residues in placenta. Evidence of peroxynitrite formation and action. *Hypertension* **28** (3), 488 (1996).

[20] Pijnenborg, R., Vercruysse, L., and Hanssens, M., The uterine spiral arteries in human pregnancy: facts and controversies. *Placenta* **27** (9-10), 939 (2006).

[21] Brosens, J. J., Pijnenborg, R., and Brosens, I. A., The myometrial junctional zone spiral arteries in normal and abnormal pregnancies: a review of the literature. *Am J Obstet Gynecol* **187** (5), 1416 (2002).

[22] Hsu, C. D. et al., Elevated circulating thrombomodulin in severe preeclampsia. *Am J Obstet Gynecol* **169** (1), 148 (1993).

[23] Levine, R. J. et al., Circulating angiogenic factors and the risk of preeclampsia. *N Engl J Med* **350** (7), 672 (2004).

[24] Maynard, S. E. et al., Excess placental soluble fms-like tyrosine kinase 1 (sFlt1) may contribute to endothelial dysfunction, hypertension, and proteinuria in preeclampsia. *J Clin Invest* **111** (5), 649 (2003).

[25] Jauniaux, E., Poston, L., and Burton, G. J., Placental-related diseases of pregnancy: Involvement of oxidative stress and implications in human evolution. *Hum Reprod Update* **12** (6), 747 (2006).

[26] Tjoa, M. L. et al., Trophoblastic oxidative stress and the release of cell-free feto-placental DNA. *Am J Pathol* **169** (2), 400 (2006).

CHAPTER FIVE

SUMMARY AND DISCUSSION

The placenta of a developing fetus has several roles including an immune interface between mother and fetus, serving to transport nutrients and waste products, and serving as a source of many peptide and steroid hormones that influence fetal, placental and maternal metabolism and development. The mammalian placenta is in a dynamic state of growth and differentiation throughout gestation; specifically human placentas show a 40-fold increase in fetal/placental weight ratio (a measure of placental efficiency) from weeks 6 to term. This increased placental efficiency is achieved by both a 10-fold increase in the villous volume occupied by vasculature and an increase in trophoblast surface area from 0.08 to 12.5m^2 and a decrease in mean trophoblast thickness from 18.9 to 4.1μm ultimately resulting in a decreased fetal-maternal diffusion distance from 55.9 to 4.8μm [1].

Each physical placental change is connected to highly organized growth phases involving branching events linked to angiogenesis, trophoblast differentiation, and syncytium formation; each step is governed by a complex gene profile carefully coordinated with placental specific angiogenic factors. Disruption in the normal pattern of placental development will lead to altered placental function. More specifically, the timing of these alterations during gestation and the extent of the disruption may cause critical implications on placental function leading to pregnancy complications.

My central hypothesis implicates the necessity of the homeodomain-containing transcription factor, Distal-less (Dlx) 3, along with its gene profile, in proper murine placental development. Initial studies of the Dlx3 mouse model have indicated a mid-gestational lethality associated with complete loss of Dlx3 [2]. Further studies have linked placental insufficiency in the Dlx3 mouse to the early fetal demise [3]. In the developing primate placenta, Dlx3 has been shown to activate the α subunit of the glycoprotein hormone gene by binding to the junctional regulatory elements found in

the promoter region [4]. Activation of the glycoprotein hormone a subunit gene is necessary for expression of chorionic gonadotropin (CG) in the placental, effectively resulting in early maintenance of pregnancy. Loss of Dlx3 in choriocarcinoma cells results in decreased expression of the α subunit. Immunostaining of human placental section obtained from 8 weeks gestation implicate the expression of Dlx3 in human cyto- and syncytiotrophoblasts at the time of peak CG production [5]. These studies support the theory that Dlx3 is involved in the molecular regulation of CG biosynthesis, indicating the novel role of Dlx3 in maintenance of early pregnancy.

Investigation of molecular interacting partners of Dlx3 in a human placental cDNA library identified Smad6 as a binding partner through yeast two-hybrid analysis (Chapter 2) [3]. Smad proteins are a group of transcriptional regulators that are categorized into 3 subclasses: receptor-regulated Smads (R), common Smads (C), and inhibitory Smads (I). The R-Smads acquire signals through two distinct pathways. Smad 1, 5, and 8 are regulated through the bone morphogenic pathway (BMP), while Smads 2 and 3 obtain signals through the transforming growth factor-β (TGF-β) pathway. Both BMP and TGF-β activate the Smad pathway by interacting and phosphorylating specific R-Smads. Phosphorylation of the R-Smads causes dissociation from the receptor and induces assembly of a complex with Smad4, a C-Smad. This heterodimeric complex then translocates to the nucleus and functions as a transcriptional comodulator by recruiting various coactivators and corepressors to the Smad DNA binding machinery [6]. The I-Smads, Smad6 and 7, function as potent antagonists by binding to either TGF-β or BMP receptors and blocking the phosphorylation of R-Smads or, in the case of Smad6, by binding to the phosphorylated Smad1 and preventing the formation of a complex with Smad4 [7]. Transcription of the I-Smads is stimulated by not only TGF-β family members [8] indicating a possible negative feedback mechanism, but also epidermal growth factor

(EGF), phorbol ester -12-*O*-tetradecanoylphorbol 13-acetate (TPA), and interferon-γ [9]. The findings imply the signaling governing Smad6, such as BMP and TGF-β, may also indirectly effect Dlx3 expression.

Further immunostaining of trophoblast cells indentified Smad6 and Dlx3 co-localized to the nuclear compartment [3]. Similarly, in human term placenta, Smad6 and Dlx3 were nuclear localized in both the cytotrophoblast and syncytial trophoblast cells within the microvilli [3]. This observation demonstrates that the interaction of Smad6 and Dlx3 is not restricted to a temporal pattern in gestation; Dlx3 expression can be maintained within the trophoblast population until term in the human placenta. The co-nuclear localization of Dlx3 and Smad6 implies Smad6 has the capability of modulating Dlx3 transcriptional expression in the placenta. For example, Smad6 disrupts the Dlx3-dependent gene expression of the placental specific promoter, Extraembryonic, spermatogenesis, homeobox-1 like protein (Esx-1) promoter (Chapter 2) [3]. The interaction between Dlx3 and Smad6 may play a role in the abnormal placental phenotype observed in the Dlx3 mouse model [3].

Further assessment of the Dlx3 gene profile was investigated by conducting an Affymetrix microarray using RNA from E9.5 wildtype and $Dlx3^{-/-}$ placentas [10]. Results identified 401 genes that were differentially expressed following the loss of Dlx3, including expression of matrix metalloproteinase (MMP-) 9, an extracellular matrix (ECM) remodeler. Microarray analysis and subsequent q-PCR revealed loss of Dlx3 at E9.5 in the $Dlx3^{-/-}$ mouse placenta resulted in decreased expression of MMP-9 [10]. MMP-9 is part of a larger family of MMPs. These molecules are mainly involved in extracellular matrix degradation (ECM). Necessary for my studies are the essential role MMPs play in placental remodeling. Degradation of ECM is critical to remodel the maternal vascular network from high resistance, low capacity structures to low resistance, high capacity vessels necessary for appropriate placental perfusion [11]. The

link between aberrant Dlx3 expression and MMP-9 transcript levels, as well as the placental abnormalities identified in the Dlx3 mouse, indicate the potential association of MMP-9 in the gene profile associated with the Dlx3 mouse model.

My studies indicate Dlx3 is capable of binding to the MMP-9 mouse and human promoters, as indicated by EMSA and ChIP assays, respectively. Further characterization indicates a Dlx3 dose dependent transcriptional activation on the murine MMP-9 gene promoter. Additional experiments linked loss of Dlx3, either by si-RNA knockdown in choriocarcinoma cells, or genetic loss as in $Dlx3^{-/-}$ placentas, to a significant decrease in MMP-9 activity as measured by zymography. Moreover, the misregulation throughout gestation, of both MMP-9 and Dlx3 transcript levels, in the BPH/5 mouse model of preeclampsia indicate a potential interplay between these two molecules underlying the abnormal placental phenotype observed in this mouse model [12].

Abnormal placentation is not the only phenotype associated with preeclampsia. Numerous studies have found that preeclampsia also is associated with uteroplacental vascular insufficiency, altered intervillous hemodynamics, oxidative stress, anti-angiogenic molecules and generalized maternal endothelial cell dysfunction [13]. However, the exact cause(s) of the disease is still unknown. Unfortunately, the disease state cannot be detected until it presents as maternal symptoms in late gestation. Finding a potential biomarker for early detection of preeclampsia in the placental transcriptome would be beneficial and could possibly lead to the development of novel treatments.

Many studies have focused on angiogenic factors as potential biomarkers of preeclampsia. For example, a nested case-control study investigated the association between fms-like tyrosine kinase 1 (sFlt1), endoglin (ENG) and placental growth factor (PGF) and preeclampsia. ELISA measurements indicated sFlt1 levels remained

unchanged between control and pregnancies complicated by preeclampsia. However, ENG levels were higher ($p<0.001$) and PGF levels were lower ($p<0.001$) in pregnancies complicated by preeclampsia compared to controls [14]. Yet, this study does not correlate with other recent data that indicates sFlt1 levels are increased in preeclamptic patients compared to control [15]. The reason for such discrepancies may have to do with maternal factors including gestational age, diet, parity. Regardless of the reason for the inconsistency, the conflicting reports in the literature only demonstrate the necessity of a reliable biomarker for preeclampsia.

Recent findings have focused on microRNA's (miRNAs), a family of small non-coding regulatory RNAs involved in human development and pathology, as effective biomarkers of human disease. miRNAs have a critical role in posttranscriptional regulation of protein-coding genes and are present in bodily fluids making them easily accessible for identification. Serum miRNA profiles have already been shown to change during physiological or pathological conditions as in pregnancy; moreover, these alterations in miRNA profiles correlate to pregnancy stage [16]. Further, studies have characterized increased expression of specific placental miRNAs in pregnancies complicated by preeclampsia in contrast to controls [17]. Future studies should seek to examine the shared miRNA profile of the Dlx3 mouse model and other models of placental insufficiency, such as the BPH/5 mouse model. These approaches would ultimately yield more precise information about the miRNA determinants found in abnormal placentation and result in a useful biomarker for placental insufficiency.

Important lessons are still to be learned from the $Dlx3^{-/-}$ placental microarray study. As mentioned above, loss of Dlx3 resulted in the differential gene expression of 401 genes [10] indicating numerous direct and indirect Dlx3 interacting partners. Future studies should investigate the definitive relationship between Dlx3 and other

highly differentially expressed genes and their collective correlation to placental insufficiency.

A deeper investigation of the Dlx3 mouse model placental vasculature is necessary for complete understanding the effect Dlx3 haploinsufficiency has on the developing placenta. Initial investigation of the Dlx3 mouse model using micro-computed tomography (micro-CT) revealed abnormal placental vascularization in the $Dlx3^{+/-}$ mouse. More specifically, $Dlx3^{+/-}$ placental and maternal spiral artery volumes tended an observed decrease ($p<0.01$) compared to wildtype controls. As discussed in Chapter 4, these studies only represent preliminary evidence. The volumetric measurements should be repeated on the Dlx3 mouse model for a better statistical representation of the data.

Antioxidant therapy using the superoxide dismutase (SOD) mimetic ameliorated the observed placental and IUGR phenotype found in the Dlx3 mouse model. These findings indicate the potential benefits of antioxidant therapy in cases of placental insufficiency.

Additionally, future studies should use the refined spacial imaging resolution associated with 2-photon excited microscopy (2-PE). Initial studies I undertook using a GFP-transgenic mouse model under the transcriptional control of a fetal endothelial cell promoter (Tie-2) resulted in marvelous images of the placental vasculature using 2-PE. However, numerous obstacles do exist for this imaging technique. The vasculature of the placenta is a very complex network of fetal and maternal blood vessels in the murine labyrinth layer [18]. Studies have indicated the labyrinth layer in the Dlx3 mouse model exhibits a restricted growth pattern in contrast to wildtype controls [3] thereby identifying the labyrinth layer as potential instrumental factor underlying the observed IUGR phenotype. Thus for the purposes of my studies, I will require a labeling tool to define fetal and maternal contributions to the labyrinth. I

originally designed a congenic animal mating the $Dlx3^{+/-}$ x Tie-2 GFP mouse for the purposes of visualizing the fetal vasculature without exogenous addition of a fluororphore. Maternal vasculature was to be labeled with addition of a designated fluorophore so subsequent imaging would allow assessment of both fetal and maternal vasculature in the mouse placenta. Limitations on imaging capabilities restricted the progress of this project. Currently those limitations are being resolved and future studies should take advantage of this congenic $Dlx3^{+/-}$ x Tie-2 GFP mouse model. Further investigation using 2-PE of Dlx3 placental vasculature in conjunction with gestational antioxidant therapy will expand on these initial studies. Potential future findings will broaden our understanding of the placental insufficiency exhibited in this mouse model and the effect of antioxidant therapy on placental vasculature.

Dlx3 has multiple mechanisms of control in the placental as described in this dissertation. In some instances, the impact of Dlx3 on placental function may be dependent on its interacting partners. For example, Smad6 down-regulates Dlx3-mediated transcription of the important placental angiogenic factor PGF in JEG3 cells [10]. Additionally, the combined effects of Dlx3 and its interacting partners can have implications on a variety of placental functions including hormone production, vascular remodeling, and angiogenesis. Alterations in the interplay of Dlx3 and its interacting partners may have detrimental effects leading to ROS-mediated placental insufficiency, IUGR, or preeclampsia. Future studies should examine not only the singular role of Dlx3 in the placenta, but also the combined effects of Dlx3 and its interacting partners.

REFERENCES

[1] Myatt, L., Placental adaptive responses and fetal programming. *J Physiol* **572** (Pt 1), 25 (2006).

[2] Morasso, M. I. et al., Placental failure in mice lacking the homeobox gene Dlx3. *Proc Natl Acad Sci U S A* **96** (1), 162 (1999).

[3] Berghorn, K. A. et al., Smad6 represses Dlx3 transcriptional activity through inhibition of DNA binding. *J Biol Chem* **281** (29), 20357 (2006).

[4] Roberson, M. S. et al., A role for the homeobox protein Distal-less 3 in the activation of the glycoprotein hormone alpha subunit gene in choriocarcinoma cells. *J Biol Chem* **276** (13), 10016 (2001).

[5] Berghorn, K. A. et al., Developmental expression of the homeobox protein Distal-less 3 and its relationship to progesterone production in mouse placenta. *J Endocrinol* **186** (2), 315 (2005).

[6] Heldin, C. H., Miyazono, K., and ten Dijke, P., TGF-beta signalling from cell membrane to nucleus through SMAD proteins. *Nature* **390** (6659), 465 (1997).

[7] Whitman, M., Smads and early developmental signaling by the TGFbeta superfamily. *Genes Dev* **12** (16), 2445 (1998).

[8] Afrakhte, M. et al., Induction of inhibitory Smad6 and Smad7 mRNA by TGF-beta family members. *Biochem Biophys Res Commun* **249** (2), 505 (1998).

[9] Ulloa, L., Doody, J., and Massague, J., Inhibition of transforming growth factor-beta/SMAD signalling by the interferon-gamma/STAT pathway. *Nature* **397** (6721), 710 (1999).

[10] Han, L. et al., Analysis of the gene regulatory program induced by the homeobox transcription factor distal-less 3 in mouse placenta. *Endocrinology* **148** (3), 1246 (2007).

[11] Pijnenborg, R., Vercruysse, L., and Hanssens, M., The uterine spiral arteries in human pregnancy: facts and controversies. *Placenta* **27** (9-10), 939 (2006); Hibbs, M. S., Hoidal, J. R., and Kang, A. H., Expression of a metalloproteinase that degrades native type V collagen and denatured collagens by cultured human alveolar macrophages. *J Clin Invest* **80** (6), 1644 (1987).

[12] Dokras, A. et al., Severe feto-placental abnormalities precede the onset of hypertension and proteinuria in a mouse model of preeclampsia. *Biol Reprod* **75** (6), 899 (2006).

[13] Roberts, J. M. and Lain, K. Y., Recent Insights into the pathogenesis of pre-eclampsia. *Placenta* **23** (5), 359 (2002); Sibai, B., Dekker, G., and Kupferminc, M., Pre-eclampsia. *Lancet* **365** (9461), 785 (2005).

[14] Srinivas, S. K. et al., The use of angiogenic factors in discriminating preeclampsia: are they ready for prime time? *J Matern Fetal Neonatal Med*.

[15] Levine, R. J. et al., Circulating angiogenic factors and the risk of preeclampsia. *N Engl J Med* **350** (7), 672 (2004); Thadhani, R. et al., First trimester placental growth factor and soluble fms-like tyrosine kinase 1 and risk for preeclampsia. *J Clin Endocrinol Metab* **89** (2), 770 (2004).

[16] Gilad, S. et al., Serum microRNAs are promising novel biomarkers. *PLoS One* **3** (9), e3148 (2008).

[17] Pineles, B. L. et al., Distinct subsets of microRNAs are expressed differentially in the human placentas of patients with preeclampsia. *Am J Obstet Gynecol* **196** (3), 261 e1 (2007).

[18] Cox, B. et al., Comparative systems biology of human and mouse as a tool to guide the modeling of human placental pathology. *Mol Syst Biol* **5**, 279 (2009).